IDŐJÁRÁS

QUARTERLY JOURNAL
OF THE HUNGARIAN METEOROLOGICAL SERVICE

CONTENTS

****

http://www.met.hu/firat/ido-e.html

VOL. 101 * NO. 2 * APRIL–JUNE 1997

IDŐJÁRÁS

Quarterly Journal of the Hungarian Meteorological Service

Editorial Office: P.O. Box 39, H-1675 Budapest, Hungary or
Gilice tér 39, H-1181 Budapest, Hungary
E-mail: gmajor@met.hu or *antal@met.hu*
Fax: (36-1) 290-7387

Subscription by

mail: IDŐJÁRÁS, P.O. Box 39, H-1675 Budapest, Hungary;
E-mail: gmajor@met.hu or *antal@met.hu*; *Fax: (36-1) 290-7387*

IDŐJÁRÁS

Quarterly Journal of the Hungarian Meteorological Service
Vol. 101, No. 2, April–June 1997, pp. 73–92

The atmosphere as a colloidal medium: absorption of solar radiation

K. Ya. Kondratyev

Research Center for Ecological Safety
Nansen International and Remote Sensing Center,
18, Korpusnaya str., 197110 St. Petersburg, Russia
E-mail: nansen@sovam.com

(Manuscript received 20 December 1996; in final form 17 March 1997)

Abstract—An overview of recent studies on "excess" absorption of solar radiation by the atmosphere has been made. The main result of the overview is the demonstration of the multicomponent nature of shortwave radiation (SWR) absorption in the atmosphere. Clouds are significant absorbers of SWR and it is very important to take into account the 3-D spatial inhomogeneity of cloud cover as well as the cloud pollution due to both natural and anthropogenic sources of aerosol pollution. There are, however, other important contributors to SWR absorption. For example, contribution of water vapor is far from being adequately assessed. Much more reliable observations and assimilation techniques (to consider observation data from different sources) are necessary to avoid relevant biases. The unacceptably high level of the underestimation of SWR absorption in the atmosphere by the present-day climate models (the disagreement with observations is an order of magnitude larger than the enhancement of the atmospheric greenhouse effect due to CO_2 concentration increase) requires further research with the two principal purposes: (1) complex dedicated field experiments to study SWR absorption in real atmosphere; (2) more adequate radiation parameterization in models.

Key-words: absorption, solar radiation, clouds, spatial inhomogeneity, multiple scattering, climate models.

1. Introduction

As it is well known, cloud dynamics and cloud–radiation interaction belong to the basic uncertainties of present-day climate modeling (*Borisenkov* and *Kondratyev*, 1988; *Kondratyev*, 1992; *Ma et al.*, 1996; *Marchuk et al.*, 1986; *Ridout* and *Rosmond*, 1996 and many other publications including the three recent volumes of the Intergovernmental Panel on Climate Change reports). An issue of critical importance in this context is the existence of uncertainties

relevant to the redistribution of solar energy transformed by the atmosphere due to impacts of various optically active components: gases, aerosols, and clouds.

Li et al. (1995) have recently emphasized that "...after more than 40 years of work, both theory and observations of the absorption of solar radiation by clouds are still fraught with uncertainties" (see also *Crutzen* and *Ramanathan*, 1996). A new illustration to this conclusion is the very intensive discussion of the problem of so called "excess" or "anomalous" absorption of solar radiation by clouds. *Ramanathan et al.* (1996) are correct in their statement that there is no reason to talk about "anomalous absorption" but "...it is safe to consider this phenomenon as simply, 'excess absorption' to point out that there is excess solar absorption in cloudy atmospheric columns when compared with clear sky column absorption".

The basic problem under discussion is the relationship between absorption of shortwave radiation (SWR) by the atmosphere and the Earth's surface which has been obtained on the basis of observations and numerical modeling. *Cess et al.* (1995) have concluded that "globally, GCMs that constrain their planetary albedos with satellite data, may overestimate the solar energy reaching the surface by as much as 8% or equivalently 25 W/m^2" (*Ramanathan et al.*, 1996).

Wild et al. (1995) showed that the ECHAM 3 General Circulation Model (GCM) calculated global mean surface SWR absorption (around 165 W/m^2) is higher by 10–15 W/m^2 compared to observations from the Global Energy Balance Archive (GEBA) data. A similar or higher overestimate is present in several other GCMs. Deficiencies in the clear sky absorption of the ECHAM 3 radiation scheme under clear sky conditions have been assumed as contributors to the flux discrepancies. A stand-alone validation of the radiation scheme under clear sky conditions revealed overestimates of up to 50 W/m^2 for daily maximum values of incoming shortwave fluxes. The lack of shortwave absorption by model clouds contributes to the overestimation of surface absorbed SWR. There is, however, a compensation between the overestimation of shortwave and underestimation of incoming longwave radiation by 10–20 W/m^2, which results in realistic enough values of the calculated surface radiation budget.

This survey paper answers the question: why may models overestimate the solar energy reaching the surface? The answer to this question is not at all simple, especially because the problem has a number of aspects to be considered. It has long been known (*Arking*, 1991; *Kiehl* and *Briegleb*, 1993, *Kondratyev*, 1969, 1972, 1988a, 1992, 1996; *Kondratyev* and *Binenko*, 1984; *Marchuk et al.*, 1986; *Stephens et al.*, 1978; *Stephens* and *Tsay*, 1990) that models underestimate SWR absorbed by clouds, but it is just one aspect of the problem, the other aspect is the "excess" absorption in the clear atmosphere.

2. *Observational data*

The problem of reliability of observational data is fairly complex. What we need to know is SWR absorption by the atmosphere (SWRA) in order to determine, how much solar energy is absorbed by the surface. SWRA may be found from combined surface and satellite observations. While the latters are really of global scale, surface solar radiation measurements are rather fragmentary and the existing global data set can therefore not be considered as adequately representing the global distribution of SWR. Besides, different spatial scales of surface point observations and satellite data averaged over large territories complicate a combined analysis of such data (important comments in this respect have been made by *Arking et al.*, 1996).

What we need to determine is the difference of shortwave radiation balances — SWRB (net SWR) at the top of the atmosphere (TOA net SWR values) and at the surface. SWRB itself is the difference between upward and downward SWR fluxes (irradiances). Thus, a necessity arises to differentiate twice the measured values of SWR fluxes. Undoubtedly, it might lead to serious errors. Unfortunately, persuasive assessments of such errors do not exist as yet. Certain efforts have been made to estimate errors in case of aircraft and balloon observations of SWR vertical profiles in the atmosphere (*Hayasaka et al.*, 1996; *Kondratyev*, 1969; *Kondratyev et al.*, 1976; *Kondratyev* and *Binenko*, 1984; *Stephens et al.*, 1978; *Pilewskie* and *Valero*, 1995, 1996; and others).

In view of the absence of reliable enough estimates of observational errors we would like to emphasize here an urgent necessity of the careful consideration of this problem. An important aspect of the problem is the use of various assimilation techniques to process inhomogeneous (in space and time) data series, which also requires a critical analysis. An illustration of this problem is the determination of clear sky radiative forcing (RF) values which is unavoidably based on various kinds of extrapolation (see *Arking et al.*, 1996).

3. *Effect of clouds on atmospheric absorption of solar radiation*

The discussion of the redistribution of solar energy between the atmosphere and the surface was mainly focused on assessments of cloud impacts on the atmospheric absorption of solar radiation (*Cess et al.*, 1995; *Li* and *Moreau*, 1996, 1997; *Li et al.*, 1995; *Ramanathan et al.*, 1995), since models obviously underestimated cloud absorption. *Ramanathan et al.* (1996) correctly noted that "Some of the fundamental flaws of our radiation models, at least those used to assert the zero net cloud effect, is that they assume: (1) clouds are flat plates with horizontally homogeneous properties, (2) cloud drops and crystals are made of pure water; and, (3) the absorption is by Lorentzian lines with arbitrary specified wavelength cut-offs, and (4) poor treatment of aerosol

effect". One more important feature to be mentioned is 3-D spatial inhomogeneity of cloud cover.

To assess the SWR absorption by clouds *Cess et al.* (1995) have undertaken an analysis of the data of simultaneous satellite and surface observations of the SWR fluxes at four locations: American Samoa (14.25°S; 170.56°W), Barrow (71.32°N; 157°W), Boulder (40.05°N; 105.01°W), Cape Grim (40.67°S; 114.69°E), and at 11 stations located in the state of Wisconsin. The data of pyranometric observations of the upward and downward SWR fluxes make it possible to calculate the shortwave radiation budget (SWRB), and satellite data contain information on the outgoing shortwave radiation (OSWR). The SWRB and OSWR differences for real cloud conditions and clear sky cases characterize the shortwave radiative forcing $C_s(S)$ and $C_s(TOA)$ at the surface and at the top of the atmosphere, respectively (the satellite data were averaged over 1° × 1° or 2.8° × 2.8° latitude-longitude grid).

From the data for Boulder, mean diurnal $C_s(S) = -92.6$ W/m^2 and $C_s(TOA) = -63.2$ W/m^2, that is $C_s(S)/C_s(TOA) = 1.46$, whereas the calculated $C_s(S)/C_s\ (TOA) \approx 1$, from which it follows that the calculated SWR absorbed by the cloudy atmosphere is substantially underestimated (by $C_s(S) - C_s(TOA) = 30$ W/m^2).

In view of possible errors in the estimates, an alternative technique has been applied based on estimation (by linear regression) of the variable

$$\beta = \frac{-dA_{TOA}}{d(Q_s/Q_{TOA})}, \tag{1}$$

where A_{TOA} is the albedo of the surface-atmosphere system, Q is the insolation at the levels of surface (S) and at the top of the atmosphere (TOA). From the data of observations in Boulder, $\beta = 0.59$, whereas calculations with the ECMWF (the European Centre for Medium Range Weather Forecasts) and CCM2 (the National Center for Atmospheric Research Community Climate Model) models gave 0.79 and 0.81, respectively.

An agreement of the calculated β values with observations is only possible with the calculated absorption supposedly underestimated. It is obvious that

$$\frac{C_s(S)}{C_s(TOA)} = \frac{1 - A_s}{\beta}, \tag{2}$$

where A_s is the surface albedo. For the Boulder conditions ($A_s = 0.17$) the quantity $\beta = 1.41$ agrees well with the estimate given above. All the other locations are also characterized by underestimated calculated absorption (with an exception of the cases of high snow surface albedo).

Cess et al. (1995) believe that though the water vapor content in the cloudy atmosphere is greater than in the clear one, this circumstance, as illustrated by respective estimates, cannot explain the growth of the SWR absorption. The universal character of the considered "anomalous" ("excessive") absorption by clouds (its independence on the location of the observation point) prompts one to reject also a possible role of the aerosol effect on the optical properties of clouds in view of the strong spatial and temporal variability of the aerosol concentration and properties.

Thus the problem consists, presumably, of the inadequacy of the present ideas of the optical properties of clouds. With the mean global surface albedo assumed to be 0.1, the excess absorption of solar radiation by clouds not considered in present climate models turns out to be about 25 W/m^2, i.e. it exceeds the $2 \times CO_2$ — induced enhancement of the greenhouse effect by almost an order of magnitude (*Borisenkov* and *Kondratyev*, 1988). Therefore there is an urgent need to understand the nature of this absorption and its consideration in the numerical climate modeling. In accordance with *Cess et al.* (1995), the mean global mean annual value of the shortwave cloud-radiation forcing $C_s(TOA)$ characterizing the effect of clouds on the shortwave radiation budget of the surface – atmosphere system (the difference of the SWRB of the mean conditions of clouds and clear sky cases) varies from –45 to –50 W/m^2. The value

$$C_s(TOA) = C_s(S) + C_s(A) \tag{3}$$

is determined by the sum of the contributions from the surface (S) and atmosphere (A). If SWR absorption grows in the presence of clouds, then $C_s(A) > 0$.

To analyse the formation of $C_s(TOA)$, the observational data of the surface heat balance and heat transport in the ocean for the region of the "warm pool" (WP) in the western Pacific (140–170°E; 10°N–10°S) have been processed by *Ramanathan et al.* (1995). In this region the SST reaches a mean annual value of ~302.5K, maximum for the World Ocean. The WP region is characterized by a humid and cloudy atmosphere with a frequent occurrence of cumulus clouds (60% of cases). An unexpected feature of WP turned to be a small mean annual dynamical heat transport (D) out of the WP mixed layer due to horizontal advection and vertical diffusion: $0 \leq D \leq 20$ W/m^2, which constrains the long-term annual mean net downward surface heat flux (H) to small values, since over an annual cycle no net heating of the mixed layer should take place. This condition

$$H - D = 0 \tag{4}$$

is used to close the WP heat balance from the observational data. It turned out that the closing is only possible in the case of strong reduction of total radiation

by clouds (> 100 W/m^2) which, in its turn, requires high values of $C_s(A)$ (~ 35 W/m^2) in the region of the WP, i.e. an anomalously intensive SWR absorption by clouds.

The resulting heat flux H at the ocean surface is

$$H = S_c + C_s(S) - F - E - h, \tag{5}$$

where S_c is the clear sky SWRB, F is the net longwave radiation, E is the heat loss due to evaporation, h is the turbulent sensible heat flux. The mixed layer net heating $Q = H - D$ is determined by two components: horizontal advection in the mixed layer (D_a) and downward entrainment of heat into the thermocline zone below (D_e). From the available data of ship and satellite observations all the heat balance components of Eq. (5) can be estimated, except for $C_s(s)$, which is calculated as a residual term.

Calculations made by *Ramanathan et al.* (1995) show that the mean annual values of the components of Eq. (5) turned out to be: $S_c = 275$ W/m^2 (with possible variations within 270–280 W/m^2) and $F = -45$ W/m^2. In this case $C_s(S) = -100$ W/m^2 (80–135 W/m^2).

The following relationship corresponds to the optimal values of the components of Eq. (5)

$$f_s = C_s(S)/C_s(TOA) = 1.5, \tag{6}$$

whereas calculations give $f_s < 1.2$. The results obtained by *Ramanathan et al.* (1995) reveal the fundamental gap in the present understanding of the effects of clouds on the SWR transport mentioned above. The value $f_s = 1.5$ means an increase of absorption by the atmosphere in the WP region by 35 W/m^2, compared to 100 W/m^2 for the cloud-free atmosphere. The oceanic mixed layer heating due to solar radiation absorption is thus reduced by 35 W/m^2. All this means a change in the meridional energy transport by the ocean and the atmosphere from the tropics to mid-latitudes within 25–50%, which, of course, is of fundamental importance from the viewpoint of climate formation.

To check these results from the data of direct observations, *Pilewskie* and *Valero* (1995) carried out simultaneous aircraft pyranometric measurements of total upward and downward SWR fluxes (the wavelength interval is 0.3–4.0 μm) in the tropical Pacific (140–180°E; 0–15°S) using aircraft measurements at altitudes from 8 to 12 km as well as at about 20 km, near the tropical tropopause. The goal of these measurements was to obtain data on the contribution of clouds to the SWR absorption by the atmosphere between the two altitudes. Through an extrapolation, data for the whole atmosphere were obtained.

The analysis of the observational results revealed a strong SWR absorption by clouds: on the average, the SWR absorbed by clouds reached 165 W/m^2, whereas, according to calculations, it was negligible. These results agree well with the estimates from the data on the ocean heat balance mentioned above. Since the results of spectral measurements revealed only specific selectivity typical of water, a supposition of the possible explanation of absorption by cloud pollution cannot be accepted. Therefore *Pilewskie* and *Valero* (1995) believe that the nature of absorption remains unclear (probably, the effects of the broken cloud morphology causing an increase of the length of the free path of photons play some role).

The problem of "anomalous" absorption by clouds would not have been highlighted as has been done in some publications (*Cess et al.*, 1995; *Ramanathan et al.*, 1995) if their authors had been acquainted with the results of complex studies of cloud–radiation interaction carried out under the programs CAENEX (Complex Atmospheric Energetic Experiment), GAAREX (Global Atmospheric Aerosol Experiment), and FGGE (First GARP (Global Atmospheric Research Programme) Global Experiment) (*Kondratyev*, 1972, 1988, 1992; *Kondratyev et al.*, 1976, 1996a; *Marchuk et al.*, 1986), and with recent results of radiation transport calculations for overcast and partial cloudiness (*Kondratyev et al.*, 1996b). Here are some illustrations of the respective results. The vertical soundings of the cloudy (5 October, 1972) and cloud-free (6 October, 1972) atmosphere over the Azov Sea revealed a strong transformation of both total and spectral radiative characteristics of the atmosphere on these days, determined by the emission of aerosol from the industrial zone of the cities Donezk and Zaporozhye, where the aerosol optical thickness of the atmosphere according to actinometric measurements was $\tau_a = 0.35$. The analysis of aircraft spectral measurements in the cloudy atmosphere carried out during the CAENEX period (*Kondratyev* and *Binenko*, 1984) revealed: (1) the SWR absorption by clouds is close to neutral in the visible; (2) the cloud top plays an active role in the SWR absorption; (3) maximum wavelength dependence on absorption in the oxygen and water vapor absorption bands; (4) strong cloud aerosol-induced absorption at $\lambda = 0.5$ μm (up to 0.15) compared to more "clean" clouds over the Black Sea (10 April, 1971), when the relative absorption was 0.03 (the optical thickness of clouds was 25 and 19, respectively).

Simultaneous measurements of the attenuation coefficient ϵ and size distribution parameters of stratified clouds of 550 m (5 October, 1972) and 450 m (10 April, 1971) thickness revealed: (1) the cloud top (within 50–100 m) has maximum ϵ, maximum values of water content, number concentration and modal radius of droplets; (2) a possibility to estimate the average droplet radius r with the use of the dependence $r = 0.9\ w/\rho\epsilon$, where w is the water content, ρ is the water density, and $\epsilon = \sigma + \kappa$ is the volume attenuation coefficient expressed as a sum of scattering and absorption coefficients; (3) the characteristic feature of marine clouds compared to clouds over land, consisting in a

greater contribution of large particles into the size distribution spectrum and in water content which could result from the impact of industrial aerosol pollution of clouds over land.

Processing the data of measurements of the SWR total fluxes (0.3–3.0 μm) showed that the SWR absorbed by the layer 0.2–1.2 km in cloudless conditions (6 October, 1972) for the sun elevation 38° was 35 W/m^2 but for the same layer in the presence of clouds the absorbed SWR reached 91 W/m^2 (5 October, 1972). Thus the contribution of absorption due to the cloud (as a difference of these values) constitutes 56 W/m^2. If we estimate the residual absorption by cloud, both total (0.3–3.0 μm) and in the visible wavelength range, in the climatological terms of other studies (*Cess et al.*, 1995; *Ramanathan et al.*, 1995) for the atmospheric layer 0.2–8.5 km, then $C_s(S)/C_s(TOA) = 140/118 = 1.16$, and for $\lambda = 0.5$ μm: $C_s(S)/C_s(TOA) = 45/18 = 2.5$, which points to an excess absorption by clouds in the visible. Since the object of the study was very extended horizontally homogeneous stratified cloudiness (it should be reminded that an element of the sub-grid climatological analysis is 250 × 250 km^2), the results of local aircraft soundings of the atmosphere could be used to assess the radiative forcing of clouds in the layer up to 8.4 km. The same estimates for more clean clouds over the Black Sea at the sun elevation 53° gave values $f_s = C_s(S)/C_s(TOA) = 1.11$ and 1.18, respectively. The radiation measurements performed on clear and cloudy days over the industrial town of Rustavi (Georgia) enabled one to estimate the ratio $C_s(S)/C_s(TOA)$ at 1.07 from the data of pyranometric measurements and 1.33 for $\lambda = 0.5$ μm.

Complex measurements carried out under the GAAREX program over Zaporozhye at sun elevation of 50°, and outside the city (on the windward side) showed that the city intensified the SWR absorption by clouds over the city compared to conditions outside the city within 21 W/m^2 to 77 W/m^2 (depending on the optical thickness of clouds at the wavelength 0.5 μm varying from 16 to 38). Therefore the SWR absorption prevails over the cloud longwave cooling. The values of $C_s(S)/C_s(TOA)$ varied from 1.2 to 2.6, which reflects an intensifying effect of clouds and pollution aerosols on the SWR absorption. Analysis of the data of sounding of the cloudy atmosphere over the Ladoga Lake (sun elevation 26°, $\tau = 80$) gave $C_s(S)/C_s(TOA) = 1.13$ and 1.18 within the wavelength interval 0.5–1.8 μm and 1.8 for $\lambda = 0.5$ μm.

In case of high surface albedo (ice or snow) the $C_s(TOA)$ differences for clear and cloudy weather are small and therefore the relative errors in estimating the radiative flux divergence, cloud absorptance and the ratio $C_s(S)/C_s(TOA)$ can reach 60% and more. Thus, the estimates of the SWR absorption by clouds become unreliable.

Based on the use of measured values of spectral downward and upward radiation fluxes and asymptotic formulas of the theory of radiation transfer in clouds, the spectral dependencies of the coefficient of scattering σ and absorption κ for a polydisperse turbid medium have been retrieved. With the

use of analytical formulas the single scattering albedo $\omega_0 = \rho/(\rho + \kappa)$ and the imaginary part of the complex refraction index were estimated from the data of the aircraft soundings of the cloudy atmosphere mentioned above (*Kondratyev et al.*, 1996b).

The calculated values of ρ and κ agree with the measured values of the attenuation coefficients and cloud optical thickness. The results of calculations with account of multiple scattering (both molecular and on droplets) for $\rho = 30\ km^{-1}$ as well as with account of the mean aerosol absorption coefficient in the cloud ($0.08\ km^{-1}$) make it possible to explain the excess absorption of solar radiation by clouds in the spectral interval 0.4–0.7 μm by the effect of multiple scattering, which enhances aerosol and cloud droplet absorption (a certain contribution is, apparently, made by changing optical properties of dirty clouds). An excess SWR absorption by clouds in the visible occurs always, and the presence of aerosol in clouds enhances this effect depending on its scattering and absorbing properties (ρ and κ) and on the place of its location: between droplets (interstitial aerosol), inside them, or on the surface.

4. Further discussion

The results published by *Cess et al.* (1995) and *Ramanathan et al.* (1995) have stimulated a rather hot discussion concerning the reality of "excess absorption". The viewpoints supported by the results of both observations and numerical modeling varied from completely negative (clouds do not absorb solar radiation) to partly supportive and to fully recognizing the significance of cloud absorption of shortwave radiation.

For instance, *Stephens* (1996) has pointed out that "current understanding predicts that absorption of solar radiation by the entire atmospheric column containing clouds is only slightly enhanced over absorption by an equivalent clear sky column" and emphasized that "...this absorption occurs in place of rather than in addition to clear sky absorption".

In their reply *Cess* and *Zhang* (1996) have emphasized again that "differences between the current observations and models...are large and constitute a signal in excess of uncertainties associated with the measurements...the model's clouds are underpredicting cloud SW absorption by overestimating cloud-sky surface insolation relative to clear sky; we see no other plausible explanation".

Pilewskie and *Valero* (1996) have pointed out in their reply that they found several errors in Stephens' arguments and made relevant comments. Pilewskie and Valero have correctly noted, for instance, that only some cloud absorption occurs in place of clear sky absorption. They have substantiated the reliability of their observations.

Let us dwell now upon a number of recent publications discussing both observation and numerical modeling results.

Hayasaka et al. (1995) conducted simultaneous observations of upward and downward total shortwave radiation fluxes below and above stratocumulus clouds in the western Pacific with the help of two aircraft equipped with pyranometers. The results of observations compared with Monte Carlo calculations show that as a result of horizontal inhomogeneity of cloud cover and respective divergence or convergence of radiation fluxes an additional absorption seemed existing which actually did not exist. Relevant corrections to remove the influence of horizontal inhomogeneity has been suggested resulting in complete coincidence of measured and calculated (for horizontally homogeneous cloud layer) absorption values. It may be concluded that, in fact, excess absorption of shortwave radiation by clouds does not exist in reality. It has been pointed also out by *Hayasaka et al.* (1995) that observed variations of cloud droplet size distribution do not influence shortwave radiation absorption by clouds.

Pinkus et al. (*Abstracts..*, 1996) have accomplished aircraft observations (the University of Washington's C-131A cloud physics aircraft) with the help of the Cloud Absorption Radiometer (CAR) which measures the distribution of radiation at 13 wavelengths in the visible and near-infrared region as a function of zenith angle in a plane perpendicular to the aircraft flight track. The measured radiance distribution and *in situ* measurements of the droplet size distribution have been analysed using radiative transfer theory for optically thick clouds to determine the spectrally dependent optical thickness, similarity parameter, and single scattering albedo of the cloud droplets and water vapor. Cloud horizontal inhomogeneity has been taken into account.

O'Hirok and *Gautier* (*Abstracts..*, 1996) have demonstrated through model calculations that specific spatial distribution of solar radiation due to the effects of 3-D cloud structure acts to enhance atmospheric absorption. Monte-Carlo calculations have indicated that the plane-parallel assumption used in radiative transfer models contributes significantly to the discrepancy between measurements and theoretical estimates and that the exclusion of 3-D effects in standard radiative transfer models may be a partial explanation for enhanced absorption. The assessments of an impact of cloud cover spatial inhomogeneity on radiative transfer have also been made by *Kinne et al.* (*Abstracts..*, 1996) and *Georgdzhaev et al.* (*Abstracts..*, 1996) who accomplished Monte-Carlo simulations as well as by *Zuidema* and *Evans* (*Abstracts..*, 1996) who applied a stochastic radiative transfer approach.

New approaches to 3-D radiative transfer calculations have been recently suggested, including the spherical harmonic discrete ordinate method (*Evans*: *Abstracts..*, 1996) and the Lattice-Boltzmann method (*Caudill* and *Mozer*: *Abstracts..*, 1996).

Using a Monte-Carlo technique, *Batey* and *Harshvardhan* (*Abstracts..*, 1996) have studied the radiative properties of inhomogeneous cloud fields for typical near-infrared conditions. The results of calculations indicate that an in-

homogeneous cloud field is less absorbing as well as less reflecting when compared to the corresponding field having the same optical depth.

Várnai and *Davies* (*Abstracts..*, 1996) have undertaken an effort to establish a theoretical framework which allows to define and calculate the various processes through which cloud inhomogeneities influence solar radiation. Using satellite information on irregular cloud fields they have shown that even for overhead sun, the dominant 3-D effects of decreasing the albedo takes place which often results not from the flow of radiation from thick to thin areas (where photons can pass through the cloud layer more easily), but rather, from thin to thick areas. This is why counter-intuitive phenomena arise such as that both spatial averaging and the addition of an underlying plan-parallel cloud can strengthen 3-D radiative effects in decreasing cloud albedo, even if the sun is overhead and if no absorption occurs. The numerical modeling indicates that radiative properties change significantly if the horizontal optical thickness variations which are observed from satellites are attributed not to variations in the volume extinction coefficient (like it was done before), but to variations in geometrical cloud thickness (which is probably a more realistic attribution for many cumulus cloud fields).

Presence of low level stratocumulus clouds is a case of inhomogeneities in microphysical and radiative properties over a wide range of scales. *Taylor* and *Hignett* (*Abstracts..*, 1996) have used aircraft observations for such a case off the coast of Namibia to constrain 3-D Monte-Carlo model calculations of the reflectance of the cloud field through relevant intercomparison. The results obtained show a significant negative albedo bias when the inhomogeneous cloud is compared to a plan-parallel cloud with the same average liquid water content.

Liou et al. (*Abstracts..*, 1996) have applied 3-D inhomogeneous radiative transfer program based on successive-order-of scattering approach to study the effects of cirrus cloud geometry and inhomogeneity on the spectral reflection and absorption.

Absorption of solar radiation by optically thin clouds over highly reflective surface has been investigated by *Otterman* and *Fraser* (*Abstracts..*, 1996). The absorption of solar radiation by clouds, surface and gaseous atmosphere has been expressed as an explicit function of the cloud-absorption, fraction a_0 of the downleg flux and a_r of the upleg (surface-reflected) flux, cloud-backscattering, fraction b_0 of the downleg and b_r of the upleg, gaseous absorption and the surface spectral albedo A. It has been shown that in the explicit expression for R (the ratio of CF at the surface to that at the TOA) the parameter a_0 appears only in a ratio a_0/b_0 which both increase with the solar zenith angle Θ. Since the b_0 increase is stronger than that of a_0 (in case of b_0 an additional contribution of an enhancement of backscattering with Θ is substantial), at large Θ the value of R tends to be close to 1.0 for zero surface albedo A, and changes only slowly with A. In case of $\Theta = 0$ (the sun near the zenith) the upleg absorption is, by a factor of at least 2.0, higher than that of the downleg. *Otterman* and

Faser have emphasized that the factor of more the 3.0 by which the combined downleg and upleg absorption exceeds the absorption for a dark surface (sun near the zenith) may explain, to some extent at least, the anomalous cloud absorption. Since for many surfaces spectral albedo in the infrared is high, the use of albedo averaged over the solar spectrum can result in an erroneous assessment of the cloud absorption.

The reflection and transmission properties of spatially inhomogeneous water-cloud fields above a dark surface have been simulated by *Macke et al.* (*Abstracts..*, 1996) by means of a Monte-Carlo radiative transfer program. A three-dimensional broken cloud field was constructed by applying a cellular automation model for cloud formation.

Francis et al. (*Abstracts..*, 1996) have analysed aircraft measurements from the C-130 aircraft of the broadband and narrow-band radiation fields in and around different cloud types. These observation were made over a number of years in several different locations around the globe. An attempt to identify "enhanced" absorption as a result of increased condensed-phase water absorption in the infrared has not been successful. Therefore it has been concluded that the observational results "...can be explained much better, both qualitatively and quantitatively, by current accepted theory".

In this context *Li* (*Abstracts..*, 1996) has pointed out that contrary to some recent claims of cloud absorption anomaly, the systematic discrepancy is attributed primarily to the treatment of clear-sky radiative processes including the negligence of aerosol and the use of dated schemes for computing water vapor absorption. After assessing various estimates, Li has come to the conclusion that the following disposition of solar energy appears to best represent our current knowledge: 30% reflection to space, 25% absorption in the atmosphere and 45% at the surface on a global and annual mean basis. *Long* and *Ackerman* (*Abstracts..*, 1996) also believe (on the basis of the observational data for the tropical western Pacific warm pool) that the proposed anomalous SW cloud absorption does not exist. The same conclusion has been made by *Davis et al.* (*Abstracts..*, 1996) who have emphasized the significance of cloud horizontal inhomogeneity and relevant horizontal radiative fluxes for the interpretation of atmospheric absorption data in presence of clouds.

One more suggestion has been made by *Chen* and *Lu* (*Abstracts..*, 1996) who discussed a possibility of an impact due to the neglect of the variation of water refractive index with temperature.

Crisp and *Zuffada* (*Abstracts..*, 1996) used a sophisticated atmospheric radiative transfer model to compute solar fluxes and heating rates for clear sky and cloudy conditions (line-by-line approach was applied for molecular absorption calculations; non spherical water, ice and aerosol particles were taken into account; multilevel, multistream, discrete ordinate algorithm was used to solve the equation of radiative transfer). The results of calculations indicate that the model accounts for a large fraction of the anomalous

absorption. For example, a standard, mid-latitude summer model atmosphere with a single, horizontally uniform, stratocumulus cloud absorbs 20 to 30 W/m^2 more sunlight at altitudes within the cloud (1 to 1.5 km) than the associated clearsky case. However, the cloudy atmosphere absorbs about 12 W/m^2 less than the clear atmosphere at altitudes below the cloud base because the cloud reduces the amount of solar radiation available at these levels. Water vapor absorption above the cloud base account for most of the additional flux divergence associated with the cloud. This contribution to anomalous absorption is proportional to the water vapor abundance and the photon path lengths within the cloud, and inversely proportional to the solar zenith angle. Crisp and Zuffada have emphasized a necessity to also consider other factors of anomalous absorption, such as horizontal inhomogeneity of cloud abundance.

Line-by-line adding-doubling computations of solar radiation absorption by clouds made by *Ramanathan* and *Freidenreich* (*Abstracts..,* 1996) were made to assess the relative roles of water vapor and clouds.

An important field study of radiative effects of tropical clouds (convection in the tropical Pacific) has been accomplished by *Collins et al.* (1996) within the program of the Central Equatorial Pacific Experiment (CEPEX) from November 1992 to February 1993. Radiation fluxes at the tropopause level were measured from ER-2 aircraft between 18 and 20 km. The ship R/V "John Vickers" and Lockheed P-3 turboprop aircraft were used to measure surface fluxes. Calculations of radiative forcings indicate that at the tropopause SW and LW forcings are nearly equal and opposite, even on daily time-scales. Therefore the net effect of an ensemble of convective clouds is small compared to other radiative terms in the surface–troposphere heat budget. The heat budget at the tropopause is determined primarily by the sum of the clear sky SW and LW fluxes, and during the CEPEX observing period the net clear sky flux across the tropopause was approximately 120 W/m^2. At the surface the net effect of clouds is to reduce the radiant energy absorbed by the ocean. Under deep convective clouds the diurnally averaged reduction exceeds 150 W/m^2. Calculations of the flux divergence in the cloudy atmosphere indicate that the atmospheric cloud forcing is nearly equal and opposite to the surface cloud forcing. Being dependent on the frequency of convection, the atmospheric forcing approaching 100 W/m^2 was observed when the surface temperature was 303K. During the CEPEX period the surface net radiative cooling due to SW forcing increased at a rate of 22 W/m^2 K.

Taylor et al. (1996) made in situ observations of SW radiation fluxes from the UK Met. Office C–130 aircraft (three cases of clear sky and four cases where a liquid-water boundary-layer cloud was present). A comparison with calculations (a new two stream radiative-transfer formulation) has revealed in case of clearsky an agreement within 3%. In the cloudy cases the albedo and transmittance agree within $\pm$ 0.1 but the absorption in the model is higher than that observed, sometimes by a factor of two. *Taylor et al.* (1996) have

concluded that there is no evidence of anomalous absorption in the observations. The observed absorptions do not exceed 6% for the stratocumulus cases considered. It is important, however, to take into account cloud spatial inhomogeneity.

To continue a discussion of "balance of evidence" one has to point out (in the contradiction with the results just mentioned) conclusions made by *Ward* (1995) on the basis of a comparison of the monthly mean SW radiation budget (SRB) obtained from the World Climate Research Programme (WCRP) shortwave global dataset with that simulated by the National Center for Atmospheric Research Community Climate Model version 2.0 (CCM2). Large differences were found in monthly mean surface solar fluxes, the largest discrepancies being in the summer mid-latitude regions where CCM2 overestimates surface SW radiation fluxes relative to retrieved from satellite data by as much as 100 W/m^2. *Ward* (1995) believes that most of the differences are associated with deficiencies in CCM2's prediction of cloud optical properties and cloud amount. However significant differences also occur in clearsky fluxes and surface albedo. CCM2 was found to have larger clearsky surface insolation than retrieved from satellite data over nearly all land areas by more than 60 W/m^2 in some locations.

There are still a few examples of a combined analysis of simultaneous surface and satellite radiation budget data which allow to obtain information on atmospheric radiation budget and its components. In this context *Yamanouchi* and *Charlock* (1995) have considered such kind of data for the Antarctic with the main purpose to assess cloud radiative effects. Radiative fluxes at the top of the atmosphere (TOA) and the surface were compared at two Antarctic stations, Syowa and the South Pole, using Earth Radiation Budget Experiment (ERBE) data and surface observations for the time period from February 1987 to January 1988. Cloud amounts were derived from surface synoptic observations.

Throughout the year over the snow and ice covered Antarctic cloud radiation impact consisted in heating the surface and cooling the atmosphere. Cloud longwave (LW) effects were greater than cloud shortwave (SW) effects. Clouds have a negligible effect on the absorption of SW by the atmosphere in the interior and clouds slightly increase the absorption of SW by the atmosphere along the coast. The atmospheric SW heating due to Antarctic clouds is much smaller than the 25–40 W/m^2 SW cloud forcing which was inferred for other latitudes. At the TOA, the LW cloud effect was heating along the coast in summer and winter, heating in the interior during summer, and slight cooling in the interior during winter. This unique TOA cloud LW cooling was due to the extremely low surface temperature in the interior during winter. At the TOA, clouds induced SW cooling in the interior and along the coast. The comparison of the monthly averaged fluxes has shown that the atmospheric column loses net radiation energy through the year with an asymmetrical

seasonal variation. The largest cooling for the atmospheric column, about 140 and 125 W/m^2, appears in May at Syowa and in April at the South Pole, respectively. The loss of net radiation energy by the atmosphere is much larger than the loss by the surface.

A very important study has been accomplished by *Evans* and *Puckrin* (1996) who made spectral measurements of the solar flux in the near-infrared region (3,000–10,000 cm^{-1}) using FTIR spectrometer under clear and overcast sky conditions. These results also yielded information concerning the absorption of direct solar radiation by clouds. A comparison of the spectra of solar fluxes for clear and overcast sky measured from the ground for a northern mid-latitude location (Nova Scotia, Canada: 43.8°N; 66.2°W) in August and September 1995 indicates that about 118 W/m^2 of the solar radiation is absorbed preferentially by clouds in the spectral region mentioned. The cloud RF ratio was estimated to be 1.24. *Evans* and *Puckrin* (1996) believe that the absorption by cloud liquid water may contribute, in part, to the anomalous cloud absorption effect.

Summarizing some of the results discussed above and their own results of processing a four-year global record of solar flux observed from both space and the Earth's surface *Li et al.* (1995) have pointed out that f_s values are highly variable in the tropics with a median of about 1.1, and consistently less than 1.0 in polar regions. They have proposed that "large values and high variations of f_s may be related to the presence of absorbing aerosols and the uncertainties in both the observed and inferred solar flux data used here. Therefore, a substantial revision of our understanding of cloud absorption and its impact on the atmosphere's energy budget may not, after all, prove to be necessary if the effects of absorbing aerosols are properly incorporated" (unfortunately, like *Cess et al.* (1995), *Ramanathan et al.* (1995), *Li et al.* (1995) and some others have failed to refer to older publications on this subject by *Kondratyev* (1972, 1988a, b, etc.) as well as by *Kondratyev et al.* (1976, 1983), *Kondratyev* and *Binenko* (1984, etc.)).

The assumption made by *Li et al.* (1995) that $f_s > 1$ due to the impact of absorbing aerosol is based on the facts that in the tropics strong absorbing aerosols produced by biomass burning could play an important role, whereas in mid-latitudes maximum f_s values were obtained near Hamburg and the Rhine Valley i.e. in heavily polluted areas. In all cases for a sizable fraction of months $f_s < 1$ which may be the influence of cirrus clouds (backscattering by cirrus clouds leads to a reduction of absorption by aerosols located below the clouds). *Li et al.* (1995) have pointed out that although the observed variation of f_s has been explained by changes in solar zenith angle and aerosol effects, the potential dependence of f_s on cloud structure (morphology) also deserves examination. They conclude that their study "...does not rule out the existence of the cloud absorption anomaly, but rather indicates that its magnitude (if it exists) on a global scale may not be as large as suggested in some recent reports".

In a later study *Li* and *Moreau* (1996) have investigated two parameters employed in recent attempts to address cloud absorption anomaly: the ratio R discussed above and the slope s, of the regressional relationship between TOA albedo and atmospheric transmittance. Li and Moreau have emphasized that neither R nor s is a direct measure of cloud absorption: they both are sensitive to many factors, especially cloud height and surface condition. In spite of that, R can indicate the effect of clouds on the atmospheric absorption of solar radiation, if the clearsky conditions remain the same. However, modeled R exceeds 1.25, and modeled s is generally less than –0.7, except for bright surfaces. Observational values of R and s from the Earth Radiation Budget Experiment (ERBE) and the Global Surface Energy Balance Archive (GEBA) (four years worth of monthly mean data) demonstrate that R is highly variable with both location and season and also shows strong interannual variations. Low to moderate values of R tend to occur over relatively clean areas, while large R values appear to be associated with heavy pollution in the mid-latitudes or frequent occurrence of biomass burning in the tropics. The overall value of R obtained with the use of various approaches is about 1.1, which is in good agreement with model calculations. In general, $R < 1$ and > 1 over the polar and tropical regions, respectively. Thus, polar and tropical clouds have opposing effects on total atmospheric absorption, while midlatitude clouds have relatively little impact on absorption. *Li* and *Moreau* (1996) have pointed out, however, that large R values for the tropical areas are less reliable than the moderate values for midlatitude areas. *Li* and *Moreau* (1996) have repeated their earlier conclusion that their study does not rule out cloud absorption anomaly, but indicate, however, that its magnitude (if it exists) is not as large, and its occurrence is not as widespread, as suggested in some recent studies. In the most recent papers *Li et al.* (1997) have come to the conclusion that the difference between model calculations and observations is primarily due to deficiencies in clearsky calculations: the use of dated schemes for water vapor absorption and the neglect of absorbing aerosols.

Arking (1996) and *Arking et al.* (1996) have confirmed the conclusion that the present-day global climate models underestimate the amount of solar energy absorbed by the atmosphere within the range of up to 25–30 W/m^2 but suggested quite different explanation of this facts. *Arking* (1996) has found on the basis of both observations and models that clouds have little (~ 5 W/m^2) or no effect on atmosphere absorption. Therefore his conclusion is that "water is the dominant influence on atmospheric absorption, and improvements in our models lie in improving the parameterization of water vapor absorption and, perhaps discovering of additional absorption in the clear atmosphere".

Chou et al. (1995) have pointed out in this context that for the ratio of cloud forcing at the surface to that at the top of the atmosphere to reach 1.5, cloud specific absorption would be required to increase by a factor of about 40 beyond what has been determined by in situ aircraft measurements.

The discussion on the nature of excess absorption of solar radiation by clouds still continues and has resulted (as we have already seen) in controversial judgments. It is obvious that further theoretical and, first of all, complex field studies are necessary with specific emphasis on 3-D inhomogeneity of cloud cover and cloud optical properties (it should be also reminded that even an old problem of IR continuum absorption by water vapor has not been solved as yet). New efforts in this direction have been started within the ARM (Atmospheric Radiation Measurement) Programme (*Wiscombe*, 1995).

5. Aerosol impact on atmospheric absorption of solar radiation

At the end of the 1940s V. Kastrov from the Central Aerological Observatory (Moscow) started his long-term pyranometric observations of SWR fluxes in the free atmosphere under various conditions over the European part of the former USSR territory (see *Kondratyev*, 1956, 1969). The most important result was the discovery that atmospheric aerosol absorption of solar radiation is close, by its magnitude, to water vapor absorption. Later on balloon and aircraft observations within CAENEX and GAREX Programmes were conducted which confirmed Kastrov's results (*Kondratyev*, 1972; *Kondratyev et al.*, 1976; *Kondratyev* and *Binenko*, 1984). Of special significance were aircraft spectral measurements of SWR fluxes under clear sky and overcast cloudiness conditions with simultaneous measurements of aerosols and clouds properties (aerosol counters and filters were used which allowed to obtain information on not only number concentration and size distribution of aerosol and cloud particles, but also their chemical composition and hence-optical properties).

Aircraft measurements made in the former USSR (European territory, Central Asia, The Arctic, Kamchatka and Chukotka) as well as over the tropical Atlantic confirmed the principal result mentioned above: aerosol absorption of solar radiation is always significant and on the average, is approximately equal to absorption by water vapor. Observations in the presence of overcast (horizontally homogeneous) cloud cover in polluted atmosphere of industrial regions revealed the existence of exceedingly strong SWR absorption by dirty clouds (see also *Chýlek* and *Wong*, 1995; *Stephens*, 1994).

It is quite clear, thus, that in the context of the problem discussed, aerosol impact on atmospheric absorption of solar radiation requires serious attention (*Kondratyev*, 1996). This conclusion has been recently confirmed by *Li* (1997) and *Li et al.* (1997).

6. Conclusions

The basic conclusion is simple and obvious: our knowledge of radiation transfer in the real atmosphere is far from being adequate: there is neither "anomalous" not "excess" absorption of solar radiation. The reality is such that there are several processes which may be responsible for the disagreement between observed and modeled redistribution of absorbed SWR between the atmosphere and the surface, including:

- multiple scattering in clouds with absorbing droplets (they never consist of pure water) which leads to the enhancement of cloud absorption;
- specific features of radiation transfer in a 3-D inhomogeneous medium (broken clouds);
- unknown contribution by water vapor (besides that is known);
- peculiarities of radiation transfer in clouds consisting of a mixture of water droplets and aerosol particles;
- absorbtion of aerosols of various origin.

Last but not least, the reliability of observations should be further assessed. The necessary improvement of radiation parameterization in climate will become possible only on such a basis. Important steps forward are *"A Plan for Research Program on Aerosol Radiative Forcing and Climate Change"* (1996), the CERES Programme (*Wielicki et al.*, 1996) as well as the intercomparisons between numerical modeling results and observations like it has been recently done by *Ellingson* and *Wiscombe* (1996), *Rossow* and *Zhang* (1995), *Salathé* and *Smith* (1996).

References

Abstracts, 1996: *International Radiation Symposium*. The University of Alaska. Fairbanks, August 19-24.

A Plan for Research Program on Aerosol Radiative Forcing and Climate Change, 1996: National Academy Press, Washington, DC.

Arking, A., 1991: The radiative effects of clouds and their impact on climate *Bull. Amer. Meteorol. Soc. 71*, 795-813.

Arking, A., 1996: Absorption of solar energy in the atmosphere: discrepancy between a model and observations, *Science 273*, 779-782.

Arking, A., Chou, M.-D. and *Ridgway, W. L.*, 1996: On estimating the effects of clouds on atmospheric absorption based on flux observations above and below cloud level. *Geophys. Res. Lett.* (in print).

Borisenkov, E. P. and *Kondratyev, K. Ya.*, 1988: *Carbon Dioxide and Climate*. Gidrometeoizdat, Leningrad.

Cess, R.D., Zhang, M.H., Minnis, P., Corsetti, L., Dutton, E.G., Forgan, B.W., Garber, D.P., Gates, W.L., Hack, S.S., Harrison, E.E., Jing, X., Kiehl, J.P., Long, C.N., Morcrette, J.J., Potter, G.L., Ramanathan, V., Subasilar, B., Whitelock, C.K., Young, D.F. and *Zhou, Y.*, 1995: Absorption of solar radiation by clouds: observations versus models. *Science 267*, 496-499.

Cess, R.D. and *Zhang, M.H.*, 1996: Response. *Science 271*, 133-134.

Chou, M.-D., Arking, A., Offerman, J. and *Ridgway, W.L.*, 1995: The effect of clouds on atmospheric absorption of solar radiation. *Geophys. Res. Lett., 22*, 1885-1888.

Chýlek, P. and *Wong, J.*, 1995: Effect of absorbing aerosol on global radiation budget. *Geophys. Res. Lett. 22*, 929-931.

Collins, W.D., Valero, F.P.J., Flatou, P.J., Lubin, D., Grassl, H. and *Pilewskie, P.*, 1996: Radiative effects of convection in the tropical Pacific. *J. Geophys. Res. 101*, 14999-15012.

Crutzen, P.S. and *Ramanathan, V.* (eds.), 1996: *Cloud, Chemistry and Climate.* Springer-Verlag, Berlin.

Ellingson, R.G. and *Wiscombe, W.J.*, 1996: The Spectral Radiance Experiment (SPECTRE): Project description and sample results. *Bull. Amer. Meteorol. Soc. 77*, 1967-1985.

Evans, W.F.J. and *Puckrin E.*, 1996: Near-infrared spectral measurements of liquid water absorption by clouds. *Geophys. Res. Letters 23*, 1941-1944.

Hayasaka, T., Kikuchi, N. and *Tanaka, M.*, 1995: Absorption of solar radiation by stratocumulus clouds: aircraft measurements and theoretical calculations. *J. Appl. Meteorol. 34*, 1042-1055.

Kiehl, J.T. and *Briegleb, B.P.*, 1993: The relative roles of sulfate aerosols and greenhouse gases in climate forcing. *Science 260*, 311-313.

Kiehl, J.T., Hack, J.J. and *Briegleb, B.P.*, 1994: The simulated Earth radiation budget of the National Center for Atmospheric Research community climate model CCM2 and comparisons with the Earth Radiative Budget Experiment (ERBE). *J. Geophys. Res. 99*, 20815-20827.

Kondratyev, K. Ya., 1956: *Actinometry* (in Russian). Gidrometeoizdat, Leningrad.

Kondratyev, K. Ya., 1969: *Radiation in the Atmosphere.* Academic Press, New York.

Kondratyev, K. Ya., 1972: *Complex Atmospheric Energetics Experiment (CAENEX)*, GARP Publ. Ser. 12, WMO, Geneva.

Kondratyev, K. Ya., 1988a: *Earth's Radiation Budget, Aerosols, and Clouds* (in Russian). Progress in Science and Technol., 10, VINITI, Moscow.

Kondratyev, K. Ya., 1988b: *Climate Shocks: Natural and Anthropogenic.* Wiley & Sons, New York.

Kondratyev, K. Ya., 1992: *Global Climate* (in Russian). Nauka Publ., St. Petersburg.

Kondratyev, K. Ya., 1996: Aerosol climate impact in the context of global climate change. *Időjárás 100*, 1-12.

Kondratyev, K. Ya., Barteneva, O.D., Chapursky, L.I., Chernenko, A.P., Grishechkin, V.S., Ivanov, V.A., Korzov, V.L., Lipatov, V.B., Prokofyev, M.A., Tolkachev, M.K., Vasilyev, O.B. and *Zvalev, V.F.*, 1976: Aerosol in the GATE area and its radiative properties. *Atmospheric Sci. Paper 247.* Colorado State Univ., Fort Collins, Co.

Kondratyev, K.Ya., and *Binenko, V.I.*, 1984: *Impact of Clouds on Radiation and Climate* (in Russian). Gidrometeoizdat, Leningrad.

Kondratyev, K.Ya., Binenko, V.L. and *Melnikova, I.N.*, 1996b: *On excessive absorption of solar radiation by clouds in the visible* (in Russian). Doklady Russian Acad. Sci. (in print).

Kondratyev, K. Ya., Moskalenko, N.I. and *Pozdnyakov, D.V.*, 1983: *Atmospheric Aerosols* (in Russian). Gidrometeoizdat, Leningrad.

Li, Z., Bakker, H.W. and *Moreau, L.*, 1995: The variable effects of clouds on atmospheric absorption of solar radiation. *Nature 376*, 486-490.

Li, Z. and *Moreau, L.*, 1996: Alteration of atmospheric solar absorption by clouds: simulation and observations. *J. Appl. Meteorol. 35*, 653-670.

Li, Z., 1997: Influence of absorbing aerosols on the influence of surface solar radiation budget. *J. Climate* (in print).

Li, Z., Moreau, L. and *Arking, A.*, 1997: On solar energy disposition: a perspective from observation and modeling. *Bull. Amer. Meteorol. Soc.* (in print).

Ma, C.-C., Mechoso, C.R., Robertson, A.W. and *Arakawa, A.*, 1996: Peruvian stratus clouds and the tropical Pacific circulation: a coupled ocean-atmosphere GCM study. *J. Climate 9*, 1635-1645.

Marchuk, G.I., Kondratyev, K. Ya., Kozoderov, V.V. and *Khvorostyanov, V.I.*, 1986: *Clouds and Climate.* Gidrometeoizdat, Leningrad.

Pilewskie, P. and *Valero, F.P.J.*, 1995: Direct observations of excess solar absorption by clouds. *Science 267*, 5197, 1626-1629.

Pilewskie, P. and *Valero, F.P.J.*, 1996: Response. *Science 271*, 1134-1136.

Ramanathan, V., Subasilar, B., Zhang, G.J., Conant, W., Cess, R.D., Kiehl, J.D., Grassl, H. and *Shi, L.*, 1995: Warm pool heat budget and shortwave cloud forcing: a missing physics? *Science 267*, 499-503.

Ramanathan, V., Valero, F.P.J. and *Cess, R.D.*, 1996: Excess solar absorption in cloudy atmospheres. *GEWEX News 6*, 6-7.

Rossow, W.B. and *Zhang, Y.-C.*, 1995: Calculation of surface and top atmospheric radiative fluxes from physical quantities based on ISCCP data sets II. *J. Geophys. Res. 100* , 1167-1197.

Ridout, J.A. and *Rosmond, T.E.*, 1996: Global Modeling of cloud radiation effects using ISCCP cloud data. *J. Climate 9*, 1479-1496.

Salathé, E.P. Jr. and *Smith, R.B.*, 1996: Comparison of 6.7 μm radiances computed from aircraft soundings and observed from GOES. *J. Geophys. Res. 101*, 21303-21310.

Stephens, G.L., Paltridge, G.W. and *Platt C.M.R.*, 1978: Radiation profiles in extended water clouds. III: Observations. *J. Atmos. Sci. 35*, 2133-2141.

Stephens, G.L. and *Tsay, S.C.*, 1990: On the cloud absorption anomaly. *Quart. J. Roy. Meteorol. Soc. 116*, 671-704.

Stephens, G.L., 1994: Dirty clouds and global cooling. *Nature 370*, 420.

Stephens, G.L., 1996: How much solar radiation do clouds absorb? *Science, 271*, 1131-1133.

Taylor, J.P., Edwards, J.M., Glew, M.D., Hignett, P. and *Slingo, A.*, 1996: Studies with a flexible new radiation code II: Comparison with aircraft short-wave observations. *Quart. J. Roy. Meteorol. Soc. 122*, 839-361.

Ward, D.M., 1995: Comparison of the surface solar radiation budget derived from satellite data with the simulated by the NCAR CCM2. *J. Climate 8*, 2824-2842.

Wielicki, B.A., Bankstorm, B.R., Harrison E.F., Lee R.B. III, Smith G.L. and *Cooper J.E.*, 1996: Clouds and the Earth's Radiant Energy System (CERES): An Earth Observing System Experiment. *Bull. Amer. Meteorol. Soc. 77*, 853-868.

Wild, M., Ohmura, A., Gilgen, H. and *Roeckner, E.*, 1995: Validation of General Circulation Model radiative fluxes using surface observations. *J. Climate 8*, 1309-1324.

Wiscombe, W.J., 1995: An absorbing mystery. *Nature 376*, 466-467.

Yamanouchi, T. and *Charlock, T.P.*, 1995: Comparison of radiation budget at the TOA and surface in the Antarctic from ERBE and ground surface measurements. *J. Climate 8*, 3109-3120.

IDŐJÁRÁS

Quarterly Journal of the Hungarian Meteorological Service
Vol. 101, No. 2, April–June 1997, pp. 93–103

Meteorological journals — A scientometric approach

S. Zsindely[1] and **G. Major**[2]

[1]*Information Science and Scientometric Research Unit,*
Library of the Hungarian Academy of Sciences,
P.O. Box 1002, 1245-Budapest, Hungary

[2]*Hungarian Meteorological Service,*
P.O. Box 39, 1675-Budapest, Hungary; E-mail: gmajor@met.hu

(Manuscript received 15 January 1997; in final form 22 March 1997)

Abstract—A survey of meteorological journals registered in bibliographical databases is given in this paper. The brief historical review is followed by the publication characteristics: the number of articles published and the impact factors. The difference of journals edited by scientific societies and by profit-oriented publishing houses are shown from the point of view of the prestige, circulation and publication frequency of the journals in question.

Key-words: scientific journal, meteorological journal, bibliographic database, impact factor, demography of journals.

1. Introduction

It was about 300 years ago, when a French nobleman, Denis de Sallo, and nearly at the same time, the Secretary of the Royal Society in London, Henry Oldenburg, lost interest in writing and disseminating between his scholar friends the hundreds of letters related to the newest scientific discoveries. Instead of sending private letters with individual content to each addressee, they wrote only one per topic, which was multiplied by typographical means and the earliest scientific journals, the *Journal des Sçavans* (Paris) and the *Philosophical Transactions* (London) were born (1665): a new era began in the communication system of science (*Ziman*, 1969; *Brookes*, 1980). The scientific journal became the chief carrier, disseminator and preserver of scientific information.

During the years, the number of scientific journals has grown exponentially (*Price*, 1963). In the beginning the content of the journals had a more universal character, but with the development of modern scientific trends, more and more specialized journals appeared.

2. The scientific journals in meteorology

Modern meteorology began when the daily weather maps were developed as a device for weather analysis and forecasting, and the instruments (thermometer, barometer, hygrometer, pluviometer, anemometer) for measuring the most important parameters as well as the telegraph became wide-spread (*Fierro*, 1991).

In spite of the fact that descriptions of meteorological observations can be also found just among the articles published in the abovementioned incipient scientific journals, the first scientific journal serving exclusively the meteorology, the *Ephemerides Societatis Meterologicae Palatinae* appeared in Mannheim in 1781. The *Ephemerides* published meterological data measured by a European network of observing sites. Among these sites was Buda, the capital of the Kingdom of Hungary. The political troubles during and after the French Revolution destroyed this initiative, and the last issue of the *Ephemerides* appeared in 1795 containing the data measured in 1792.

After some attempts for nearly a century, it was only the time of the foundation of the first meteorological observatories when the first viable, regularly published scientific journals appeared in this discipline (*Quarterly Journal of the Royal Meteorological Society*, 1871–; *Annalen der Hydrographie und maritime Meteorologie*, 1873–1944), *Meteorologische Zeitschrift,* (1884–1944, 1948–).

The evolution of the scientific journals of meteorology has shown the same trend as in the case of other scientific journals. As an example let us look at *Időjárás* (the name means: weather). Its first issue appeared in April, 1897. It was a private journal founded by *Dr. Héjas* Endre, a meteorologist of the state meteorological service. His basic purposes were: to increase the meteorological knowledge as well as to help the development of the Hungarian meteorological language. In that time several misbeliefs were frequent about the weather phenomena and even about the climate and its possible modifications. For example it was argued against the regulation of rivers that it would decrease the precipitation. In 1925 the journal was taken over by the Hungarian Meteorological Society and became more scientific. In 1945 it became the official scientific journal of the Hungarian Meteorological Service. Besides the Hungarian ones, papers appeared in English, French, German and Russian as well. Since 1992 the only accepted language is English. The recent policy is to publish original scientific articles in any field of atmospheric sciences from authors of any nationality. Less than half of the papers is written by Hungarian authors, the larger part comes from all the five continents, mainly from Europe, Asia and Africa.

Nowadays scientific journals of this discipline (similarly to other fields of the science) are edited partly by learned societies and partly by profit-oriented publishing houses.

3. Meteorological journals in bibliographical databases

The titles and main data of several journals publishing articles and observed data of meteorological interest for the years 1994-1995 can be found in *Ulrich's International Periodicals Directory* (1994) under the headline "Meteorology". This compilation is, although not exhaustive, but impressive: it includes 466 journals from 58 countries (plus United Nations). Knowing the highly developed meteorological service of Japan, it is not surprising that 161 of the titles there stem from this country.

Besides the name of the periodical, the Directory registers the ISSN Number, the language(s) of the texts, the date of foundation, the editor's name, the address of the publisher, the names of abstract journals indexing the journal in question, the formerly used name(s), if any, amongst others.

Unfortunately, the title of *Időjárás* is missing, but two other Hungarian journals can be found in this chapter of the Directory. These are: *Acta Geographica ac Geologica et Meteorologica Debrecina* (rather geographical in nature, and with irregular publishing sequence) and *Acta Universitatis de Attila József Nominatae. Acta Climatologica*, which focuses on general climatology, bio- and agrometeorology. These periodicals publish those works of university professors or lecturers that are meteorological ones or strongly connected to the different applications of climatological data series.

It is supposed that any given population of periodicals follows, at least in part, the rules of human demography (*Zsindely* and *Schubert*, 1992). For illustrating the "age distribution" of the "still living" meteorological journals, an age-pyramid of the journals registered in *Ulrich's Directory* has been compiled for the years 1994 and 1995 (*Fig. 1*). This diagram depicts separately the journals edited by institutions (societies, institutes, observatories, etc.) and by profit-oriented publishing houses; it includes 284 meteorological journals with regular publication and known year of foundation.

From the figure it can be seen that the oldest, still edited journal containing meteorological information, the *Monthly Notices of the Royal Astronomical Society* (London), was first published in 1827. The profit oriented publication of meteorological journals began mainly after World War II.

The Science Citation Index (SCI) of the Institute of Scientific Information (ISI, Philadelphia, U.S.A.) processes 3430 journals in 160 subfields; the subfield of Meteorology and Atmospheric Sciences is represented by 33 titles in 1995. It is worth mentioning that the list of *Ulrich's Directory* and that of SCI do not overlap perfectly. The selection for the SCI is based, among others, on the average citation rate (impact factor) of the journal to be registered. SCI's journals for meteorology are compiled for the year 1994 in the rank order of their first year of publication in *Table 1*.

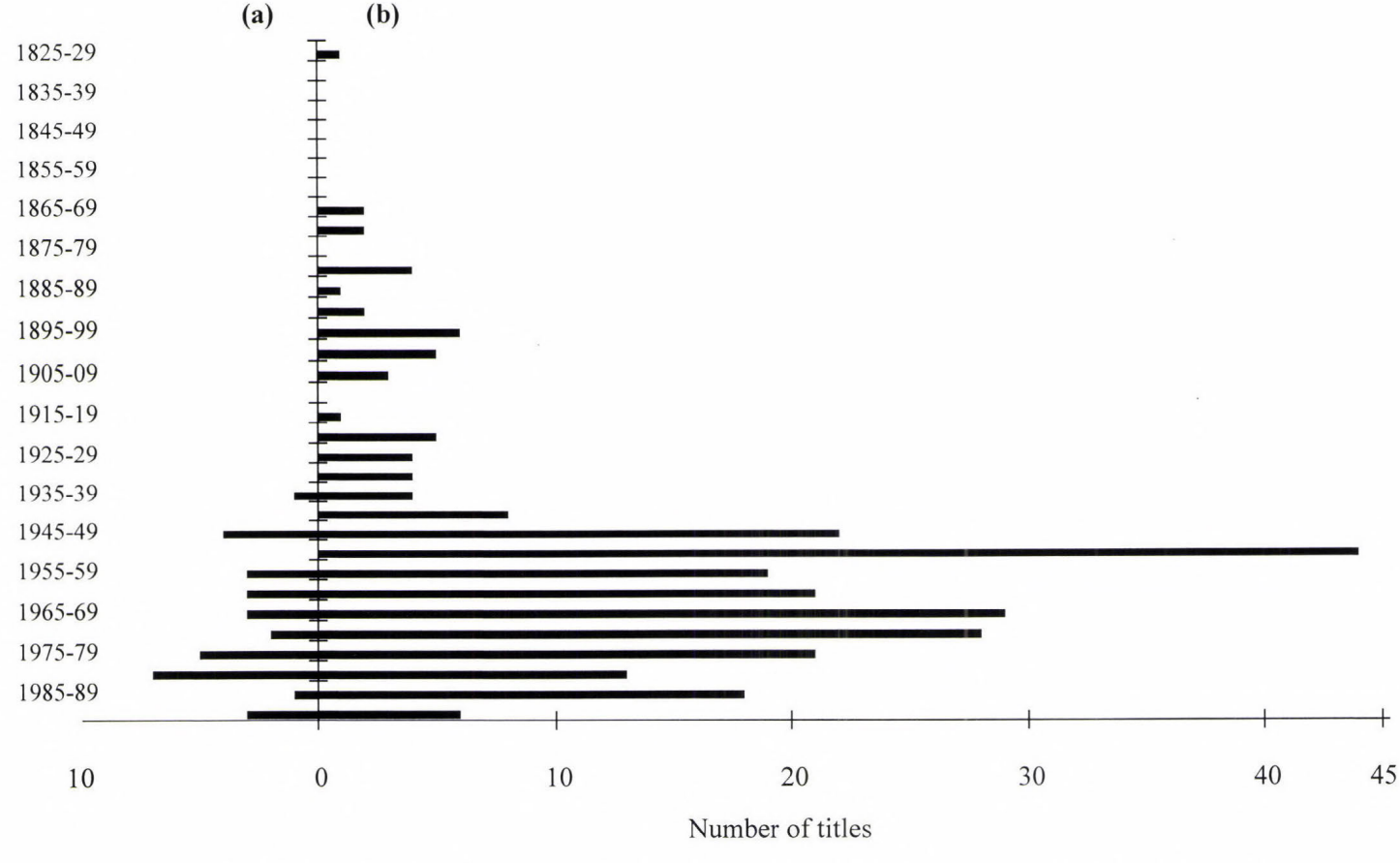

Fig. 1. Age-pyramid of journals registered in *Ulrich's Directory* for the subfield meteorology for 1994 and 1995; (*a*) journals published by publishing houses, (*b*) journals published by scientific societies and institutions.

Table 1. Meteorological journals registered in SCI in 1995

Title	First year of publication	Registration in SCI	Publisher
Q. J. Roy. Meteor. Soc.	1871	1975	Royal Meteor. Soc., Reading, Berkshire
Monthly Weather Review	1872	1975	American Meteorol. Soc., Boston
J. Meteor. Soc. Japan	1882	1982	Meteorological Soc. Japan, Tokyo
J. Geophys. Res. (Atmos.)	1896	1975	American Geophys. Union, Washington
J. Geophys. Res. (Space Ph.)	1896	1975	American Geophys. Union, Washington
Bull. Amer. Meteor. Soc.	1920	1975	American Meteorol. Society, Boston
J. Atmospheric Science	1944	1975	American Meteorol. Society, Boston
Meteor. Atmos. Physics	1949	1975	Springer Verlag, Vienna
Tellus A	1949	1975	Munksgaard Internat. Publ., Copenhagen
Tellus B	1949	1975	Munksgaard Internat. Publ., Copenhagen
Theor. Appl. Climatol.	1949	1987	Springer Verlag, Vienna
J. Atmos. Terr. Physics	1950	1975	Elsevier Science Ltd., Oxford
J. Air Waste Management	1951	1975	Air & Waste Manag. Assoc., Pittsburgh
Australian Meteor. Magazine	1952	1954	Australian Bureau of Meteor., Canberra
Int. J. Biometeorology	1957	1975	Springer Verlag, Berlin
J. Applied Meteorology	1962	1975	American Meteorol. Society, Boston
Atmosphere – Ocean	1963	1987	Canadian Meteorol. Oceanogr. Society
Agricultural Forest Meteor.	1964	1984	Elsevier Science B.V., Amsterdam
Izv. A. N. Fiz. Atmos. Ok.	1965	1980	Izdatelstva Nauka, Moscow
Atmospheric Environment	1967	1975	Elsevier Science Ltd., Oxford
Boundary-Layer Meteorology	1970	1981	Kluwer Scientific Publishers, Utrecht
J. Aerosol Science	1970	1981	ELsevier Science Ltd., Oxford
Climate Change	1977	1977	Kluwer Acad. Publishers, Dodrecht
Dynam. Atmos. Oceans	1977	1977	Elsevier Science B.V. Amsterdam
Advances in Space Research	1981	1993	Elsevier Science Ltd., Oxford
Int. J. Climatology	1981	1982	John Willey Ltd., Journals, Sussex
Annales Geophysicae	1983	1983	Springer Verlag, Heidelberg
J. Atmospheric Chemistry	1983	1984	Kluwer Acad. Publishers, Dodrecht
J. Atmos. Ocean Tech.	1984	1991	American Meteorol. Society, Boston
Climate Dynamics	1986	1992	Springer Verlag, Heidelberg
J. Climate	1986	1986	American Meteorol. Society, Boston
Wheather Forecast	1986	1992	American Meteorol. Society, Boston
Global Biogeochem. Cycl.	1987	1993	American Geophys. Union, Washington

4. The impact factor

From the very beginning of the scientific publication the recognition by the scientific community had been the reward for well done scientific research. This is reflected, inter alia, in the citation of the work in question by fellow researchers in their own publication. The SCI is built on the principle that there is some meaningful relationship between one paper and some other through citations, so a citation index can be constructed. The ISI publishes such an index in each year. On the basis of citation data of articles published in a given journal a so called "impact factor" can be calculated for the journal in question as a tool for evaluation. The impact factor is the measure of the frequency with which the "average cited article" in a journal has been cited by other articles in a particular year. The impact factor of a journal is basically a ratio between citations and citable items published. Thus the 1994 impact factor of a given journal would be calculated by dividing the number of all the SCI source journals' 1994 citations of articles of the given journal published in 1992 and 1993 by the total number of papers it published in 1992 and 1993 (*Garfield*, 1972).

Table 2 shows the rank order of the meteorological journals of ISI by average number of articles. In *Table 3* the annual impact factor for the years 1985–1994 is given. From the latter it can be deduced that the general average value of the impact factor for these meteorological journals is 1.02.

As it can be seen in Table 3, the highest average impact factor (3.989) was reached by *Journal of Geophysical Research*, which is not strictly a meteorological journal. One of the most renowned interdisciplinary journals, *Nature*, which publishes highly cited articles in the whole field of science, announced its impact factor by subfields separately for 1996. These data can be found in *Monthly Nature*, a (since then ceased) collection of the most interesting articles of the weekly *Nature*. It can be seen that the impact factor of *Nature*'s articles in the subfield of earth sciences is 14.01, substantially lower than the value calculated for all of the publications in *Nature* (25.5), but fourteen-times higher than the average impact factor for meteorological journals included in ISI's SCI. In our opinion this difference is not only due to the fact that the greater part of *Nature*'s articles about earth sciences does not deal with meteorology, but deals with more "fashionable" topics, e.g. space research. However, the few meteorological articles published in *Nature* are altogether certainly outstanding.

The values of the impact factor show some changes during the "life" of a given periodical. The changes are more pronounced if they are caused by some "demographical" events (i.e. "change of name", "multiplying by partition", etc). *Tables 4* and *5* give some examples for these phenomena in the "population" of meteorological journals. *Fig. 2* shows the consequences of such changes for the values of the impact factor of the journals in question.

Table 2. Rank order of journals by annual average number of articles (1985–1994) (*Journal Citation Report*)

Rank	Title	Average no. of articles
1	J. of Geophysical Research	961.1
2	J. of Geophysical Research – Solid Planets	431
3	Atmospheric Environment A – General	285
4	Atmospheric Environment	277
5	J. of Geophysical Research – Atmospheres	248.17
6	J. of Geophysical Research – Oceans	242
7	J. of Atmospheric Science	217.5
8	Monthly Weather Review	180.1
9	Izv. Akad. Nauk. Fizika Atmosfery i Okeana	129.22
10	J. of Climate and Applied Meteorology	126.3
11	J. of Air Pollution Control Association	122.6
12	J. of Atmospheric and Terrestrial Physics	121.4
13	J. of Applied Meteorology	121
14	J. of the Air and Waste Management Association	118.4
15	J. of Aerosol Science	105.3
16	J. of Climate	92
17	Boundary-Layer Meteorology	91.5
18	J. Atmos. Ocean Technology	90.25
19	Annales Geophysicae	85
20	Agricultural and Forest Meteorology	80.5
21	Annales Geophysicae B – Terr. Planet. Physics	68
22	J. of Meteorological Society of Japan	62.67
23	Quarterly J. of Royal Meteorological Society	61.2
24	Bull. of the American Meteorological Society	57.8
25	Int. J. of Climatology	55
26	Indian J. of Radio Space	54.78
27	Annales Geophysicae A – Upper Atm. Space Sci.	52
28	J. of Climatology	42.5
29	Theoretical and Applied Climatology	40
30	Atmospheric Environment B – Urban	39.5
31	J. of Atmospheric Chemistry	38.9
32	Climatic Change	38.7
33	Meteorology and Atmospheric Physics	38.67
34	Climate Dynamics	38.33
35	Meteorological Magazine	38.14
36	Tellus B	34
37	Tellus A	33
38	Int. J. of Biometeorology	32.4
39	Atmosphere – Ocean	26.67
40	Australian Meteorological Magazine	25
41	Wheather Forecast	22.5
42	Dynamics of Atmospheres and Oceans	18.5
43	Arch. for Meteorology, Geophys. and Bioclim. A	18
44	Arch. for Meteorology, Geophys. and Bioclim. B	16

Table 3. Rank order of journals by annual average impact factor (1985–1994) (*Journal Citation Report*)

Rank	Title	Average impact factor
1	J. of Geophysical Research	3.989
2	J. of Climate	2.712
3	Climate Dynamics	2.278
4	J. of Atmospheric Science	1.905
5	J. of Atmospheric Chemistry	1.874
6	Tellus B	1.860
7	Quarterly J. of Royal Meteorological Society	1.814
8	Bull. of the American Meteorological Society	1.795
9	Climatic Change	1.615
10	J. of Climatology	1.599
11	Monthly Weather Review	1.544
12	Atmospheric Environment	1.444
13	Atmospheric Environment A - General	1.240
14	Annales Geophysicae	1.200
15	Tellus A	1.191
16	J. of Climate and Applied Meteorology	1.188
17	J. of Geophysical Research - Atmospheres	1.096
18	J. of Atmos. Ocean Technology	1.066
19	Boundary-Layer Meteorology	1.020
20	J. of Atmospheric and Terrestrial Physics	1.006
21	Dynamics of Atmospheres and Oceans	0.895
22	J. of Applied Meteorology	0.888
23	Int. J. of Climatology	0.885
24	J. of Geophysical Research - Solid Planets	0.875
25	Atmosphere – Ocean	0.871
26	Agricultural and Forest Meteorology	0.835
27	J. of Air Pollution Control Association	0.831
28	J. of Geophysical Research - Oceans	0.790
29	J. of Aerosol Science	0.679
30	J. of the Air and Waste Management Association	0.675
31	J. of Meteorological Society of Japan	0.647
32	Atmospheric Environment B - Urban	0.571
33	Wheather Forecast	0.535
34	Meteorology and Atmospheric Physics	0.497
35	Int. J. of Biometeorology	0.337
36	Arch. for Meteorology, Geophys. and Bioclim. B	0.316
37	Theoretical and Applied Climatology	0.293
38	Australian Meteorological Magazine	0.273
39	Arch. for Meteorology, Geophys. and Biocklim. A	0.273
40	Izv. Akad. Nauk. Fizika Atmosfery i Okeana	0.223
41	Meteorological Magazine	0.220
42	Indian J. of Radio Space	0.089
	General average:	1.02

Table 4. Causes of changing names of meteorological journals

Cause	Original title	New title
Internationalization, extended readership	Journal of Climatology	International Journal of Cimatology (1990)
Change in scope	Journal of the Air Pollution Control Association	Journal of the Air and Waste Management Association (1990)
Focusing in scope (bipartition)	Journal of Climate and Applied Meteorology	Journal of Applied Meteorology (1989) Journal of Climate (1989)
Merging	Journal of Geophysical Research, – Atmospheres, – Oceans, – Solid Planets	Journal of Geophysical Research (1991)
Becoming independent	Archives for Meteorology, Geophysics and Bioclimatology, Series A: Meteorol. and Geophys.	Meteorology and Atmospheric Physics (1986)

Table 5. Effects of splitting and reuniting of a journal

Atmospheric Environment (A – General; B – Urban)

	1985	1986	1987	1988	1989	1990	1991	1992	1993	1994
A						300	256	299	285	
Papers published	235	264	274	284	266					339
B						49	26	53	30	
A							1.033	1.358	1.259	1.310
Impact factor	1.465	1.634	1.529	1.340	1.473	1.358	1.312			0.000
B							0.592	0.692	0.389	0.611

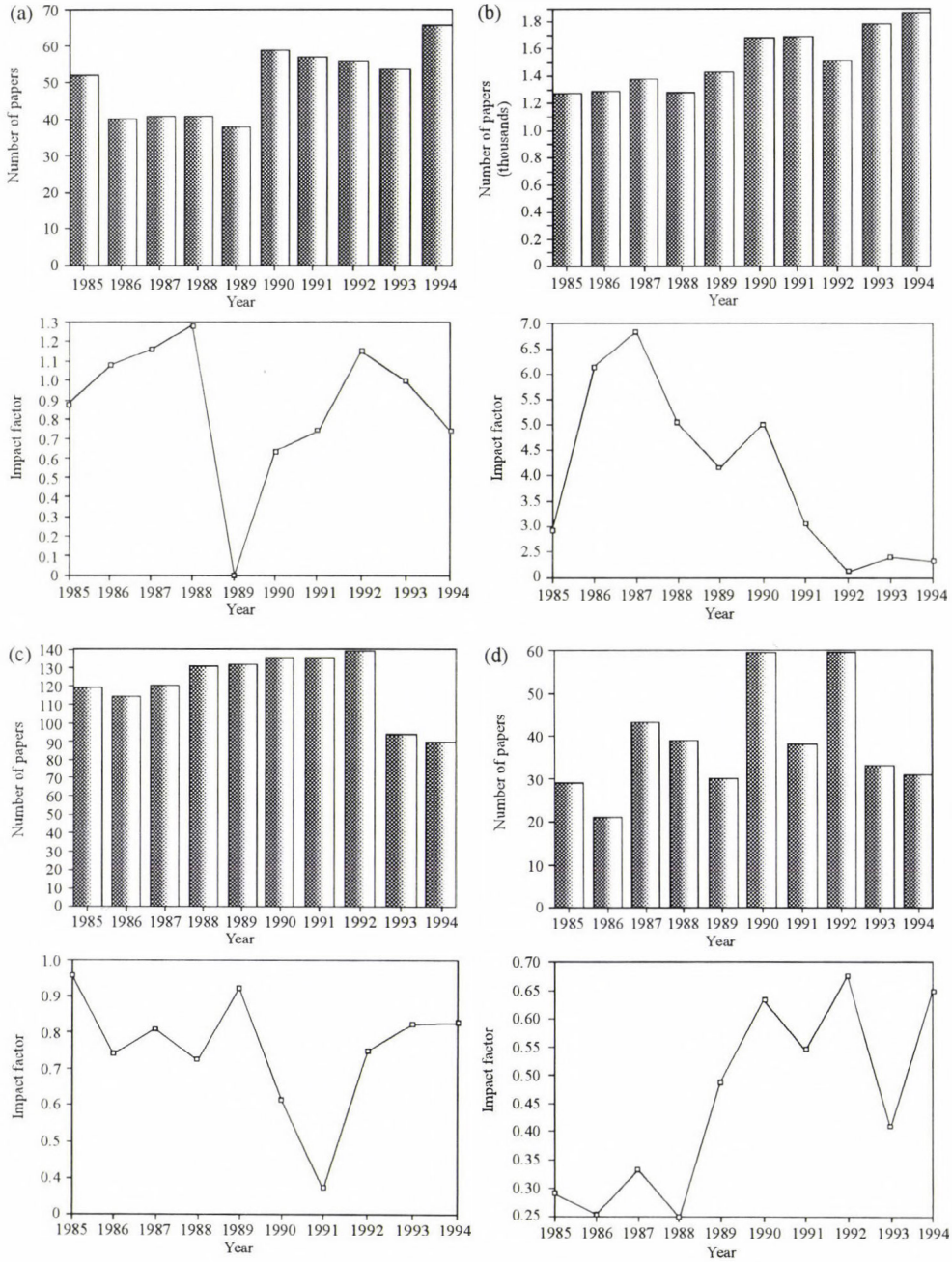

Fig. 2. Changes in the number of papers and impact factors during 10 years (1985–1994) for some meteorological journals: (*a*) Int. Journal of Climatology; (*b*) Journal of Geophysical Research; (*c*) J. of the Air and Waste Management Association; (*d*) Meteorology and Atmospheric Physics.

5. Where to publish?

Now, we can come to the conclusion that a great variety of journals are available for the scientist in meteorology for publication. Especially the journals in SCI's list are worth to mention, from the points of view of prestige, circulation and frequency (*Day*, 1983). There are namely differences between, e.g., a new, attractive journal, published by a commercial publisher without sponsorship of a society; an old, well-known, small journal, published by a famous institute, and a journal, published by a leading scientific society, representing the subfield in question. Perhaps, the latter has the largest circulation, whereas the old, well-known small journal has very limited space, and this is mainly reserved for the members of its publishing institute. Usually, a new, attractive journal, published by a profit-oriented publishing house, is the most specialized periodical in the respective topic, but because of the high subscription price, it has certainly the disadvantage of a low circulation (*Day*, 1983).

In any case, if somebody wants his/her article to be read by as many as possible scientists interested in its topic, the paper has to go to a journal of international prestige. Nowadays, the language of such journals is almost exclusively English. The contents of scientific articles, which appear in obscure periodicals, written in a rarely spoken language, will fail the aim of large scale dissemination of its results and will sink into oblivion.

The quotation: "everybody talks about the weather, but nobody does anything about it" (*Warner*, 1890) is not quite valid today . The meteorologists, even if being unable to do much about the weather, can write about the atmosphere in appropriate scientific journals of international reputation. Perhaps this modest paper will help to find the right one.

Acknowledgement—The authors thank *Prof. T. Braun* for stimulating remarks and discussions.

References

Brookes, B. C., 1980: Aging in scientific literature. *J. Docum. 36*, 164.

Day, Robert A., 1983: *How to Write and Publish a Scientific Paper*. ISI Press, Philadelphia.

Fierro, A., 1991: Histoire de la météorologie. Denoël, Paris.

Garfield, E., 1972: Citation analysis as a tool in journal evaluation. *Science 178*, 471-479.

Journal Citation Report, 1985–1994, Institute for Scientific Information, Philadelphia.

Price, D. J. de Solla, 1963: *Little Science, Big Science*. Columbia Univ. Press., New York, London.

Science Citation Index, 1985-1994, Institute for Scientific Information, Philadelphia.

Ulrich's International Periodicals Directory, 1994-95. 33rd Edition, Vol. 3. The Bowker International Serials Database (ed.: *R.R. Bowker*). New Providence, New Jersey.

Warner, C. D., 1967: Editorial. Hartford, Conn., Courant cont. 1890. In *The Home Book of Quotations* (ed.: *B. Stevenson*). Classical and Modern. 10th Edition, Dodd, Mead & Comp., New York. Often attributed to Mark Twain.

Ziman, M., 1969: Information, communication, knowledge. *Nature 224*, 318.

Zsindely, S. and *Schubert, A.*, 1992: The demography of journals. *New Library World 93* (1102), 17-20.

IDŐJÁRÁS

Quarterly Journal of the Hungarian Meteorological Service
Vol. 101, No. 2, April–June 1997, pp. 105–121

Area averages of ammonia concentrations in high emission areas; measurements and model results

Jan Willem Erisman and **Joris Boermans**

National Institute of Public Health and Environmental Protection, RIVM, P.O. Box 1, 3720 BA Bilthoven, The Netherlands; E-mail: janw@rivm.nl

(Manuscript received 15 October 1996; in final form 22 March 1997)

Abstract—Atmospheric concentrations and deposition of ammonia in the Netherlands and Europe have been described using the long-range transport model TREND (*Asman* and *van Jaarsveld*, 1992). In this paper results are reported of a program aimed at evaluating the TREND model in high ammonia emission density areas. In such areas emissions and concentrations show large horizontal variations. Average concentrations for two areas in the Netherlands were obtained by continuous ammonia measurements at a fixed point. Due to technical problems the time coverage of one of the sites was too low and therefore these data are not taken into account. The representativeness of the Vredepeel fixed point measurements was investigated using mobile measurements, a detailed emission inventory and a short-term/short-range transport model for ammonia (SLAM). The measuring strategy developed for this research provides a good tool for assessing the representativeness of a single point measurement for a larger area surrounding the fixed point. Yearly average concentration during July 1991–July 1992 at Vredepeel was 19.4 μg m^{-3}. The results of the assessment of the representativity of the fixed point showed that the Vredepeel location is representative within 10% in comparison with the surrounding 5 × 5 km area. It is concluded from this study that there was no significant difference between TREND results and the annual average measured concentration for the high emission area at Vredepeel.

Key-words: ammonia, high emission density area, measurements, modeling, representativity.

1. Introduction

Only recently has ammonia been recognized as one of the potential acidifying air pollutants (*van Breemen et al.*, 1982; *Heij* and *Schneider*, 1991, *Sutton et al.*, 1993). Nitrification of deposited ammonia and ammonium by microbial processes in forest soils in the Netherlands has been demonstrated by *van Breemen et al.* (1982). Through this process, acids in gaseous form, in aerosols or in rain droplets initially neutralized by gaseous NH_3 can form two

equivalents of acid when deposited: one can be considered as derived from NH_3 and one from the neutralized acid. Because of incomplete nitrification in the soil or uptake of nitrogen by vegetation the contribution of NH_3 and/or NH_4^+ may be less than one equivalent H^+ per mole NH_3 deposited. This contribution depends on type of soil and vegetation. Furthermore, NH_3 may play an important role in the enrichment of nutrient poor ecosystems (*Heil* and *Diemont*, 1983; *Heij* and *Schneider*, 1991; *Grennfelt* and *Thörnelöf*, 1992). The contribution of NH_3 to the total potential acid deposition in the Netherlands in 1989 was estimated to be 46% (*Erisman*, 1993).

Ammonia is emitted primarily from low level agricultural sources, with varying source strengths (*Buijsman et al.*, 1987; *Erisman*, 1989; *Asman*, 1992). Gaseous NH_3 has a short atmospheric residence time (*Erisman et al.*, 1988). Thus, concentrations (and deposition) will vary substantially over short distances. Measurements at 2 m height, of the horizontal gradient of NH_3 concentrations over a heathland located next to an emission area, showed gradients up to a factor of 20 within 5 km (*Asman et al.*, 1989). Consequently, accurate representative measurement of NH_3 concentrations in the Netherlands, especially in high emission density areas, would require many measuring sites. There are only very few attempts to monitor ammonia concentrations (*Erisman et al.*, 1986; *Allen et al.*, 1988; *Langford et al.*, 1992; *Sutton et al.*, 1993). Large scale monitoring of ammonia concentrations has been limited by a lack of an accurate and reliable measuring method. The number of measurements made in the Netherlands is far too small to obtain an accurate spatial distribution of the concentration. Therefore, the spatial distribution has been estimated from dispersion calculations by a transport model (TREND model, *Asman* and *van Jaarsveld*, 1992), using yearly average meteorological statistics and detailed emission maps. In this way, NH_3 and NH_4^+ concentration estimates on a 5×5 km grid have been obtained over the country. These concentration maps are used together with meteorological measurements, surface characteristics and wet deposition measurements to estimate the total NH_x deposition (*Erisman*, 1993).

From an analysis using all available NH_3 and NH_4^+ concentration measurements in air and in precipitation, it appeared that evaluation of model results in high emission density areas is difficult because of the difficulty of measuring representative area average concentrations (*Asman* and *van Jaarsveld*, 1992; *van Aalst* and *Erisman*, 1991). For this reason a program was started for estimating concentrations of ammonia in high emission areas aimed at further evaluation of the emission–dispersion–concentration–deposition system described in the TREND model (*Boermans* and *Erisman*, 1991, 1993). A measuring strategy based on a phenomenological description of available measurements was developed to account for the complex behavior of NH_3 in the atmosphere. It turned out during the execution of the measuring program that an extra tool was needed for the interpretation of the measurements. This

became the *S*hort-term *L*ocal-scale *A*mmonia transport *M*odel SLAM (*Boermans* and *van Pul*, 1993). SLAM can be used to calculate short-term (hourly) and local-scale (< 15 km) concentrations due to the dispersion of air pollution emitted from a large number of ground-level sources. In this paper the measuring strategy will be explained and the results of the measuring program will be presented.

2. Experimental set-up

2.1 Measuring/modeling strategy

Two regions with high ammonia emission density were selected; one region with predominantly intensive chicken breeding (Lunteren) and one region with predominantly intensive pig breeding (Vredepeel). Cheap and accurate ammonia concentration measuring devices for extensive application were not available. Continuous measurement devices were still under development. A fixed point in each region was therefore selected and equipped with a prototype continuous ammonia measurement instrument (*Wyers et al.*, 1992). Continuous measurements were made during one year at each fixed point. The fixed points were chosen by visual inspection together with detailed emission maps. The sites had to be representative for the region, with no direct influence of nearby sources in relation to emission strength and distribution of wind direction. Representativity of the concentration measured at the fixed point for the average surrounding area of 5 × 5 km (TREND model resolution) was evaluated by mobile measurements at eight sites (see Figs. 1a and 1b). These sites were selected by local inspection together with detailed emission maps. These sites were selected so as to represent parts with high, average and low emission in the grid square.

The mobile measurements were made by using a van in which the same measuring system was installed. Measurements were carried out on 23 days during the year according to a meteorological classification. The meteorological classification was based on a phenomenological study using long-term NH_3 concentration measurements at two sites: Elspeetsche Veld (hourly measurements, *Erisman et al.*, 1993) and Vredepeel (24 hour average measurements, *Erisman et al.*, 1986) (*Boermans* and *Erisman*, 1991). The main results of this study showed a positive correlation between air temperature and NH_3 concentrations. Furthermore, a dependence of wind direction (sources) and stability (mixing) was observed. The classification was based on wind direction, wind speed and temperature and is given in *Table 1*. Meteorological conditions were averaged over the hours the mobile measurements were carried out, to define a meteorological class. The aim was to measure all meteorological classes at least once. Annual averages could then be obtained by weighting the

occurrence of a class during the year. Usually nine measurements were made per day, starting at the fixed point (instrument calibration), then at the remaining eight sites (changing the order each day). If the instrument calibration showed more that 25% deviation, an extra measurement was made at the fixed point at the end of the measuring period.

Table 1. Meteorological classes used for the selection of measuring days in the mobile measuring program (*Boermans* and *Erisman*, 1990)

Wind directions: north, east, south and west, each divided into four classes:

Meteo class	Wind speed $m\ s^{-1}$	Temperature °C
1	≥ 3	> 11
2	≥ 3	≤ 11
3	< 3	> 11
4	< 3	≤ 11

The TREND model was originally developed for estimating concentration and deposition of sulfur compounds and oxidized nitrogen compounds in the Netherlands (*van Jaarsveld*, 1995). Recently the model was extended to treat reduced nitrogen compounds (*Asman* and *van Jaarsveld*, 1992). The more general model concept was validated by comparing model results with measurements of concentrations in air and in precipitation (*van Jaarsveld*, 1989; *Asman* and *van Jaarsveld*, 1992). The model resolution is 5 × 5 km. Within the grid cells the variation in concentration can be very high, especially in high emission density areas. It was desirable to have a tool which could serve as an explanatory model for the hourly measurements at the fixed point and additional measurements within the 5 × 5 km areas. For this purpose the SLAM model was developed (*Boermans* and *van Pul*, 1993). The SLAM model resolution is 100 m, when appropriate emission inventories are available. SLAM is used as an extension to the measurements, because measurements can be simulated and extended for periods where the equipment failed. The results of the SLAM calculations are extensively described in *Boermans* and *van Pul* (1993).

2.2 Measuring method

The NH_3 measurements were performed with an automated thermodenuder system developed at ECN (*Keuken et al.*, 1989; *Wyers et al.*, 1992). The method is based on collection of NH_3 by a V_2O_5-coated annular denuder, desorption and conversion of NH_3 to NO_x at 700°C and measurement of the resulting NO_x concentration by a NO_x-monitor (Ecophysics CLD 700 AL). A data logger controls the system and calculates the sampled NH_3 concentration

from the integrated NO_x signal, the sampling flow rate, the sampling time and a calibration constant. The sampling period was set to 5 minutes within a measuring cycle of 45 minutes. The sampling flow rate was kept at 3.3 ℓ min^{-1}. Two systems were installed in portable cabins at Lunteren and Vredepeel, while one system was installed in a van. Ambient air was sampled through 3 m long tubes (FEP Teflon, 6.35 mm outside diameter), which were renewed every month to prevent adsorption of NH_3 on dirty inlet tubes. Systems were calibrated at the site once every two weeks using a portable calibrator (Environment, model VE3M) provided with an NH_3 permeation tube and a zero-air dilution system. The performance of the thermodenuder system was examined in two field campaigns (*Mennen et al.,* 1992; *Mennen* personal communication) and in a calibration chamber under controlled conditions (*van Putten et al.,* 1992). From the latter, a detection limit of 0.2 $\mu g\ m^{-3}$ was found; precision was better than 0.3 $\mu g\ m^{-3}$ at low concentrations and better than 2% at high concentrations, and the measuring range is 0–300 $\mu g\ m^{-3}$.

2.3 Site description and ammonia emissions

The two locations are Vredepeel (51°32'N; 5°51'E) in the region "de Peel" and Lunteren (52°6'N; 5°38'E) in the region "Gelderse Vallei". In order to generate realistic calculations using TREND and SLAM, detailed emission inventories are needed for both areas. *Erisman* (1989) reports ammonia emissions in the Netherlands on a 5 × 5 km scale for 1988. In this inventory, emissions were assessed per municipality and generated by land use to a 5 × 5 km scale. The inventory is used on a national scale as input for the TREND model. For the two areas more detailed emission inventories were made. The inventory around Vredepeel consists of ammonia sources in an area of 15 × 20 km around the fixed point (*DHV Raadgevend Ingenieursbureau*, 1991). This inventory contains point sources (emissions from stables) and land use specific area sources (application of manure and pasture emissions) and it is an update for 1991 in comparison with the emissions according to *Erisman* (1989). The Lunteren inventory consists of ammonia sources in an area of 15 × 15 km around the fixed point (*Heidemij Adviesbureau*, 1989), this inventory is an update for 1989 in comparison with the emissions according to *Erisman* (1989). *Figs. 1a* and *1b* show point sources of the central 5 × 5 km grid cell of the Vredepeel (a) and Lunteren (b) inventories. In the figures the fixed point (a) and the eight additional sites (1 to 8) are also plotted. Source strength is categorized by annual average emission estimates.

As it can be seen in Fig. 1, the Lunteren area shows many more but smaller point sources in comparison with the Vredepeel area. This difference is caused by a different housing of animals. In Lunteren mainly smaller stables with chickens can be distinguished in comparison with larger stables in the Vredepeel area holding mainly pigs. The Lunteren area is characterized by being rural area

split up by forest from the center to the southeast of the 15 × 15 km area. The Vredepeel area is more homogeneous, showing small forest and a military air base in the south of the 5 × 5 km area and a forest in the west of the 15 × 20 km area. The annual average ammonia emission for the 5 × 5 km grid in Vredepeel was estimated to be 344 t yr^{-1}, and for Lunteren 464 t yr^{-1}. Within the program it was tried to obtain information about agricultural practices, especially about spreading of manure, by sending out an inquiry. Unfortunately only a few questionaires were returned so the results were not used.

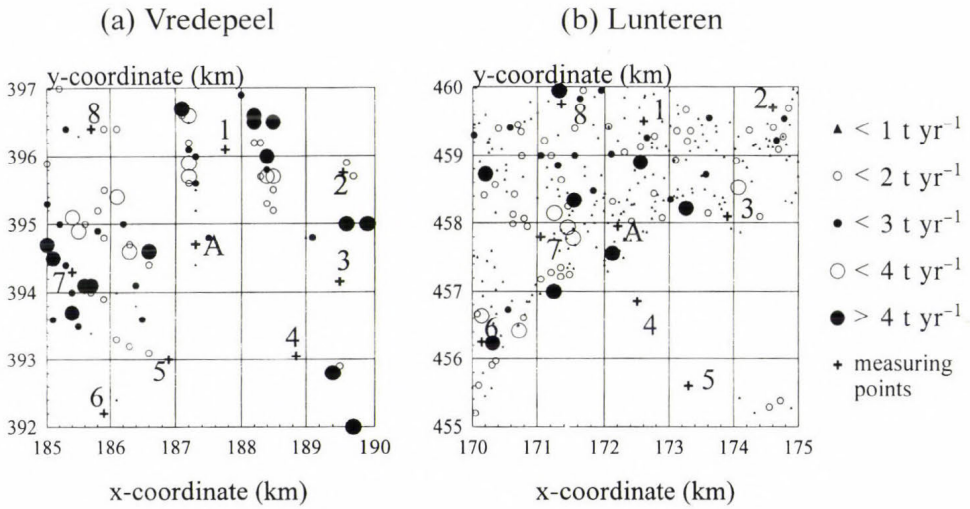

Fig. 1. Emission inventory of point sources in the surrounding 5 × 5 km area arround the location Vredepeel (*a*) and Lunteren (*b*). The measuring sites (A and 1–8) are also plotted. The axes represent coordinates of the Dutch coordinate system.

3. Phenomenology of ammonia at the fixed points

The measurements at the locations Vredepeel and Lunteren were carried out from July 1991 until July 1992. Due to technical problems, mainly bad performance of the data loggers, but also defective ovens, mechanical problems and failure of mains voltage, many measurements failed at the two fixed points, Vredepeel and Lunteren. The Lunteren data show a percentage of cover of only 31%, whereas the Vredepeel data show 69% of coverage during a one year of continuous measurements. Although less operational problems occurred with the mobile measurements, not all 16 meteorological (meteo) classes were covered. Differences between weather forecasts and actual meteorological conditions caused overlaps in meteo classes for the selected measuring days. Operational failures at the fixed points during mobile measurements also resulted in loss of successful days.

Phenomenology of ammonia concentrations show various relationships to meteorological conditions and seasons. *Fig. 2* shows monthly average measured concentrations at the fixed point at Vredepeel (*a*) and at Lunteren (*b*). The percentages of coverage of the monthly measured concentrations are also plotted. Monthly average concentrations show lowest values during the months from July until November. The concentrations show low levels during summer despite of high temperatures (positive relation to emission). This is caused by the growing season and therefore the absence of spreading of manure. The effect on the monthly average concentration of spreading manure in spring is not as clear as expected. Mobile measurements also show that the effect of spreading manure as measured (and visually seen) at one of the eight additional sites in the 5 × 5 km area does not always lead to an increase in concentration at the fixed point depending on the wind direction. In spite of low response to the inquiry to register the spreading of manure in Vredepeel, results also show a lower peak of spreading activities than the expected. Another explanation might be that, despite of the regulations which state that application of manure is not allowed during winter months, spreading activities occur during the whole year. Annual average concentrations are 19.4 $\mu g\ m^{-3}$ (σ = 22 $\mu g\ m^{-3}$) and 32.9 $\mu g\ m^{-3}$ (σ = 55 $\mu g\ m^{-3}$) for Vredepeel and Lunteren, respectively.

Fig. 3 shows measured concentrations in relation to temperature and stability for the whole dataset of Vredepeel. In general, the measured concentrations show a small decrease with increasing temperature. This effect is mainly caused by the high measured concentrations at temperatures below –5°C at stable conditions and the higher concentrations measured within the interval 0–10°C at unstable conditions. Near to neutral conditions the concentrations show no variation with the temperature classes. The effect of stability and wind speed on the measured concentrations is clearly demonstrated. Low wind speed and stable conditions show high concentration levels. These conditions are typical for early morning inversion situations where there is no vertical mixing of pollutants. Due to the high number of ground-level sources, ammonia will accumulate in the thin surface layer during these conditions. This effect can also be seen in the summer and winter average diurnal variation, shown in *Fig. 4*, where high concentration levels occur during nighttime with a maximum of 32 $\mu g\ m^{-3}$ in summer and, a less pronounced maximum of 19 $\mu g\ m^{-3}$ in winter. These daily variations are different from the observations in background areas where smallest concentrations are observed during nighttime and highest during the day (*Langford et al.,* 1992). An example of a time series of continuous measurements of NH_3 concentration during 18–30 October 1991 at Vredepeel, given in *Fig. 5*, clearly illustrates the NH_3 behavior observed here. In this figure variation in temperature is also plotted. This figure also demonstrates that relations between concentrations and temperatures are not simple.

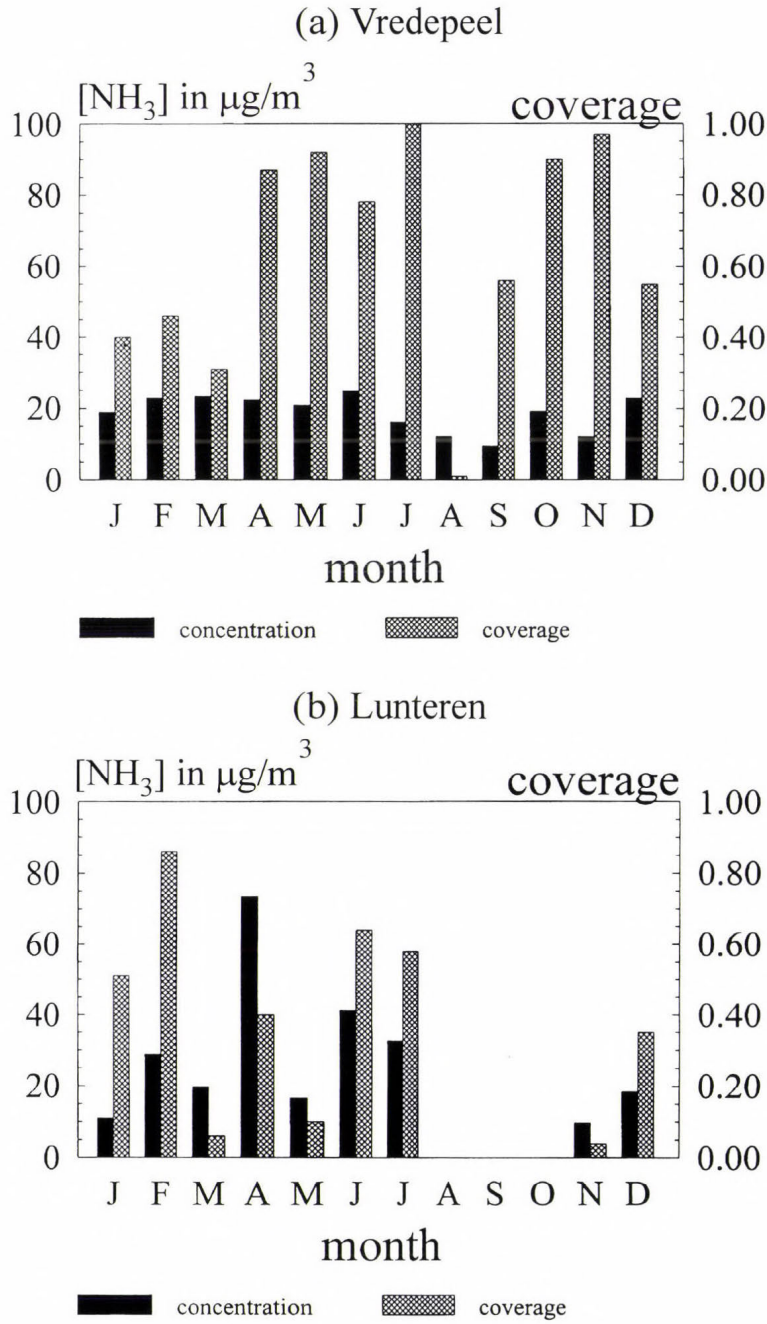

Fig. 2. Monthly average concentrations for Vredepeel (*a*) and for Lunteren (*b*). The percentages of coverage of the monthly measured concentrations are also plotted.

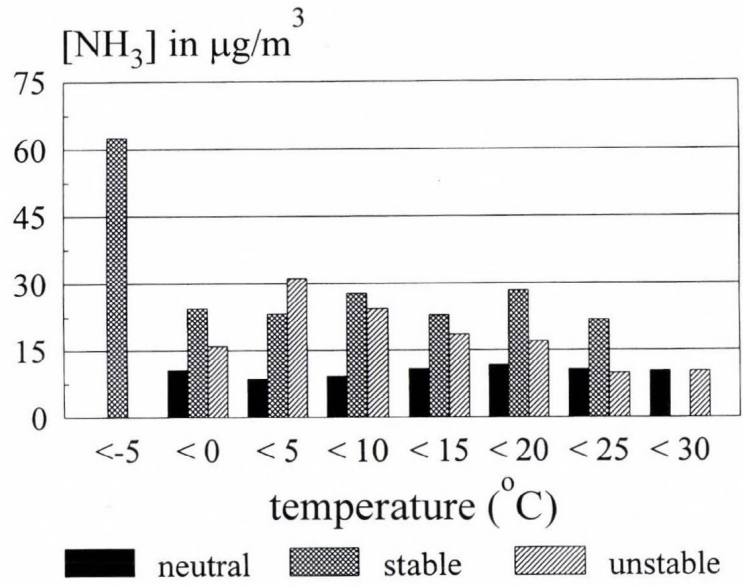

Fig. 3. Measured concentrations of the Vredepeel data related to a temperature and stability classification.

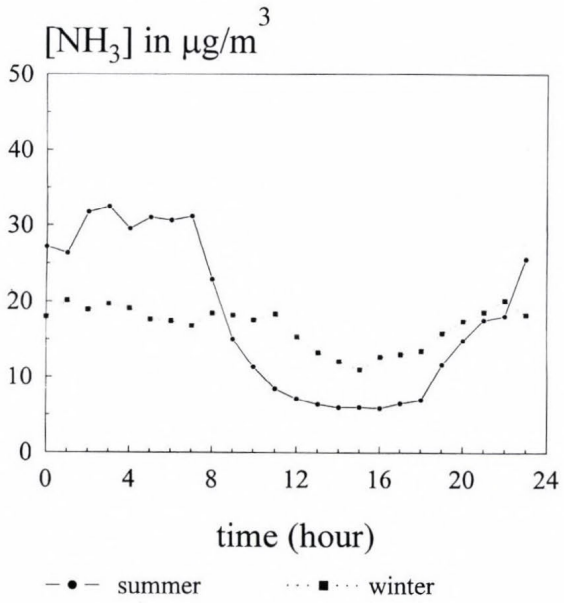

Fig. 4. Annual average diurnal variations of ammonia concentrations at Vredepeel.

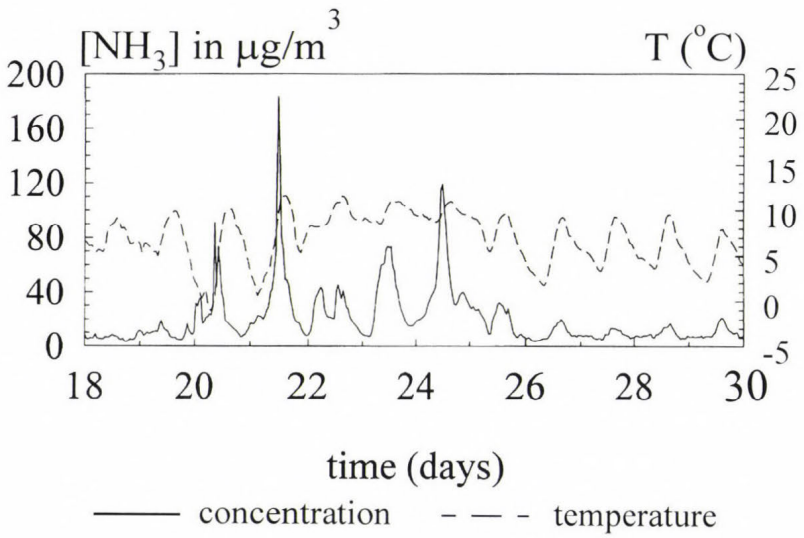

Fig. 5. An example of time series of continuous measurements of NH_3 concentration during 18–30 October 1991 at Vredepeel.

4. Fixed point and mobile measurements

In order to evaluate the representativeness of the fixed points, mobile measurements were made according the measuring strategy developed by *Boermans* and *Erisman* (1991, see Section 2.1). Because of the low coverage of the measurements at Lunteren, this site is not taken into account for model validation purposes. *Fig. 6* shows the fixed point measurements in comparison with the arithmetic averages of the mobile measurements for Vredepeel. Averaged mobile measurements for the Vredepeel area (23 days) show 25% lower concentrations compared to the yearly average fixed point concentration. This underestimation is mainly caused by the high number of meteo classes with wind speed conditions >3 m s^{-1} (19 of a total of 23 days). These conditions show clearly lower concentrations (Section 3). The deviations between the fixed point and the mobile measurements is probably due to the small amount of point sources in the area with high emissions resulting in large concentration gradients (Fig. 1). The average concentration for all mobile measurements at Vredepeel is 15.3 μg m^{-3}, for the fixed point during the same hours this is 14.2 μg m^{-3}. Fixed point results are averaged for all hours of all measuring days and therefore differ slightly in comparison with values presented in Section 3.

In this section a statement has to be made about the spatial representativeness of the fixed points for the 5 × 5 km area around Vredepeel on an annual basis. According to the measuring strategy, a yearly average grid

concentration (5 × 5 km) should have been assessed by averaging the mobile measurement results for all 16 meteo classes multiplied by the occurrence of each class during the year. Even though the fixed point measurements agree well with the mobile measurements, no yearly average grid concentration could be assessed due to the inadequate number of measured meteo classes.

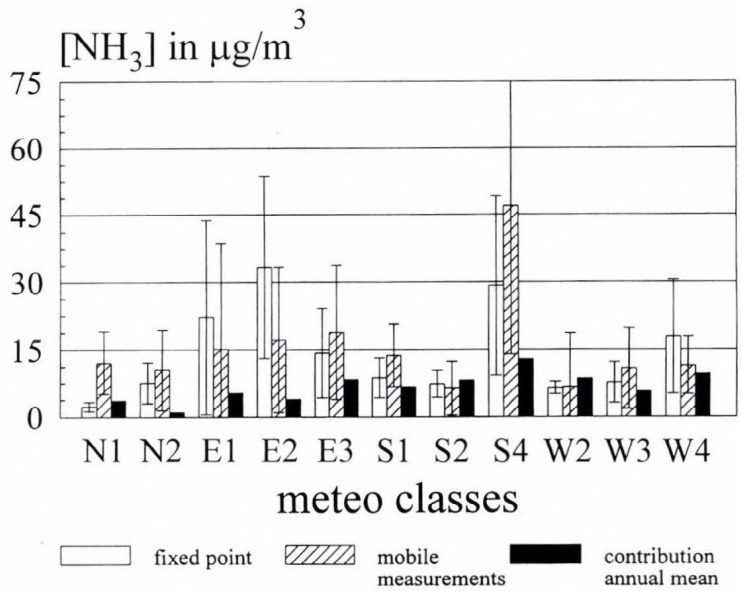

Fig. 6. Fixed point measurements in comparison to the average of mobile measurements in the 5 × 5 km area of Vredepeel for the different meteorological classes. The contribution of the meteo class average concentration to the annual mean concentration, weighted according to the occurrence of the meteo class, is also given.

For Vredepeel the time weighted contribution (%) of the meteorological classes to the annual average concentration based on the fixed point measurements is plotted. The classes for which measurements are available cover 73.6% of the annual (fixed point) concentration. Therefore, measurements have been made during the most important classes. Because no more representativeness measurements could be made, the representativity was investigated further using a model.

At this stage the SLAM model was used to further examine the representativity of the fixed point concentrations relative to the grid averages. The model was tested using measurements presented here (*Boermans* and *van Pul*, 1993). SLAM input consists of all point sources (Fig. 1) and area sources in the studied areas. Model calculations were made to estimate average

concentrations for the fixed points and for the 5 × 5 km grids for all meteo classes (*Boermans* and *Erisman*, 1993). As the model tends to overpredict concentrations at wind speed below 1.5 m s^{-1} (*Boermans* and *van Pul*, 1993), only calculations for wind speed above this value were used. The modeled fixed point concentration at Vredepeel amounted 18.1 $\mu g\ m^{-3}$, versus 19.4 $\mu g\ m^{-3}$ measured, and the calculated grid concentration amounted 17.1 $\mu g\ m^{-3}$. These results show that calculated and measured fixed point concentrations are in reasonable agreement with the calculated grid average concentration (< 10% deviation). As an overall conclusion it can be deduced that the Vredepeel fixed point can be considered representative for the 5 × 5 km grid.

5. Comparison of TREND results with observations

The outcome of the TREND model strongly depends on the emission input. Neither emission nor seasonal/diurnal variations of emission are well known (*Asman* and *Van Jaarsveld*, 1992; *Asman*, 1992). Temporal emission variation plays an important role in the resulting actual hourly (and annual) concentrations. Temporal variation was modeled according to *Asman* (1992). He provides a monthly relationship to agricultural practice and some relationships of emission to wind speed and temperature, characterized by increasing emissions with increasing wind speed and temperature.

TREND calculations were made for three different emission options and two emission files. The results of these calculations are given in *Boermans* and *Erisman* (1993). Here only the results for the best option are given and the variation in input is used to estimate uncertainty in the output. Following options were taken into account: option A is the original model configuration with a diurnal emission variation characterized by an increasing emission during daytime; option B describes constant emissions and option C describes a diurnal emission variation, as well as a seasonal emission variation. Two different emission files were used as input: (1) emissions according to *Erisman* (1989); and (2) a detailed update for the areas Vredepeel (1991) and Lunteren (1989) (see Section 2.3). For each emission file and the three options calculations of annual average ammonia concentrations for the period from July 1991 until July 1992 were made by averaging monthly calculated ammonia concentrations. Calculations were made using monthly assessed national and local meteorological statistics. TREND calculation using different emission variations show different results. These results show again the importance of knowledge on emissions. Constant emissions show higher calculated yearly average concentration levels compared to a diurnal and/or seasonal emission variation. From the calculations it appeared that option C with the detailed emissions and the local meteorological statistics could be considered as the best and most realistic option. *Fig. 7* shows the monthly average measured and modeled

concentrations for Vredepeel according to option C. The error bars represent variation in the model outcome as a result of input variation (option A and B, emissions according to *Erisman* (1989) and national meteorological statistics). This variation might be regarded as uncertainty in model results.

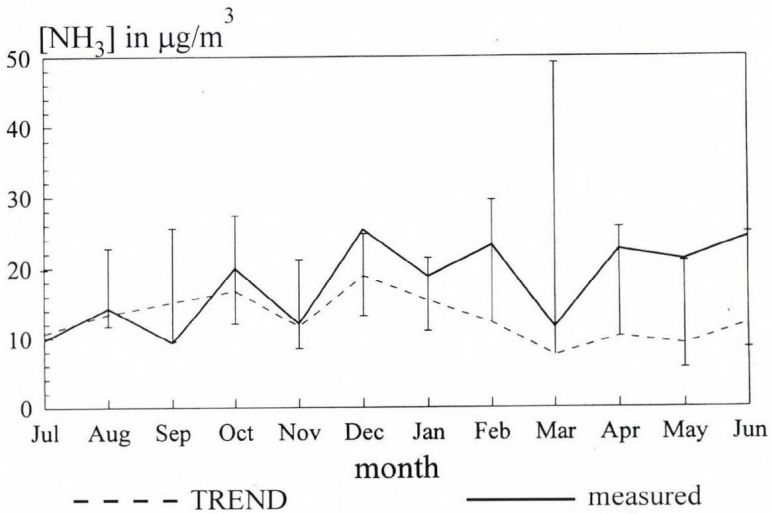

Fig. 7. Comparison of the Vredepeel measured fixed point concentration with the monthly calculated TREND concentrations.

Fig. 7 shows that the variation in monthly average modeled and measured concentrations is similar, but measured concentrations tend to be somewhat higher in spring and in winter. It must be stressed that the representativity of the fixed point is studied on an annual basis. Monthly averaged measurements at the fixed point might not be representative for the grid concentration, depending on meteorological conditions and emissions during the month. However, measured and modeled values at Vredepeel are not considered to be significantly different when the uncertainty in both values is taken into account. The uncertainty in annual average measured concentrations was estimated to be 20–25% (*Boermans* and *Erisman*, 1993).

For the Vredepeel area TREND calculations using local meteorological conditions and using 1991 updated emissions show reasonable agreement with the yearly average measured concentration, 16.2 and 19.4 $\mu g\ m^{-3}$, respectively. For the Lunteren area TREND calculations shows ca. 30% lower concentrations in comparison with the average measured fixed point concentration (only 30% cover), 20.5 and 32.9 $\mu g\ m^{-3}$, respectively. These results are in line with the indications obtained from the mobile measurements and SLAM calculations. A final statement however on the representativeness of the fixed point has not been made.

Up to this level comparison studies were made only looking at concentrations. A deposition estimate has been made based on hourly measured ammonia concentrations. Hourly flux of ammonia for the 5 × 5 km area has been calculated by the summation of the hourly measured ammonia concentration and the hourly estimated deposition velocity. The deposition velocity is estimated using the resistance analogy with measured meteorological parameters and a grid average roughness length value as input (*Hicks et al.*, 1987; *Erisman*, 1993). Hourly fluxes were calculated using the RIVM Laboratory of Air Research surface flux routine (*Erisman*, 1993). Yearly average ammonium deposition was generated only for the Vredepeel area. According to this method the yearly deposition of ammonium is 3510 mol ha^{-1} yr^{-1}. TREND calculations, using a surface resistance of 30 s m^{-1}, show an yearly average deposition of 3050 mol ha^{-1} yr^{-1}, which agrees reasonably well with the deposition estimate based on air concentration measurements and modeled deposition velocities.

6. Synthesis and conclusions

In this paper ambient ammonia concentration measurements are used to evaluate TREND model results. The results of this research show that fixed point measurements might be used to evaluate long-range transport models. Provided representativeness for a larger area is investigated. This is especially relevant in NH_3 source areas where large horizontal concentration gradients are expected. The measuring strategy used for the evaluation provides a good tool for estimating the representativeness measurements at a single-point location for a larger area surrounding the fixed point. An extra tool to evaluate representativeness is the SLAM model with a detailed emission map (*Boermans* and *van Pul*, 1993). The largest uncertainty in comparing model results with measurements is due to uncertainty in emission estimates and temporal variations in emissions. Treating temporal variation in emission as a function of application of manure and agricultural practice and applying a fixed statistical diurnal variation characterized by a higher emission during daytime than during nighttime (*Asman*, 1992) provided the best agreement between model and measurements. The uncertainty in the yearly average concentrations measured at the two fixed points studied is estimated at 20–25%. Evaluation of representativeness of those fixed point measurements using mobile measurements show that the fixed point concentrations at Vredepeel agree within ca. 10% with grid average concentrations. For Lunteren no statement was made for the representativeness of the fixed point for the 5 × 5 km area.

Different emission files, temporal emission variations and national and local meteorological conditions were evaluated using the TREND model to estimate uncertainty in model results. The final conclusion of this research is that there

was no significant difference between TREND results and yearly average measured concentrations at a high ammonia emission area (Vredepeel). It is recommended that measured concentrations at point locations should be evaluated on representativeness for a surrounding 5 × 5 km area and local meteorological data and best guess on emissions should be used as input for model (e.g. TREND) calculations. A comparison of TREND results with measurements made prior to this research showed that there were no systematic differences between model estimates and measurements in background areas and in moderate ammonia concentration areas (*Asman* and *van Jaarsveld*, 1992). The uncertainty in 5 × 5 km TREND results is estimated to vary from ca. 20% for background and low emission areas up to ca. 30% for high emission areas.

To evaluate the emission–transport–concentration–deposition system of NH_3 in the future, a monitoring network of about eight locations has been established in the Netherlands where hourly average NH_3 concentrations are measured. Three locations are located in high NH_3 emission density areas with different animals (pigs, chickens and cows) dominating in stables. Furthermore, two locations are located in remote areas, not directly influenced by local sources, and three locations in background areas. Evaluation of representativeness by mobile measurements is done annually in the areas showing a high emission density, once every three years in the remote areas and once every 5 to 10 years in the background areas surrounding the fixed monitoring sites. This is expected to be sufficient for annual evaluation of TREND model results used for mapping concentration and deposition of NH_3 in the Netherlands. As an important part of this evaluation it should be mentioned that the use of local updated emissions on ammonia and local assessed meteorology is necessary. Furthermore, the network should provide an evaluation of the success of abatement strategies by signaling achieved reduction in emissions.

Acknowledgements—This research was carried out with substantial assistance of colleagues at the Netherlands Energy Centre (ECN). We acknowledge the work of *Paul Wyers, Han Möls* and *others*. We also thank *Marcel Mennen, Henk Boelhouwer, Jaap Schippers, Bernard van Elzakker, Edith van Putten* and *Erik Zwart* of the Laboratory of Air Research at RIVM for their contribution to this project. We would like to thank *Hans van Jaarsveld* for his comments on the manuscript and for the assistance with the TREND model.

References

Aalst, R.M. van and *Erisman, J.W.*, 1991: Atmospheric input. In *Acidification Research in the Netherlands* (eds.: *G.J. Heij* and *T. Schneider*). Studies in Environmental Science 46, Elsevier, Amsterdam.

Allen, A.G., Harrison, R.M. and *Wake, M.T.*, 1988: A meso-scale study of the behaviour of atmospheric ammonia and ammonium. *Atmospheric Environment 22*, 1347-1353.

Asman, W.H.A., 1992: Ammonia emissions in Europe: Updated emissions and emission variations. Laboratory of Air Research, National Institute of Public Health and Environmental Protection RIVM: *Report*, No. 228471008. Bilthoven, The Netherlands.

Asman, W.A.H., Pinksterboer, E.F., Maas, H.F.M., Erisman, J.W. and *Horst, T.W.*, 1989: Gradients of the ammonia concentration in a nature reserve: model results and measurements. *Atmospheric Environment 23*, 2259-2265.

Asman, W.H.A. and *Jaarsveld, J.A. van* 1992: A variable-resolution transport model applied for NHx for Europe. *Atmospheric* Environment *26A*, 445-464.

Boermans, G.M.F. and *Erisman, J.W.*, 1991: Development of a measurement strategy for the investigation of the representativeness of measuring points for the ammonia concentration; phenomenology of ammonia. Laboratory of Air Research, National Institute of Public Health and Environmental Protection RIVM: *Report*, No. 222105001. Bilthoven, The Netherlands.

Boermans, G.M.F. and *Erisman, J.W.*, 1993: Final report on the *Additional Programme on Ammonia*. Laboratory of Air Research, National Institute of Public Health and Environmental Protection RIVM: *Report*, No. 222105002. Bilthoven, The Netherlands.

Boermans, G.M.F. and *Pul, W.A.J. van*, 1993: SLAM, a transport model for short-term and short distance applied for simulation of the dispersion of ammonia. National Institute of Public Health and Environmental Protection RIVM: *Report*, No. 222105003. Bilthoven, The Netherlands.

Breemen, N. van, Burrough, P.A., Velthorst, E.J., Dobben, H.F. van, Wit, T. de, Ridder, T.B. and *Reinders, H.F.R.*, 1982: Soil acidification from atmospheric ammonium sulphate in forest canopy throughfall. *Nature 299*, 548-550.

Buijsman, E., Maas, J.F.M. and *Asman, W.A.H.*, 1987: Anthropogenic NH_3 emissions in Europe. *Atmospheric Environment 21*, 1009-1022.

DHV Raadgevend Ingenieursbureau BV, 1991: Ammonia emission inventory in the surroundings of the measuring site of Vredepeel. *Dossier* D1907-81-001, DHV, Amersfoort, The Netherlands.

Erisman, J.W., Vermetten, A.W.M., Asman, W.A.H., Mulder, W., Slanina, J. and *Waijers-IJpelaan, A.*, 1986: Ammoniak en ammonium concentraties in de Nederlandse buitenlucht Concentrations of ammonia and ammonium over the Netherlands: Report R86-3, IMOU, State University of Utrecht, The Netherlands.

Erisman, J.W., Vermetten, A.W.M., Asman, W.A.H., Slanina, J. and *Waijers-IJpelaan, A.*, 1988: Vertical distribution of gases and aerosols: the behaviour of ammonia and related copmponents in the lower atmosphere. *Atmospheric Environment 22*, 1153-1160.

Erisman, J.W., 1989: Ammonia emissions in the Netherlands in 1987 and 1988. *Report*, No. 228471006. National Institute of Public Health and Environmental Protection. Bilthoven, The Netherlands.

Erisman, J.W., 1992: Atmospheric deposition of acidifying compounds in the Netherlands. Ph.D. Thesis. University of Utrecht, The Netherlands.

Erisman, J.W., 1993: Acid deposition onto nature areas in the Netherlands; Part I. Methods and results. *Water Soil Air Pollut. 71*, 51-80.

Erisman, J.W., Elzakker, B.G. van, Mennen, M. G., Hogenkamp, J., Zwart, E., Beld, L. van den, Römer, F.G., Bobbink, R., Heil, G., Raessen, M., Duyzer, J.H., Verhage, H., Wyers, G.P., Otjes, R.P. and *Möls, J.J.*, 1993b: The Elspeetsche Veld experiment on surface exchange of trace gases: summary of results. *Atmospheric Environment 28*, 487-496.

Grennfelt, P. and *Thörnelöf, E.*, 1992: Critical loads for nitrogen. *Report*, No. Nord 1992:41, Nordic Council of Ministers, Copenhagen, Denmark.

Heidemij Adviesbureau, 1989: Local ammonia dispersion in the research area sorrounding Ede. Research as part of the ammonia execution program. Heidemij, Arnhem, The Netherlands.

Heij, G.J. and *Schneider, T.*, 1991: Acidification research in the Netherlands. *Studies in Environmental Science 46*. Elsevier, Amsterdam.

Heil, G.W. and *Diemont, W.H.*, 1983: Raised nutrient levels change heathlands into grasslands. *Vegetatio 53*, 113-120.

Hicks, B.B., Baldocchi, D.D., Meyers, T.P., Hosker, Jr. R.P. and *Matt, D.R.*, 1987: A preliminary multiple resistance routine for deriving dry deposition velocities from measured quantities. *Water Air Soil Pollut. 36*, 311-330.

Jaarsveld, J.A. van, 1989: A model approach for assessing transport and deposition of acidifying compounds on different spatial scales. In *Changing Composition of the Troposphere*. Special Environment Report No. 17, WMO No. 724, 197-204. Geneva, Switzerland.

Jaarsveld, J.A. van, 1995: Modelling the long-term atmospheric behaviour of pollutants on various spatial scales. *Ph.D. thesis*, University of Utrecht, The Netherlands.

Keuken, M.P., Wayers-IJpelaan, A., Mols, J.J., Otjes, R.P. and *Slanina, J.*, 1989: The determination of ammonia in ambient air by an automated thermodenuder system. *Atmospheric Environment, 23,* 2177-2185.

Langford, A.O., Fehsenfeld, F.C., Zachariassen, J. and *Schimel, D.S.*, 1992: Gaseous ammoni fluxes and background concentrations in terrestrial ecosystems of the United States. *Global Biogeochem. Cycl. 6*, 459-483.

Mennen, M.G., Elzakker, B.G. van, Wyers, G.P., Otjes, R.P., Verhage, A.J.L., Wouters, L.W., Heffels, C.J.G., Römer F., Beld, L. van den, Tetteroo, J.E.H. and *Hoogervorst, A.*, 1992: A field intercomparison with five automatic ammonia monitors. *Report*, No. 223107002. National Institute of Public Health and Environmental Protection. Bilthoven, The Netherlands.

Putten, E.M. van, Mennen, M.G., Uiterwijk, J.W. and *Regts, T.A.*, 1992: Performance study of three automatic ammonia monitors under controlled conditions. *Report*, No. 223107003, National Institute of Public Health and Environmental Protection. Bilthoven, The Netherlands.

Sutton, M.A., Pitcairn, C.E.R. and *Fowler, D.*, 1993: The exchange of ammonia between the atmosphere and plant communities. *Advances in Ecol. Res. 24*, 301-393.

Wyers, G.P., Vermeulen, A.T. and *Slanina, J.*, 1992: Measurement of the dry deposition of NH_3 on a forest. *Envir. Pollut. 75*, 25-28.

IDŐJÁRÁS

Quarterly Journal of the Hungarian Meteorological Service
Vol. 101, No. 2, April–June 1997, pp. 123–142

Graupel production and agent residence time within the seeding zone of a Cb cloud

Mladjen Ćurić and **Dejan Janc**

Institute of Meteorology, University of Belgrade,
11000 Belgrade, P.O. Box 550, Yugoslavia; E-mail: curic@rudjer.ff.bg.ac.yu

(Manuscript received 1 July 1996; in final form 25 February 1997)

Abstract—A one-dimensional kinematic model with detailed microphysics is applied to investigate the graupel production in the seeding zone defined between the isotherm levels of -8°C and -12°C. We calculate the final graupel production and the agent residence time, two important parameters determining the success of an Hail Suppression Operational Project. The agents are injected at the level of -8°C. Their interaction with the cloud environment is simulated by a microphysical model with the Khrgian-Mazin (KM) size distribution of drops. The seeding agents are considered by using the maximum agent mixing ratios and corresponding agent particle masses and radii, because their chemical composition are the same. It is shown:

- Final graupel production is heavily dependent on vertical velocity at the bottom boundary of the seeding zone, while the agent residence time is independent of an agent type. The model results suggest that the PP-6 agent is the most efficient in producing graupel within the seeding zone;
- The rate of rain accreting to cloud ice formed by deposition nucleation is the most important mechanism for graupel formation although its magnitude is the smallest or nearly smallest compared to other mechanisms. This is due entirely to the numerous active deposition nuclei which convert into the cloud ice immediately.

Key-words: graupel production, seeding agents, hail suppression, seeding zone, numerical model of seedings.

1. Introduction

A Hail Suppression Project has been in operation in Serbia for more than twenty years. The main aim of hail suppression is a decrease of damages caused by the hail. The operational project for hail suppression follows the Soviet method given by *Sulakvelidze* (1967). Later, the concept and the effectiveness of the hail suppression in Serbia were described in more details by *Radinović* (1989) and *Mesinger* and *Mesinger* (1992). The silver iodide is injected in the

zone between isotherm levels of -8°C and -12°C, where the most probable formations of natural hail embryos are (*Fukuta*,1980). After seeding is performed, silver iodide produces artificial graupel particles. The final graupel production and the agent residence time in the seeding zone are the most important factors determining the success of hail suppression, according to the hypothesis of competing embryos (*Sulakvelidze*, 1967).

Great progress in the investigation of agent reaction with cloud environment in theory and experiment has been made in the last twenty years. The pioneer work in this field was the model of contact nucleation mechanisms of AgI with highly parameterized dynamics given by *Alkezweeny* (1971). Further, *Young* (1974a-c) introduced a model with uncoupled microphysics and dynamics using the continuous bin technique to examine the seeding influence. Recently, *Young* (1993) constructed the kinematic model with detailed microphysics. Most numerical models simulate the seeding operation with the Eulerian treatment using the bulk-water parameterization scheme. Some 2-D convective cloud model simulations investigate the seeding influence on precipitation enhancement as those published by *Hsie et al.* (1980), *Orville* and *Chen* (1982), *Orville et al.* (1984) or *Kopp* (1988). The application of 3-D cloud models and mesoscale models to the weather modification problems is now more and more frequent (*Levy* and *Cotton*, 1984; *Farley et al.*, 1994; *Holroyd et al.*, 1995). The more recent work by *Farley* (1987) and *Farley et al.* (1996) use a 20-category ice particle hail model to investigate the seeding effects, while the other microphysical fields are treated by the bulk-parameterization scheme. Some more complex models (for example, *Reisen et al.*, 1996) treat the complete microphysics by stochastic concept. Numerical models make it possible to simulate some of the agent nucleation mechanisms which may be measured only with difficulty with the available techniques.

The primary aim of our manuscript is to evaluate roughly the capability of the seeding agents (in use in hail suppression in Serbia) to produce the graupel within the seeding zone after agent injection at the level of -8°C for a great variety of atmospheric conditions and chosen parameters of drop size distribution. We especially focus on total graupel number concentration produced by seeding agent following the hail suppression methodology in Serbia. Under this concept, the seeding is terminated when the graupel concentration is 100 m^{-3} within the seeding zone. Therefore, we think that the bulk-water parameterization scheme is applicable in this case. A one-dimensional (1-D) kinematic model is used. The silver iodide interaction with cloud environment is simulated by help of a microphysical model. In contrast to the model version of *Ćurić* and *Janc* (1990), the one we used in this paper assumes the Khrgian-Mazin size distribution function for liquid water fraction and also include phoretic processes. The bulk microphysics is treated using the results of *Hsie et al.* (1980) and *Lin et al.* (1983). Vertical motion of graupel particles is considered by the kinematic concept.

2. Model

2.1 Microphysical model equations

The interaction of AgI particles with the cloud environment is simulated by a microphysical model version without immersion freezing with implemented Khrgian-Mazin size distribution function (hereafter called KM) for the entire drop spectrum. In an earlier version of the model we have used the monodisperse size distribution for cloud droplets and the *Marshall-Palmer* (1948) one for raindrops (*Ćurić* and *Janc*, 1990). This conventional approach produces an unnatural gap in the size range of the drop spectrum. Therefore the drop spectrum is now approximated by the unique KM size distribution function. The lower boundary for the raindrop spectrum is taken to be R_{min} = 50 μm, in agreement with *Hsie et al.* (1980). Graupeln in the model are distributed according to the exponential size distribution.

Following the model scheme the cloud ice is produced by both contact (Brownian and inertial collection rates due to cloud droplets; phoretic processes) and deposition nucleation mechanisms. The accretion of cloud ice by raindrops is the sink term for cloud ice. The graupel is produced via the Brownian and inertial collection rates due to raindrops and accretion of generated cloud ice by raindrops. The cloud water is depleted by the Brownian and inertial collection rates as well as the accretion of cloud droplets by graupeln. The sink term for raindrops is the source term for graupel particles. The microphysical model involves only those processes which lead to cloud ice/graupel formation in an early glaciation period (just after the agent injection in the seeding zone) in agreement with *Ćurić* and *Janc* (1990). As noted, the presence of raindrops is necessary for graupel formation in accordance with *Hsie et al.* (1980) or *Lin et al.* (1983). These papers indicate that the interaction of ice crystals with raindrops is important for graupel (hail) formation in the simulation of continental clouds. Recently, *Reisen et al.* (1996) also emphasized the importance of raindrop proportion for graupel formation in both maritime and continental clouds.

The KM size distribution of drops (*Pruppacher* and *Klett*, 1978; *Ćurić* and *Vuković*, 1991) may be written as

$$f(R) = AR^2 \exp(-BR), \tag{1}$$

where

$$A = 1.46 \frac{\rho Q}{\rho_w R_M^6}, \quad \text{and} \quad B = \frac{3}{R_M}. \tag{2}$$

Here Q is the liquid water mixing ratio, R_M is the mean radius of drop spectrum, ρ and ρ_w are the air and liquid water densities, while R is the drop radius. The cloud droplet (N_c) and raindrop number concentrations (N_r) are respectively

$$N_c = \frac{2A\alpha_1}{B^3}; \quad N_r = \frac{2A\beta_1}{B^3}, \tag{3}$$

where

$$\alpha_1 = \frac{\Gamma(3; BR_{\min})}{2}; \quad \beta_1 = 1 - \alpha_1. \tag{4}$$

The microphysical production terms with implemented KM size distribution are given in Appendix A.

2.2 Kinematic model equations

A 1-D kinematic model is employed to investigate the seeding agent behavior in the seeding zone. We suppose that the agent cloud center with associated maximum agent mixing ratio moves upwards and leads to the change of the vertical velocity due to buoyancy and loading effects. The equation of motion for a seeded air parcel may be written in the form:

$$\frac{dw}{dt} = g\frac{dT}{T} - g\frac{M_i N_{ci,d}}{\rho}, \tag{5}$$

where the first term on the right-hand side of Eq. (5) represents the buoyancy effects caused by phase transitions after the agent injection in the seeding zone, while the second one represents the loading by deposition on the ice forming nuclei (AgI), which only increases its effect comparing with the non seeding case. The freezing of the water drops and the accretion mechanisms do not change the total hydrometeor mixing ratio (drops and ice particles). The temperature change dT is determined by the first law of thermodynamics given in Appendix B. The loading term depends on the number concentration of cloud ice generated by deposition nucleation ($N_{ci,d}$) and distributed according to the monodisperse size distribution. A single cloud ice crystal mass is supposed to be $M_i = 4.2 \times 10^{-13}$ kg according to *Lin et al.* (1983).

The number concentration of contact or deposition nuclei is calculated using corresponding efficiency curves proposed by *Cooper* (1974), *Hsie et al.* (1980) and *Kopp* (1988). In principle, it is possible to find the activation curves for each agent. But, due to the lack of experimental data, we use the same efficiency curve for each agent. The continuity equation for the maximum agent mixing ratio (X_s) for a 1-D

case is given by

$$\frac{dX_s}{dt} = -\mu X_s + S_{bfc} + S_{ic} + S_{br} + S_{ir} + S_d, \tag{6}$$

where the first term on the right-hand side represents the turbulent diffusion of silver iodide in the seeding zone. It is assumed that the entrainment coefficient (μ) depends on the vertical velocity in accordance with *Wisner et al.* (1972) in the following manner

$$\mu = Kw, \tag{7}$$

where $K = 5 \times 10^{-4}$ m^{-1}.

The terms on the right-hand side with subscripts *bfc, ic, br, ir* and *d* describe the Brownian collection rates due to cloud droplets and phoretic effects,the inertial collection rate due to cloud droplets, the Brownian and inertial collection rates due to raindrops and deposition nucleation, respectively. The silver iodide mixing ratio is expressed in kg kg^{-1} while the terms on the right-hand side of Eq. (6) are expressed in kg kg^{-1} s^{-1}. The sink terms of the silver iodide mixing ratio for contact and deposition nucleation mechanisms may be written as

$$S_y = -J_y \frac{X_s}{N_{cn}}; \qquad S_d = -\frac{N_d(\Delta T)X_s}{N_d(20^0)\Delta t}, \tag{8}$$

where the subscript y may be *bfc, ic, br* and *ir*, respectively. The terms J_y are given in Appendix A. $N_d(\,)$ represents the number of activated deposition nuclei at given supercooling while Δt is the time increment.

In our model the time increment is $\Delta t = 1$ s, while for substantial derivations the Lagrangian time forward scheme is used. Then the discrete form of corresponding time changes is:

$$\frac{dY}{dt} \rightarrow \frac{Y^{n+1} - Y^n}{\Delta t}, \tag{9}$$

where $n + 1$ and n designate successive time steps. The numerical techniques used prevent the appearance of the negative seeding agent mixing ratio values.

3. Experiments

3.1 Agent characteristics

Four agent types are used in the Hail Suppression Operational Project in Serbia. The available experimental data for the agents used are given in *Table 1*. Some characteristics of the TG-10 agent are published by *Huter et al.* (1988). All agents have the same chemical composition but they differ from each other in geometry and in a particle mass. The size distribution of the SAKO-6 agent particles is of a log-normal type with weak scattering around its modal radius ($R_s = 0.03$ μm). Over 80% of the agent particles are found around the modal value of the size distribution function. The size distributions for the other agents coincide well with that of the SAKO-6. Therefore, the monodisperse size distribution for the seeding agent particles seems to be justified. The maximum seeding agent mixing ratios and the agent particle mass are determined following the results of *Hsie et al.* (1980).

Table 1. The characteristics of agents used in the Hail Suppression Operational Project

Agent type	TG-10	TG-5	SAKO-6	PP-6
Pyrotechnic mixture mass (g)	400	400	400	400
AgI content (%)	15	15	25	20
Activity (-10°C) (particles per gram)	1.2×10^{12}	1.2×10^{12}	1.7×10^{12}	3×10^{12}
Particle mass (m_s) ($\times 10^{-16}$ kg)	8.3	8.3	5.9	3.3
AgI mixing ratio (X_s) ($\times 10^{-9}$ kg kg^{-1})	0.08	0.19	0.31	0.20

3.2 Initial and boundary conditions

Within the seeding zone, the initial temperature lapse rate is 7 K/km, while the pressure at $t = -10$°C is $p = 550$ hPa representing the mean climatological values for the April–October period with active hail suppression in Serbia. The seeding zone depth in our calculations is $d = 571$ m.

The initial simulated vertical velocity profile is taken from a model simulation of a hail cloud performed by *Ćurić* and *Janc* (1989) in the form:

$$w_0(z) = w_0 + k_w z, \tag{10}$$

where w_0 is the vertical velocity at the bottom boundary, while $k_w = 0.008$ s^{-1}. Eq. (10) represents in-cloud vertical velocity for unseeded case and it is held

fixed in time. It also includes the loading of total hydrometeor content (drops and ice particles).

Both cloud and rain water mixing ratios are set to be fixed with height in agreement with calculated profiles (*Ćurić* and *Janc*, 1989) within the seeding zone. Total liquid water mixing ratio is supposed to be $Q = 5 \times 10^{-3}$ kg kg^{-1} in all experiments. This implies that the mean cloud drop radius is also fixed with height in agreement with Eqs. (1) and (2). Two values of the mean drop spectrum radius are used: $R_M = 10$ and 20 μm, respectively.

At the bottom boundary temperature and pressure are respectively –8 °C and 570 hPa. Vertical velocity (w_0) at the bottom boundary of the seeding zone takes values of 5, 10, 15 and 20 m s^{-1}. At the top boundary the temperature is –12 °C, while the pressure is determined by the static equation. The vertical velocity is calculated by Eqs. (5) and (10).

3.3 Results

In order to investigate the capability of seeding agents to produce the additional cloud ice and then graupel within the seeding zone under certain atmospheric conditions, we perform numerical experiments taking into account the characteristics of seeding agents which are used in hail suppression in Serbia (Table 1). We especially focus on analyses of different mechanisms leading to graupel formation.

Fig. 1 shows the number concentration of cloud ice formed via contact nucleation ($N_{ci,cn}$, m^{-3}) versus time within the seeding zone for different cloud atmospheres and $w_0 = 5$ m s^{-1}. According to the proposed efficiency curve for contact nuclei which shows an exponential dependence on supercooling, it is reasonable that the number concentration of cloud ice grows with time for each agent. The cloud ice production is the greatest for PP-6 agent (greatest value of X_s, Table 1) because the active number of contact nuclei is proportional to X_s (*Hsie et al.*, 1980). Number concentrations of cloud ice are much smaller for $R_M = 20$ μm (Fig. 1b) than for $R_M = 10$ μm (Fig. 1a). This is entirely due to more KM distributed raindrops for $R_M = 20$ μm, which in turn, produce more efficient collisions with cloud ice to form graupeln.

In contrast to cloud ice produced by contact nucleation, with that formed by deposition one provides much higher number concentrations (*Fig. 2*; an order of magnitude 10^3 m^{-3} for PP-6 agent) due to different nature of these mechanisms. Cloud ice is formed instantaneously from activated deposition nuclei (*Lamb et al.*, 1981; *Ćurić* and *Janc*, 1990), as opposed to that formed via less efficient contact nucleation mechanisms. Consequently, the cloud ice number concentrations are only slightly smaller for $R_M = 20$ μm (Fig. 2b) than for $R_M = 10$ μm (Fig. 2a).

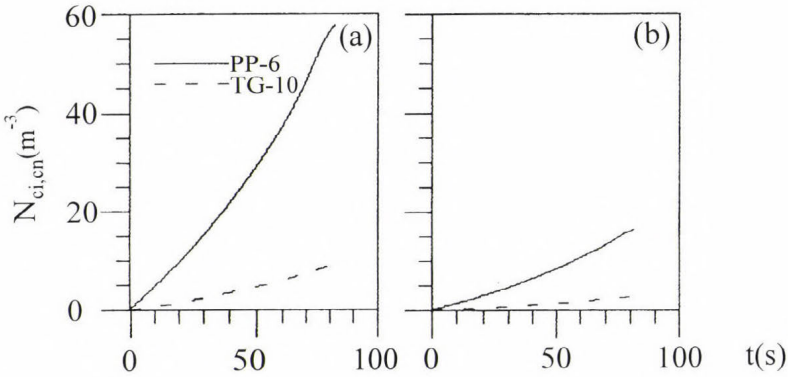

Fig. 1. Cloud ice number concentration generated via contact nucleation, ($N_{ci,cn}$, m^{-3}), versus time for TG-10 and PP-6 agents. Figures labeled *a* and *b* refer to R_M = 10 μm and R_M = 20 μm, respectively. Calculations are performed for w_0 = 5 m s^{-1}.

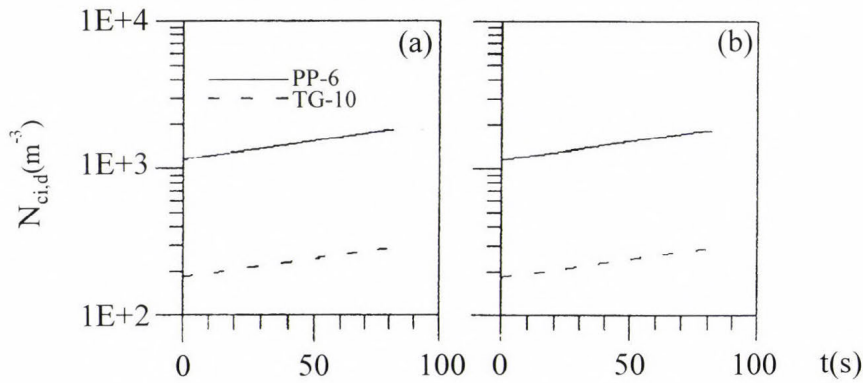

Fig. 2. As in Fig. 1, but for number concentration of cloud ice generated via deposition nucleation ($N_{ci,d}$, m^{-3}).

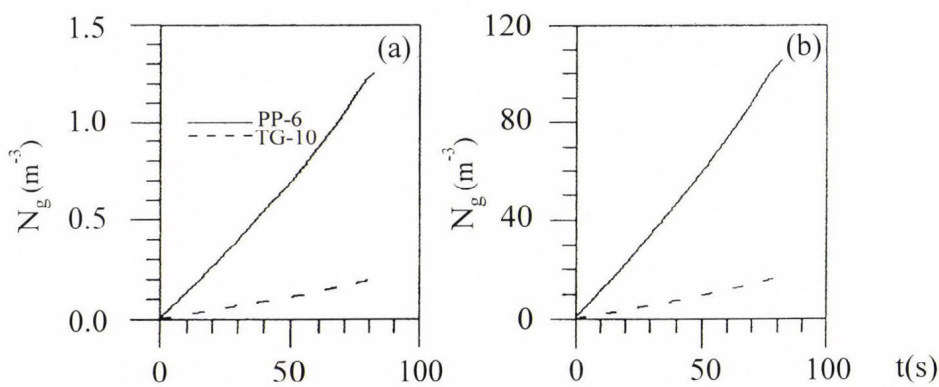

Fig. 3. As in Fig. 1 but for graupel number concentration (N_g, m^{-3}).

Fig. 3 clearly shows that the graupel number concentration grows with time as a consequence of the simultaneous cloud ice production within the seeding zone. Corresponding graupel production depends heavily on raindrop number concentration due to the rain/cloud ice collisions. Therefore graupel number concentration is several times greater for $R_M = 20$ μm (Fig. 3b) than for the smaller value of the mean cloud drop spectrum radius (Fig. 3a).

The number of active contact (or deposition) nuclei shows the rapid growth with increased supercooling (maximum at $\Delta T = 20°C$ for contact nuclei and corresponding maximum for deposition ones at still lower temperature). On the other hand, the turbulent diffusion of the agent particles (Eq. 6) cannot reduce significantly the number of active nuclei within the short time interval ($t \sim 100$ s). Therefore, the number concentrations of both contact and deposition active nuclei grow with time for each agent (*Fig. 4*).

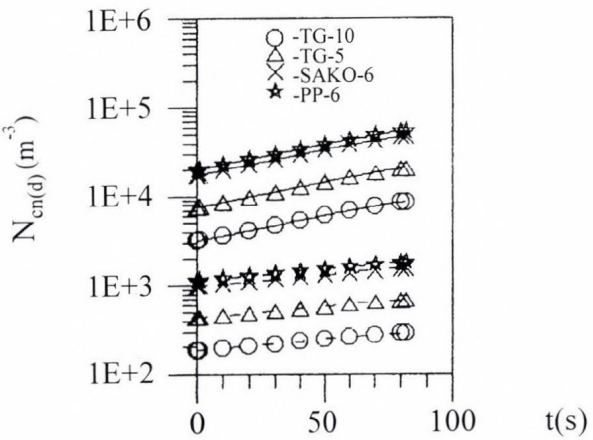

Fig. 4. Number concentrations of active contact nuclei (N_{cn}, m^{-3}; solid lines) and deposition ones (N_d, m^{-3}; dash lines) within the seeding zone for different agents and $w_0 = 5$ m s^{-1}.

Time evolution of each particular mechanism within the seeding zone for PP-6 agent and two cloud environments is presented in *Fig. 5*. It should be noted that each particular mechanism grows with time (Figs. 5a and 5b) because the number concentrations of active contact and deposition nuclei increase with time (Fig. 4) and simultaneously, cloud ice and graupel number concentrations increase. For $R_M = 10$ μm (Fig. 5a), the graupel growth rate with respect to cloud water (J_{gc}) takes the greatest value, and successively the Brownian and inertial collection rates due to cloud droplets (J_{bc} and J_{ic}), the rates of rain accreting cloud ice formed by contact and deposition nucleations (J_{rcn} and J_{rd}) and the Brownian and inertial collection rates due to raindrops (J_{br} and J_{ir}).

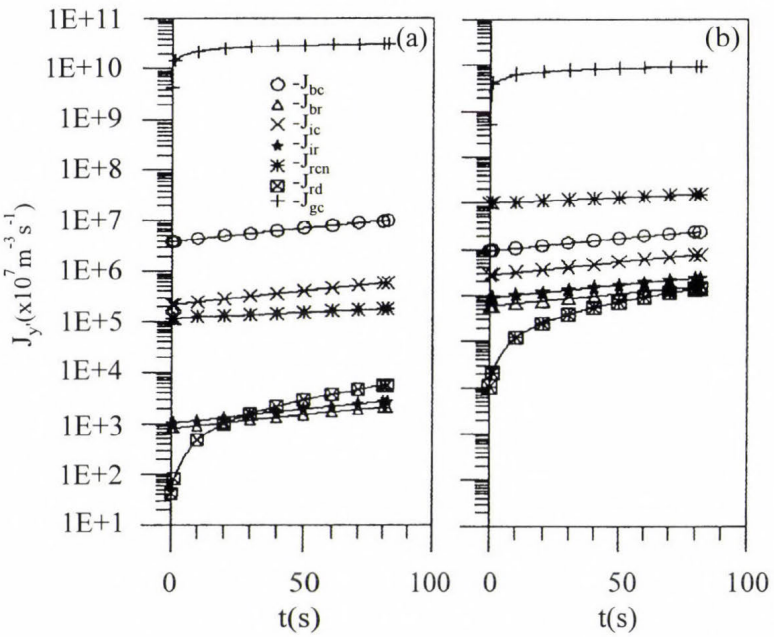

Fig. 5. Time evolution of different mechanisms, ($J_{y'}$, 10^7 m^{-3} s^{-1}) for PP-6 agent within the seeding zone for w_0 = 5 m s^{-1}. The subscript *y'* may be *bc* (Brownian collection rate due to cloud droplets), *br* (Brownian collection rate due to raindrops), *ic* (inertial collection rate due to cloud droplets), *ir* (inertial collection rate due to raindrops), *rcn* (collection rate of raindrops with respect to cloud ice generated via contact nucleation), *rd* (collection rate of raindrops with respect to cloud ice generated via deposition nucleation and *gc* (graupel growth with respect to cloud water). Figures labeled *a* and *b* refer to R_M = 10 μm and R_M = 20 μm, respectively.

In contrast to cloud environment with R_M = 10 μm, that one with R_M = 20 μm consists of more large drops and less small ones, which in turn, leads to an increase in magnitude of all mechanisms with raindrops and a corresponding decrease of those with cloud droplets (except inertial collection rate; *Fig. 6b*). Now, the term J_{rcn} surpasses terms J_{bc} and J_{ic}, while those denoted by J_{br} and J_{ir} surpass the term J_{rd}. Since the behavior of different mechanisms with time for the other agents is alike that for PP-6 agent, they are not represented graphically (number concentration of active contact or deposition nuclei shows a linear dependence of X_s).

In order to answer the question which mechanism contributes most to cloud ice, graupel formation and depletion of cloud water, we have done additional analysis whose results are represented over the coefficient

$$k_{ty'} = \frac{\dfrac{dN_{ty'}}{dt}}{\dfrac{dN_t}{dt}}, \tag{11}$$

where the subscript t refers to cloud ice formed by contact nucleation (*icn*), graupel (*g*) and cloud water (*c*), while *y'* refers to the Brownian and inertial collection rates due to cloud droplets and raindrops (*bc, ic, br, ir*), rates of rain accreting cloud ice formed by contact and deposition nucleation (*rcn, rd*) and graupel growth rate with respect to cloud water (*gc*). The quantity of a type $N_{ty'}$ or N_t refers to corresponding number concentration.

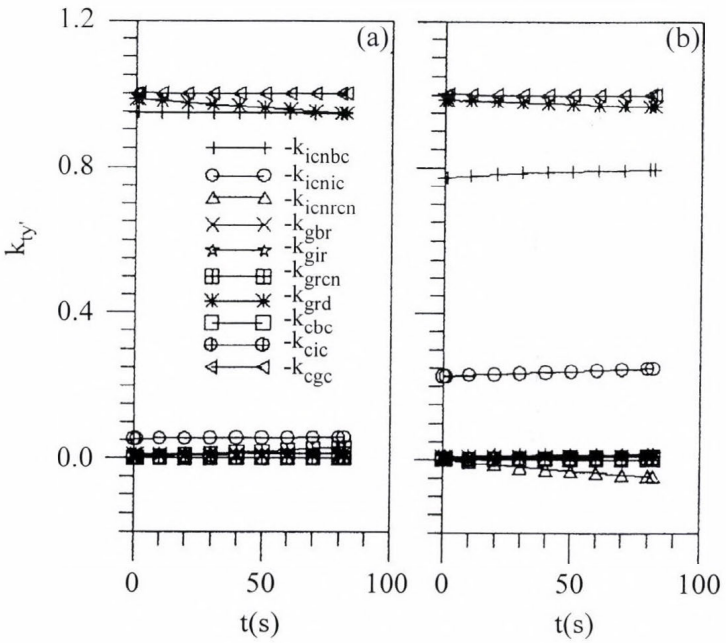

Fig. 6. Coefficient $k_{ty'}$ versus time for different mechanisms which contribute to cloud ice formed via contact nucleation (t = *icn*), graupel production (t = *g*) and depletion of cloud water (t = *c*). Figures labeled *a* and *b* refer to R_M = 10 μm and R_M = 20 μm, respectively. Calculations are performed for w_0 = 5 m s^{-1}.

The coefficient (11) versus time for w_0 = 5 m s^{-1} and two mean drop spectrum radii is represented in Fig. 6. It should be noted that the Brownian collection rate due to cloud droplets contributes most to cloud ice, the main sink

term for cloud water is the graupel accretional growth, while the collisions of raindrops and cloud ice of deposition nucleation origin is the main source for graupel. The role of the other mechanisms can be ignored ($k_{ty'}$ close to zero) except somewhat the inertial collection rate due to cloud droplets as a source term for cloud ice ($k_{ty'}$ is 0.05 for $R_M = 10$ μm, see Fig. 6a; $k_{ty'}$ varies between 0.23 and 0.25 for $R_M = 20$ μm, see Fig. 6b). Also, the role of the Brownian collection rate due to cloud droplets in cloud ice formation decreases for $R_M = 20$ μm due to smaller number concentration of small droplets in such a drop spectrum (Fig. 6b). As noted, the magnitude of the collision rate between rain and cloud ice formed by deposition nucleation is nearly the smallest compared to the other mechanisms (Figs. 5a and b), but its role in graupel production is the most important. It is in agreement with the nature of deposition nucleation where the numerous deposition active nuclei convert water vapor into cloud ice immediately (see Fig. 2).

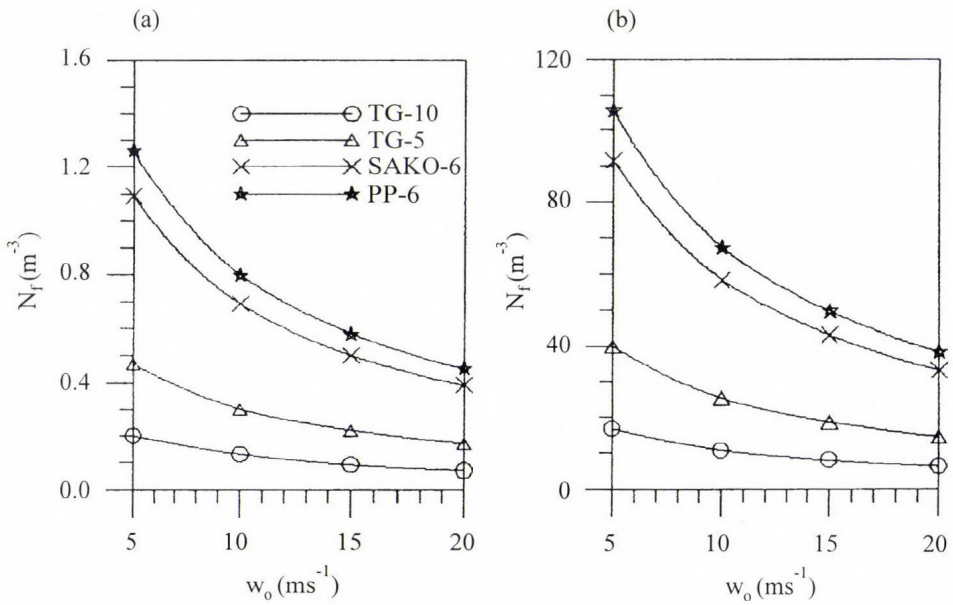

Fig. 7. Final graupel production, N_f (m^{-3}), vs vertical velocity at the bottom boundary, w_0 ($m\ s^{-1}$), for different agents. Figures labeled *a* and *b* refer to $R_M = 10$ μm and $R_M = 20$ μm, respectively.

Finally, we show the parameters which are important from the point of view of hail suppression methodology as it is applied in Serbia. They are: the graupel number concentration at the top boundary of the seeding zone called the final

graupel production (N_f) and the time need for the seeded air parcel to ascend throughout the seeding zone called the agent residence time (t_R). The final graupel production (produced from a single rocket per m^{-3}) versus vertical velocity at the bottom boundary of the seeding zone is presented in *Fig. 7.* Our findings give us the opportunity to conclude that the final graupel production shows an exponential dependence on corresponding vertical velocity. The PP-6 agent is the most efficient in graupel production. It produces the graupel number concentrations of 1.26 m^{-3} and 105.7 m^{-3} within its residence time of 82 s for $w_0 = 5$ m s^{-1}.

The agent residence time for different vertical velocities at the bottom boundary is shown in *Table 2.* As noted, it is independent of an agent type because the buoyancy effects and the loading term in Eq. (5) can be ignored. The effect of phase transitions on vertical velocity is not important due to the small amounts of the agents and the short agent residence time. Calculated residence times agree well with results of *Slinn* (1971).

Table 2. The agent residence time (t_R) for different vertical velocities at the bottom boundary of the seeding zone (w_0)

w_0 (m s^{-1})	5	10	15	20
t_R (s)	82	48	34	26

The considered graupel production refers only to that associated with the maximum seeding agent mixing ratio. Our calculations show that the representative value of the spread parameter due to the agent dispersion is 50 m within the agent residence time according to the procedure proposed by *WMO* (1980). Concentration of the agent particles decreases rapidly (most often exponentially, *Hsie et al.*, 1980) outside the agent cloud center. On such a way, most of the graupel production per unit volume is taken into account.

4. Conclusions

1-D kinematic model with detailed microphysics is used to find out the graupel production within the seeding zone after agent injection at its bottom boundary following the concept of the hail suppression in Serbia. The behavior of four seeding agents is investigated. They all have the same chemical composition but they differ from each other in geometry. For conditions close to those occurring during the seeding operation we conclude:

- The PP-6 agent gives the largest, and TG-10 the smallest graupel production within the seeding zone. The final graupel production is an

exponential function of the vertical velocity at the bottom boundary of the seeding zone, while the agent residence time is independent of an agent type. The better performance of the PP-6 agent directly depends on the ratio of its maximum mixing ratio and mean particle size;

- Among mechanisms which are responsible for graupel production, the Brownian collection due to cloudy droplets is the greatest in magnitude for the cloud atmosphere with the lack of raindrops, while the rate of rain accreting cloud ice formed via contact nucleation is the greatest for an environment with larger drops. However, the rate of rain accreting cloud ice of deposition nucleation origin is the most important for graupel production due to numerous active deposition nuclei which convert water vapor into cloud ice immediately.

Acknowledgements—The research was supported by the Hydrometeorological Service of Serbia under the contract "The Research in Hail Suppression". Two anonymous reviewers have made many suggestions in the reviewing process that increased the completeness and clarity of the paper. These contributions are appreciated.

References

Alkezweeny, A.J., 1971: A contact nucleation model for seeded clouds. *J. Appl. Meteor. 10*, 732-738.

Cooper, W.A., 1974: A possible mechanism for contact nucleation. *J. Atmos. Sci. 31*, 1832-1837.

Cotton, W.R., Stephens, M.A., Nehrkorn, T. and *Tripoli, G.J.*, 1982: The Colorado State University three-dimensional cloud/mesoscale model-1982. Part II: An ice phase parameterization. *J. Rech. Atmos. 16*, 295-320.

Cotton, W.R., Tripoli, G.J., Rauber, R.M. and *Mulvhill, E.A.*, 1986: Numerical simulation of the effects of varying ice crystal nucleation rates and aggregation processes on orographic snowfall. *J. Climate Appl. Meteor. 114*, 718-733.

Ćurić, M. and *Janc, D.*, 1989: Dynamic entrainment rate influence on products of a one-dimensional cumulonimbus model. *Atmos. Res. 24*, 305-323.

Ćurić, M. and *Janc, D.*, 1990: Numerical study of the cloud seeding effects. *Meteorol. Atmos. Phys. 42*, 145-164.

Ćurić, M. and *Vuković, Z.*, 1991: The influence of thunderstorm thunderstorm-generated acoustic waves on coagulation. Part I: Mathematical formulation. *Z. Meteorol. 41*, 164-169.

Farley, R.D., 1987: Numerical modeling of hailstorms and hailstone growth. Part III: Simulation of an Alberta hailstorm-natural and seeded cases. *J. Climate Appl. Meteor. 26*, 789-812.

Farley, R.D., Nguyen, P. and *Orville, H.D.*, 1994: Numerical simulation of cloud seeding using a three-dimensional cloud model. *J. Wea. Mod. 26*, 113-124.

Farley, R.D., Chen, H., Orville, H.D. and *Hjelmleft, H.R.*, 1996: The numerical simulation of the effects of cloud seeding on hailstorms. *Preprints 13th Conf. on Planned and Inadvertent Weather Modification*. Atlanta. GA. Amer. Meteor. Soc., 23-30.

Fuchs, N.A., 1964: *The Mechanics of Aerosols*. Pergamon Press, Oxford.

Fukuta, N.,1980: Advances in Cloud Physics. (Textbook). University of Utah.

Holroyd, E.W., Heimbach, J.A. and *Super, A.*, 1995: Observations and model simulation of AgI seeding within the winter storm over Utah's Wasatch Plateau. *J. Wea. Modif. 27*, 36-56.

Hsie, E-Y., Farley, R.D. and *Orville, H.D.*, 1980: Numerical simulation of ice-phase convective cloud seeding. *J. Appl. Meteor. 19*, 950-977.

Huter, M., Prelesnik, B., Ćurić, M., Mitić, D. and *Herak, R.*, 1988: X-ray diffraction analysis of aerosols obtained burning of the AgI based pyrotechnics. In *Atmospheric Aerosols and Nucleation* (eds.: *P.E. Wagner* and *G. Vali*). Springer, Berlin, Heidelberg. (Lecture Notes in Physics, 309).

Kopp, F.J., 1988: A simulation of Alberta cumulus. *J. Appl. Meteor. 27*, 626-641.

Lamb, D., Hallett, J. and *Sax, R.I.*, 1981: Mechanistic limitations to the release of latent heat during the natural and artificial glaciation of deep convective clouds. *Quart. J. Roy. Meteor. Soc. 107*, 935-954.

Levy, G. and *Cotton, W.R.*, 1984: A numerical investigation of mechanisms linking glaciation of the ice-phase to the boundary layer. *J. Climate Appl. Meteor. 23*, 1505-1519.

Lin, Y-L., Farley, R.D. and *Orville, H.D.*, 1983: Bulk parameterization of the snow field in a cloud model. *J. Climate Appl. Meteor. 22*, 1065-1092.

Liu, J.Y. and *Orville, H.D.*, 1969: Numerical modeling of precipitation and cloud shadow effects on mountain-induced cumuli. *J. Atmos. Sci. 26*, 1283-1298.

Marshall, J.S. and *Palmer, W. McK.*, 1948: The distribution of raindrops with size. *J. Meteor. 5*, 165-166.

Mesinger, F. and *Mesinger, N.*, 1992: Has hail suppression in Eastern Yugoslavia led to a reduction in the frequency of hail? *J. Appl. Meteor. 34*, 104-111.

Murakami, M., 1990: Numerical modeling of dynamical and microphysical evolution of an isolated convective cloud - the 1981 July 1981 CCOPE cloud -. *J. Meteor. Soc. Japan 68*, 107-128.

Orville, H.D. and *Chen, J.-M.*, 1982: Effects of cloud seeding, latent heat of fusion,and condensate loading on cloud dynamics and precipitation evolution: A numerical study. *J. Atmos. Sci. 39*, 2807-2827.

Orville, H.D., Farley, R.D. and *Hirsch, J.H.*, 1984: Some suprising results from simulated seeding of stratiform-type clouds.*J. Climate Appl. Meteor.* 12, 517-521.

Pruppacher, H.R. and *Klett, J.D.*, 1978: *Microphysics of Clouds and Precipitation*. D. Reidel, Dordrecht.

Radinović, Dj., 1989: Effectiveness of hail control in Serbia. *J. Wea. Mod. 21*, 75-84.

Reisin, T., Levin, Z. and *Tzivion, S.*, 1966: Rain production in convective clouds as simulated in an axisymmetric model with detailed microphysics. Part I: Description of the model. *J. Atmos. Sci. 53*, 497-519.

Slinn, W.G.N., 1971: Time constants for cloud seeding and tracer experiments. *J. Atmos. Sci. 27*, 299-307.

Sulakvelidze, G.K., 1967: *Showers and Hail* (in Russian). Gidrometeoizdat, Leningrad.

Young, K.C., 1974a: The role of contact nucleation in ice-phase initiation in clouds. *J. Atmos. Sci. 31*, 768-776.

Young, K.C., 1974b: A numerical simulation of wintertime,orographic precipitation:Part I. Description of model microphysics and numerical techniques. *J. Atmos. Sci. 31*, 1735-1748.

Young, K.C., 1974c:A numerical simulation of wintertime, orographic precipitation: Part II, Comparison of natural and AgI-seeded conditions. *J. Atmos. Sci. 31*, 1749-1767.

Young, K.C., 1993: *Microphysical Processes in Clouds*. Oxford University Press, Oxford.

Wisner, C.E., Orville, H.D. and *Myers, C.G.*, 1972: A numerical model of a hail-bearing cloud. *J. Atmos. Sci. 29*, 1160-1181.

WMO, 1980: *Dispersion of Cloud Seeding Reagents*. Precipitation Enhancement Project. Rep. No. 14, Weather Modification Programme. WMO, Geneva.

APPENDIX A

Microphysical production terms

The rate of change in number concentration (m^{-3} s^{-1}) of cloud ice produced by the Brownian collection rate due to cloud droplets and phoretic processes (diffusiophoresis and thermophoretic contact nucleations) is in agreement with *Cotton et al.* (1986)

$$J_{bfc} = 4\pi D_s N_{cn} F \int_0^{R_{min}} Rf(R)\,dR = \frac{24\pi D_s AFN_{cn}\alpha_2}{B^4}, \tag{A1}$$

where

$$\alpha_2 = \frac{\Gamma(4; BR_{\min})}{6}; \quad F = 1 + \frac{F_2}{D_s}\left(f_T - \frac{R_V T}{L_V}\right); \quad F_2 = \frac{G(T,p)SL_v}{p} \tag{A2}$$

and

$$f_T = \frac{0.4\left[1 + 1.45K_N + 0.4\,K_N \exp(-1/K_N)\,(K_N + 2.5\,K_N K_A)\right]}{(1 + 3K_N)(2K + 5K_A K_N + K_A)}. \tag{A3}$$

The quantities in Eqs. (A1) to (A3) are: D_s is the diffusivity of the silver-iodide, S is the saturation ratio over water, L_V is the latent heat of vaporization, R_V is the specific gas constant for water vapor, p is the in-cloud pressure, T is the in-cloud temperature, K is the thermal conductivity of the air, K_A is the thermal conductivity of the silver-iodide taken to be 5.39×10^{-9} J m^{-1} s^{-1} K^{-1}, e_S is the saturated water vapor pressure at temperature T, K_N is the Knudsen number, N_{cn} is the number concentration of contact nuclei, and $G(T,p)$ is the thermodynamic function as defined by *Cotton et al.* (1982).

The rate of change in number concentration of graupel particles formed by Brownian collection rate due to raindrops is calculated similarly to that for cloud droplets, i.e.:

$$J_{br} = 4\pi D_s N_{cn} \int_{R_{\min}}^{\infty} Rf(R)\,dR = \frac{24\,\pi D_s N_{cn} A(1 - \alpha_2)}{B^4}. \tag{A4}$$

The inertial collection rates due to cloud droplets and raindrops and the accretion terms require the knowledge of terminal velocities of drops and graupel particles. We use the expressions for terminal velocities of cloud droplets (U_c), raindrops (U_r) and graupel particles (U_g) proposed by *Murakami* (1990), *Liu* and *Orville* (1969) and *Lin et al.* (1983), respectively as follows

$$U_c = cR^d \frac{\rho_0}{\rho}; \quad U_r = aR^b \left(\frac{\rho_0}{\rho}\right)^{0.5}; \quad U_g = kR_g^{0.5}; \quad k = \left(\frac{8\rho_g}{3\rho C_d}\right)^{0.5}, \tag{A5}$$

where $c = 1.2 \times 10^8$ m^{-1} s^{-1}, $d = 2$, $a = 1465$ m$^{0.2}$ s^{-1}, $b = 0.8$, ρ_0 is the reference air density (set to 1.2 kg m^{-3}), ρ_g is the graupel density with a value appropriate for hard ice, C_d is the drag coefficient (set to 0.6) and R_g is the graupel radius.

The rate of change in number concentration of cloud ice formed by the inertial collection due to cloud droplets is in agreement with *Hsie et al.* (1980)

$$J_{ic} = \pi E_{ac} N_{cn} \int_0^{R_{\min}} U_c R^2 f(R)\, dR = \frac{720\, \pi\, c E_{ac} A N_{cn} \rho_0 \alpha_3}{\rho B^7}, \tag{A6}$$

where

$$\alpha_3 = \frac{\Gamma(7; BR_{\min})}{720} \tag{A7}$$

and E_{ac} is the collection efficiency of cloud droplets for the seeding agent particles, set to 10^{-4} (*Pruppacher* and *Klett*, 1978).

The rate of change in number concentration of graupeln produced by the inertial collection rate due to raindrops may be derived similarly to Eq. (A6) as:

$$J_{ir} = \pi E_{ar} N_{cn} \int_{R_{\min}}^{\infty} U_r R^2 f(R)\, dR = \frac{\pi a E_{ar} A N_{cn} \Gamma(5.8)(1 - \alpha_4)}{B^{5.8}} \left(\frac{\rho_0}{\rho}\right)^{0.5}, \tag{A8}$$

where

$$\alpha_4 = \frac{\Gamma(5.8; BR_{\min})}{\Gamma(5.8)} \tag{A9}$$

and E_{ar} is the collection efficiency of raindrops for the seeding agent particles set to 0.5×10^{-4} (*Fuchs*, 1964).

The rate of change in number concentration of graupeln by collisions between raindrops and cloud ice formed by contact or deposition nucleations may be derived by applying the stochastic collection equation with "sweep-out" concept in the form:

$$J_{rx} = \int_{R_{\min}}^{\infty} \pi R^2 E_{rx} U_r N_{ci,x} f(R)\, dR = \frac{\pi a E_{rx} N_{ci,x} A \Gamma(5.8)(1 - \alpha_4)}{B^{5.8}} \left(\frac{\rho_0}{\rho}\right)^{0.5}, \tag{A10}$$

where E_{rx} is the collection efficiency of raindrops for cloud ice taken to be 0.1 in accordance with *Lamb et al.* (1981), while $N_{ci,x}$ is the number concentration of cloud ice formed by contact ($x = cn$) or deposition ($x = d$) nucleations.

The rate of change in number concentration of graupeln due to the accretion of cloud water by graupeln is determined by the integration of the stochastic collection equation under the assumption that the graupel terminal velocity always exceeds that of cloud droplets as follows

$$J_{gc} = \pi E_{gc} \int_0^{R_{\min}} \int_0^{\infty} (R + R_g)^2 \, | U_c - U_g | N_g f(R) dR \, dR_g$$

$$= \pi E_{gc} N_{0g} A \sum_{i=1}^{3} C_i \left[\frac{k\Gamma(6 - i; BR_{\min})\Gamma(i + 0.5)}{B^{6-i}(2\lambda_g)^{i+0.5}} - \frac{c\Gamma(8 - i; BR_{\min})\Gamma(i)}{B^{8-i}(2\lambda_g)^{i}} \right], \quad \text{(A11)}$$

where $C_1 = C_3 = 1$, $C_2 = 2$; E_{gc} is the collection efficiency of graupel for cloud water taken to be 0.5 in accordance with *Lamb et al.* (1981); N_{0g} is the intercept value in graupel size distribution; N_g is the graupel number concentration and λ_g is the slope parameter of graupel size distribution. The graupel growth via gravitational coagulation is equal to zero for cloud droplets less than 10 μm in diameter (*Pruppacher* and *Klett*, 1978). The parameter N_{0g} in graupel size distribution is calculated by the help of number concentration and mixing ratio of graupel particles as well as their prognostic equations in the following manner.

Number concentration and mixing ratio of the graupel particles can be calculated as

$$N_g = \int_0^{\infty} N_{0g} \exp(-\lambda_g D_g) \, dD = \frac{N_{0g}}{\lambda_g}, \quad \text{(A12)}$$

$$Q_g = \int_0^{\infty} \frac{\pi}{6} \frac{\rho_w}{\rho} D_g^3 N_{0g} \exp(-\lambda_g D_g) dD_g = \frac{\rho_w}{\rho} \pi \frac{N_{0g}}{\lambda_g^4}, \quad \text{(A13)}$$

where D_g is the graupel diameter.

The prognostic equation for graupel number concentration is in accordance with *Ćurić* and *Janc* (1990)

$$\frac{dN_g}{dt} = J_{bfc} + J_{ic} + J_{br} + J_{ir} + J_{rcn} + J_{rd}, \quad \text{(A14)}$$

where the terms on the right-hand side of (A14) are (A1), (A6), (A4), (A8) and (A10), respectively. The prognostic equation for graupel mixing ratio is

$$\frac{dQ_g}{dt} = S_{bfc} + S_{ic} + S_{br} + S_{ir} + S_{rcn} + S_{rd}, \tag{A15}$$

where the first four terms on the right-hand side of Eq. (A15) are calculated by Eq. (8) and the last two by

$$S_{rcn} = J_{rcn}\frac{M_i}{\rho}; \quad S_{rd} = J_{rd}\frac{M_i}{\rho}. \tag{A16}$$

By the help of Eqs. (A13) to (A16), we can find corresponding parameters of the graupel size distribution at each time step.

APPENDIX B

The first law of thermodynamics

Latent heat of fusion or sublimation is released during the formation of cloud ice and graupel or during their growth. In an early phase both ice crystals or graupel particles and supercooled cloud droplets and raindrops may exist. The sublimation growth of crystals operates together with evaporation of the supercooled drops. Therefore, in terms of sublimation growth of ice crystals we use the latent heat of fusion instead of latent heat of sublimation (*Lamb et al.*, 1981).

The adopted rates of heat released due to the contact nucleation of cloud droplets (Q_{cnc}), accretion of cloud droplets by graupel particles (Q_{gc}) and freezing of raindrops (Q_r) for the implemented *KM* size distribution are respectively

$$\frac{dQ_{cnc}}{dt} = L_f\left(\frac{3840\pi^2 D_s N_{cn} FA\rho_w\alpha_3}{B^7} + \frac{4838\pi^2 c E_{ac} N_{cn} A\rho_w\rho_0\alpha_5}{\rho B^{10}}\right), \tag{B1}$$

where

$$\alpha_5 = \frac{\Gamma(10; BR_{\min})}{\Gamma(10)}, \tag{B2}$$

$$\frac{dQ_{gc}}{dt} = L_f\left\{\frac{4}{3}\pi^2 E_{gc} N_{0g}\rho_w A\sum_{i=1}^{3} C_i\left[\frac{k\Gamma(9-i; BR_{\min})\Gamma(i+0.5)}{B^{9-i}(2\lambda_g)^{i+0.5}} - \frac{c\Gamma(11-i; BR_{\min})\Gamma(i)}{B^{11-i}(2\lambda_g)^i}\right]\right\}, \tag{B3}$$

$$\frac{dQ_r}{dt} = L_f \left[\frac{3840\pi^2 D_s N_{cn} A(1-\alpha_3)}{B^7} + \frac{4\pi^2 a \rho_w A \Gamma(8.8)(1-\alpha_6)}{3B^{8.8}} \left(\frac{\rho_0}{\rho} \right)^{0.5} \right.$$

$$\left. \times \left(E_{ar} N_{cn} + E_{rcn} N_{ci,cn} + E_{rd} N_{ci,d} \right) \right], \tag{B4}$$

where

$$\alpha_6 = \frac{\Gamma(8.8; BR_{\min})}{\Gamma(8.8)}. \tag{B5}$$

In Eqs. (B1), (B3) and (B4) L_f is the latent heat of fusion. In the case of sublimation growth of cloud ice the corresponding heat released for frozen cloud droplets (Q_{cn}) and crystals produced by deposition nucleation (Q_d) may be written in the form (*Lamb et al.*, 1981)

$$\frac{dQ_{cn}}{dt} = L_f N_{cn} \left(4\pi \overline{R_c} D \Delta\rho \right), \tag{B6}$$

$$\frac{dQ_d}{dt} = L_f N_d \left(4\pi C_{id} D \Delta\rho \right), \tag{B7}$$

where $\Delta\rho$ is the difference between saturated water vapor density with respect to water and ice, and C_{id} the electrostatic capacity for ice crystals generated by deposition nucleation set to be 35 μm. The mean cloud droplet spectrum radius is calculated as

$$\overline{R_c} = \frac{3\alpha_2}{B\alpha_1}. \tag{B8}$$

The total rate of released heat may be obtained by summation of Eqs. (B1), (B3), (B4), (B6) and (B7).

IDŐJÁRÁS

Quarterly Journal of the Hungarian Meteorological Service
Vol. 101, No. 2, April–June 1997, pp. 143–153

Ambient air quality status assessment in industrial belts — A case study of Hazira Kawas region

Swaroop R. Mudaliar, C. S. Sunil Kumar, Pawan Kumar, S. D. Badrinath and **C. V. Chalapati Rao**

National Environmental Engineering Research Institute, Nagpur–20, India; E-mail: root%neeri@ren.nic.in

(Manuscript received 14 February 1994; in final form 10 October 1994)

Abstract—The area of Hazira (India) has several industrial establishment. For investigation of the heavy pollution a well designed air quality monitoring network of 18 stations has been installed. The measurement program includes the determination of suspended particulate matter, sulfur dioxide, nitrogen dioxide, aldehyde, ammonia and some meteorological elements. The results obtained in May of 1991 are presented.

To predict the impact of the emitted pollution a steady state Gaussian plume dispersion model has been used. The predicted ground level concentration of nitrogen oxides, found to be a significant parameter, was computed as 37 $\mu g\ m^{-3}$, 37 $\mu g\ m^{-3}$ and 41 $\mu g\ m^{-3}$ in the NE direction during 10–18 hrs, 18–02 hrs and 02–10 hrs, respectively. The distances at which the maximum concentrations are likely to occur were predicted to be 0.5 km, 6 km and 6 km, respectively from the sources.

Key-words: nitrogen oxides, suspended particulate matter, sulfur dioxide, aldehydes, ammonia, modeling.

1. Introduction

The trend towards urbanization and greater industrialization has led, among other things, to the concentration of population in residential areas and heavier use of city highways. These in turn, have resulted in more severe and widespread contamination of our atmosphere. The atmosphere contains such a great variety of elements of different concentrations in time and space that its exact composition will always be somewhat indeterminate. Analytical methods can be used for measuring special forms and low levels of concentration of many elements which pollute the ambient air. The present paper describes the application of various tools and techniques used during the studies carried out in Hazira-Kawas region, India.

1.1 Study area

The study area is located at Hazira in western India which is situated 18 km North-West of Surat city in Gujarat State. The site is located west of Surat city and north of the Arabian sea (*Fig. 1*).

The major industries located in this region include:

- Oil and Natural Gas Commission (ONGC)'s gas processing complex,
- Essar's Sponge Iron Project,
- GAIL — gas receiving and compression station,
- National Thermal Power Corporation (NTPC)'s gas based power plant,
- Plant of the Petro Polyols Ltd.,
- Narmada Cement Company,
- Petrochemical Complex of Reliance Industries Ltd.

The siting of so many industries in a small area has increased the level of pollution. The proximity of the densely populated Surat city to this area has made the issue of pollution more acute.

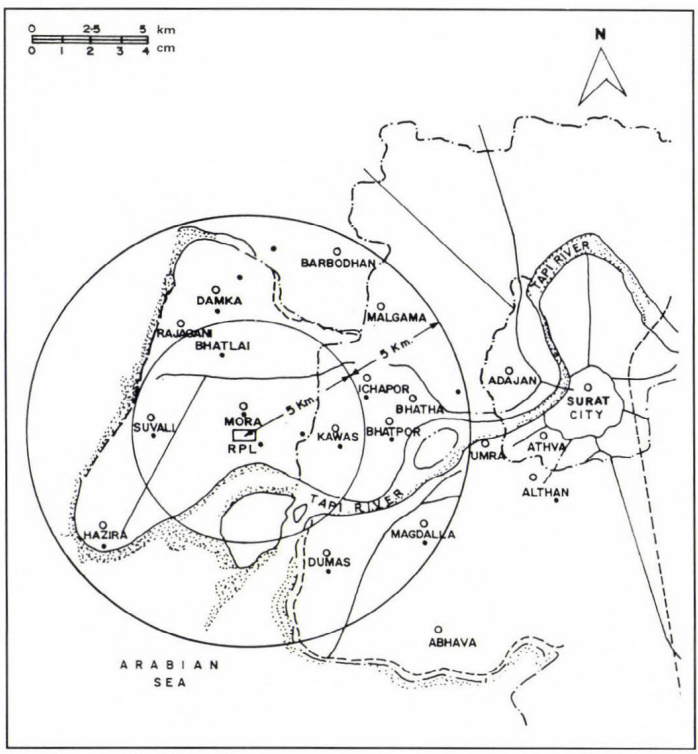

Fig. 1. Ambient air quality monitoring stations.

2. *Materials and methods*

2.1 Measurements

Ambient Air Quality was assessed through a network of 18 ambient air quality stations (*Indian Standards*, 1979) during summer season i.e. in May, 1991. Suspended particulate matter (SPM), sulfur dioxide, nitrogen oxides, ammonia and aldehydes were monitored during the study period. High volume samplers were used for collection of aerosol samples for SPM while sampling of gaseous pollutants were carried out by means of impingers of 35 ml capacity. Into the impingers the air was drawn at an impingement rate of 1 ℓ m^{-1}.

The following analytical methods were used for measuring the concentrations of various gases:

Sulfur dioxide	—	West and Gaeke method (see: *Indian Standards*, 1969)
Nitrogen dioxide	—	Jacob and Hochhiesser method (see: *Indian Standards*, 1974)
Aldehyde	—	Methyl benzothiazolone hydrozone hydrochloride method (see *Katz*, 1977)
Ammonia	—	Nesslerisation method (see *Katz*, 1977).

The various meteorological parameters e.g. wind speed, wind direction and temperature were recorded using a computerised weather monitoring unit. These data were recorded at every 10 minutes and further averaged for each hour during the whole study period. Hourly wind data were, later on, processed for wind-rose diagrams.

2.2 The model

In the study region, twenty-seven elevated point sources were identified in the proposed industrial complex out of which 21 stacks were considered as significant elevated continuous point sources for mathematical modeling (*Fig. 2* and *Table 1*).

Neither line nor area sources were considered because of the insignificant contribution of pollutants from these sources.

Hence, a short-term multiple point source Gaussian Plume Dispersion Model has been identified as the suitable model for prediction of impacts on air environment. The values of the dispersion were determined from Pasquill-Gifford dispersion curves suggested by *Turner* (1970). The hourly wind speed, solar insolation and total cloudiness during day time; and wind speed and total cloudiness during night time were used to determine the hourly atmospheric stability (*Turner,* 1970; *Pasquill*, 1974).

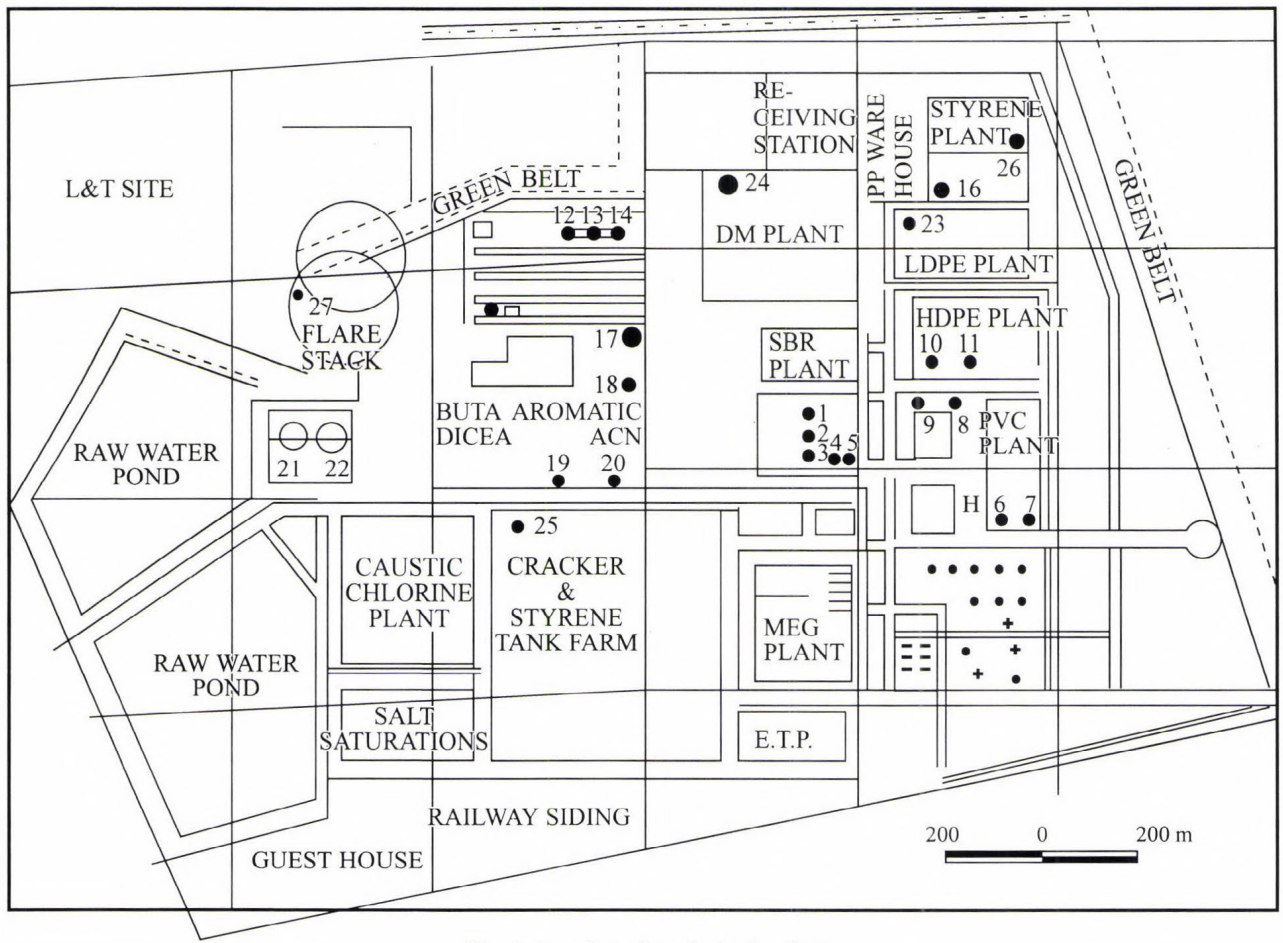

Fig. 2. Location of stacks in the plant.

Table 1. Expected emissions from different stacks

Stack No.	Stack description	NO_x emission rate 10^{-3} kg/sec
1.	Boiler-I	18.75190
2.	Boiler-II	18.75190
3.	Boiler-III	18.75190
4.	By-pass-I	9.78685
5.	By-pass-II	9.78685
6.	PVC dryer-I	0.777
7.	PVC dryer-II	0.777
8.	EDC cracking furnace-I	0.1263
9.	EDC cracking furnace-II	0.1263
10.	Incinerator	0.5277
11.	Hot oil heater	3.653
12.	Cracker furnace-I	4.311
13.	Cracker furnace-II	3.61100
14.	Cracker furnace-III	3.61100
15.	Cracker furnace-IV	3.61100
16.	Styrene reactor furnace	0.72200
17.	ACN reactor	0.34400
18.	HCN incinerator	0.08610
19.	Power plant	14.8500
20.	Power plant	12.66000
21.	Flare stack-I	4.8
22.	Flare stack-II	4.8
23.	LLDPE plant	Negligible
24.	Polypropylene plant	Negligible
25.	Polystyrene plant	Negligible
26.	Chlorine cumbercent	Negligible
27.	Flare stack	4.8

Note:
- Out of first five stacks, only three are used at a time.
- Normally gas is used as fuel.
- Flare stack emissions are normally from pilot burning.
- SO_2 from gas burning is negligible. The fuel gas supplied by ONGC is sweet gas.
- 23–26 are only vents for pneumatic conveying system. So except SPM & C12 (in the case of caustic/chlorine) other pollutants are not present.

2.3 Source data

The atmospheric emission rates from different stacks were computed based on emission factors for natural gas combustion and mass balance of raw materials and products involved in different processes.

The computed emission rates for nitrogen oxides are based on the theoretical estimates made for normal operating conditions which include all the forms of oxides of nitrogen e.g. NO, NO_2, but NO_2 forms a major portion of these oxides.

3. Results

The observed concentrations of various pollutants at all the sampling stations were processed for different statistical parameters like arithmetic mean, arithmetic standard deviation, geometric mean, geometric standard deviation, and various percentile values. The baseline levels of SPM, sulfur dioxide, nitrogen oxides, aldehyde and ammonia are expressed in $\mu g\ m^{-3}$ (*Tables 2* to *6*).

The arithmetic mean of 8 hourly SPM values at all these stations, ranged between 121 and 304 $\mu g\ m^{-3}$ whereas 95th percentile values of concentrations varied between 178 and 535 $\mu g\ m^{-3}$.

The higher SPM concentrations observed at Athwalines and Surat can be attributed to local and transportation activities.

At Reliance Petrochemicals Ltd. (RPL) site the SPM concentrations were found to be high due to construction activities and vehicular traffic through kuchha roads. At all other sites the 95th percentile values of suspended particulate matter concentrations were well within the limits stipulated by Central Pollution Control Board—India, National Ambient Air Quality Standards (NAAQS).

Lower concentrations of gaseous pollutants i.e. sulfur dioxide and nitrogen dioxide were observed during the period of study. The arithmetic mean of sulfur dioxide and nitrogen dioxide were found to be in the range of 3.0–17.8 and 3.0–7.9 $\mu g\ m^{-3}$, whereas the 95th percentile values were observed to be in the range of 3–28 $\mu g\ m^{-3}$ and 3–17 $\mu g\ m^{-3}$, respectively.

The 95th percentile values of ammonia and aldehydes varied in the range of 42–98 $\mu g\ m^{-3}$ and 13–30 $\mu g\ m^{-3}$, respectively, whereas average concentrations of ammonia and aldehydes ranged respectively between 24.2–5 $\mu g\ m^{-3}$ and 7.85–20.9 $\mu g\ m^{-3}$, thereby indicating very less concentrations in ambient air.

Aldehydes which have also been detected during ambient air quality monitoring could prove to be toxic, these are formed during the incomplete combustion and by interaction of nitrogen dioxide and hydrocarbons under influence of sunlight.

Sulfur dioxide levels were observed to be low as natural gas is used as basic raw material and fuel in the industries and hence sulfur dioxide contribution from industries is very low.

At the time of the study, KRIBHCO, ONGC and ESSAR plants were the major industries already in operation and the RPL plant was under construction.

Table 2. Ambient air quality status for suspended particulate matter (summer season; May 1991)

8 hrs avg. Unit : $\mu g\ m^{-3}$

Stat. No.	Sampling locations	Min. obs.	Percentile 10%	25%	50%	80%	95%	Max. obs.	Arithmetic Mean	S.D.	Geometric Mean	S.D.
1.	Ichchapore	59	59	111	156	192	278	316	166.2	70.16	151.1	1.58
2.	Kawas	126	126	178	223	336	454	476	265.5	108.64	243.7	1.52
3.	RPL site	74	84	130	220	310	533	549	237.9	137.43	201.8	1.79
4.	Mora	39	52	96	123	160	178	191	125.7	40.98	117.2	1.49
5.	Malgama	87	94	119	154	248	463	688	219.1	143.14	187.4	1.69
6.	Barbodhan	85	105	167	194	268	333	383	188.7	94.2	140.4	1.37
7.	Dumas	74	91	183	283	329	398	455	221.1	119.55	173.4	1.43
8.	Bhatpore	122	128	177	234	368	469	600	271.3	126.31	245.9	1.55
9.	Althan	65	68	88	159	357	435	509	215.2	137.58	174.3	1.94
10.	Adajan	127	129	180	233	304	384	403	207.6	112.74	191.9	1.39
11.	Bhata	142	148	178	256	400	475	523	292.2	120.49	267.8	1.52
12.	Suvali	150	152	167	183	269	299	300	215.1	52.67	208.9	1.27
13.	Bhatlai	48	65	164	195	344	471	545	249.3	132.66	212.7	1.83
14.	Damka	154	165	195	229	324	483	496	279.1	104.89	261.8	1.43
15.	Surat	185	187	244	290	312	535	581	303.5	99.9	289.5	1.34
16.	Umra	105	111	135	220	282	349	450	226.6	90.1	208.8	1.51
17.	Magdulla	116	124	145	191	286	354	456	212.4	103.73	178.5	1.47
18.	Hazira	47	50	75	90	157	248	303	121.3	69.59	105.7	1.67

Table 3. Ambient air quality status for sulfur dioxide (summer season; May 1991)

8 hrs avg. Unit : $\mu g\ m^{-3}$

Stat. No.	Sampling locations	Min. obs.	Percentile 10%	25%	50%	80%	95%	Max. obs.	Arithmetic Mean	S.D.	Geometric Mean	S.D.
1.	Ichchapore	3	3	3	3	3	4	6	3.7	1.1	3.0	1.3
2.	Kawas	3	3	3	3	3	3	3	3.0	0.0	3.0	1.0
3.	RPL site	3	3	3	3	3	5	7	3.4	1.11	3.2	1.27
4.	Mora	3	3	3	3	3	5	6	3.3	0.84	3.2	1.22
5.	Malgama	3	3	3	3	3	4	8	3.2	1.18	3.1	1.26
6.	Barbodhan	3	3	3	3	3	3	3	3.0	0.0	3.0	1.00
7.	Dumas	3	3	3	3	5	7	8	3.9	1.62	3.6	1.41
8.	Bhatpore	3	3	3	4	6	9	10	5.0	2.17	4.5	1.52
9.	Althan	3	3	3	3	3	6	10	3.5	1.68	3.3	1.36
10.	Adajan	3	3	3	3	0	6	7	3.5	1.19	3.4	1.31
11.	Bhata	3	3	3	3	5	6	8	3.7	1.31	3.5	1.33
12.	Suvali	3	3	3	3	3	5	9	3.6	1.46	3.4	1.33
13.	Bhatlai	3	3	3	3	4	7	9	3.8	1.25	3.5	1.39
14.	Damka	3	3	3	3	3	3	3	3.0	0.0	3.0	1.0
15.	Surat	3	3	12	20	24	28	28	17.8	7.74	15.2	1.92
16.	Umra	3	3	3	3	3	3	3	3.0	0.0	3.0	1.0
17.	Magdulla	3	3	3	3	4	7	9	3.7	1.57	3.4	1.36
18.	Hazira	3	3	3	3	3	3	3	3.0	0.0	3.0	1.0

Table 4. Ambient air quality status for nitrogen oxides (summer season; May 1991)

8 hrs avg. Unit : $\mu g\ m^{-3}$

Stat. No.	Sampling locations	Min. obs.	Percentile 10%	25%	50%	80%	95%	Max. obs.	Arithmetic Mean	S.D.	Geometric Mean	S.D.
1.	Ichchapore	3	3	3	3	3	3	3	3.0	0.0	3.0	1.0
2.	Kawas	3	3	3	3	3	9	12	4.29	2.52	3.84	1.52
3.	RPL site	3	3	3	3	3	3	3	3.0	0.0	3.0	1.0
4.	Mora	3	3	3	3	3	3	3	3.0	0.0	3.0	1.0
5.	Malgama	3	3	3	3	3	3	3	3.0	0.0	3.0	1.0
6.	Barbodhan	3	3	3	3	3	3	3	3.0	0.0	3.0	1.0
7.	Dumas	3	3	3	3	5	4	3	3.0	0.0	3.0	1.0
8.	Bhatpore	3	3	3	4	6	4	5	3.27	0.58	3.23	1.16
9.	Althan	3	3	3	3	3	6	8	3.47	1.24	3.33	1.29
10.	Adajan	3	3	3	4	7	11	11	5.38	2.89	4.73	1.64
11.	Bhata	3	3	3	3	5	6	7	3.83	1.34	3.65	1.35
12.	Suvali	3	3	3	3	3	3	3	3.0	0.0	3.0	1.0
13.	Bhatlai	3	3	3	3	4	3	3	3.0	0.0	3.0	1.0
14.	Damka	3	3	3	3	3	3	3	3.0	0.0	3.0	1.0
15.	Surat	3	3	5	6	7	17	2.5	7.89	5.37	6.63	1.76
16.	Umra	3	3	3	3	3	3	3	3.0	0.0	3.0	1.0
17.	Magdulla	3	3	3	3	4	3	3	3.0	0.0	3.0	1.0
18.	Hazira	3	3	3	3	3	3	3	3.0	0.0	3.0	1.0

Table 5. Ambient air quality status for ammonia (summer season; May 1991)

8 hrs avg. Unit : $\mu g\ m^{-3}$

Stat. No.	Sampling locations	Min. obs.	Percentile 10%	25%	50%	80%	95%	Max. obs.	Arithmetic Mean	S.D.	Geometric Mean	S.D.
1.	Ichchapore	15	14	20	40	71	142	180	59.2	48.81	44.40	2.11
2.	Kawas	3	3	6	15	49	160	236	44.5	66.52	17.90	3.87
3.	RPL site	3	3	3	20	54	67	81	29.9	66.40	15.20	3.76
4.	Mora	3	3	3	3	3	6	7	3.6	1.32	3.50	1.34
5.	Malgama	34	36	44	48	100	127	158	73.3	35.35	65.70	1.59
6.	Barbodhan	11	10	12	33	74	132	179	54.0	50.28	35.93	2.51
7.	Dumas	11	12	14	24	30	74	106	30.6	20.72	24.61	1.84
8.	Bhatpore	13	13	18	30	49	63	63	35.5	17.39	31.10	1.69
9.	Althan	3	3	3	11	78	91	105	33.0	36.11	15.13	3.77
10.	Adajan	3	3	3	41	74	95	103	44.7	35.93	21.24	4.49
11.	Bhata	4	4	7	15	26	41	44	20.0	12.92	15.01	2.16
12.	Suvali	3	3	3	3	13	31	46	10.6	12.68	6.40	2.51
13.	Bhatlai	3	3	3	3	20	35	46	12.9	13.28	7.70	2.75
14.	Damka	3	4	7	19	32	64	77	25.9	21.10	17.90	2.53
15.	Surat	11	11	25	41	50	54	57	36.6	14.18	32.90	1.66
16.	Umra	3	3	4	16	32	40	44	18.8	13.87	13.10	2.55
17.	Magdulla	3	3	6	12	38	77	140	26.4	34.37	14.01	3.01
18.	Hazira	3	3	3	3	8	12	12	5.8	3.46	4.90	1.76

Table 6. Ambient air quality status for aldehyde (summer season; May 1991)

8 hrs avg. Unit : $\mu g\ m^{-3}$

Stat. No.	Sampling locations	Min. obs.	Percentile					Max. obs.	Arithmetic		Geometric	
			10%	25%	50%	80%	95%		Mean	S.D.	Mean	S.D.
1.	Ichchapore	3	3	4	5	8	11	12	5.9	3.02	5.2	1.61
2.	Kawas	3	4	5	6	10	12	14	6.8	2.96	6.3	1.51
3.	RPL site	3	3	3	3	14	39	44	11.5	13.41	6.7	2.66
4.	Mora	3	3	3	4	6	7	9	4.3	1.71	4.0	1.41
5.	Malgama	3	3	3	6	9	19	21	7.1	5.30	5.7	1.87
6.	Barbodhan	3	3	3	4	6	14	18	6.0	4.49	4.9	1.77
7.	Dumas	3	4	7	9	11	13	14	9.0	3.12	8.1	1.52
8.	Bhatpore	4	4	4	7	9	11	112	7.1	2.68	1.6	1.49
9.	Althan	3	4	6	8	9	15	28	8.6	5.49	7.6	1.59
10.	Adajan	3	3	3	5	7	8	110	5.0	2.14	4.6	1.51
11.	Bhata	3	3	3	3	4	8	27	4.8	5.44	3.0	1.67
12.	Suvali	3	3	3	3	3	3	3	3.0	0.0	5.0	1.00
13.	Bhatlai	3	3	3	3	9	22	33	7.5	8.61	5.4	2.17
14.	Damka	3	3	4	5	7	13	20	6.2	4.07	5.4	1.66
15.	Surat	3	3	3	5	9	11	17	6.3	3.56	4.3	1.67
16.	Umra	3	3	3	4	5	8	9	4.6	1.84	3.0	1.43
17.	Magdulla	3	3	3	3	3	3	3	3.0	0.00	3.2	1.00
18.	Hazira	3	3	3	3	3	5	8	3.4	1.25	3.0	1.28

3.1 Micrometeorology

The 24 hour wind-rose at RPL shows the maximum occurrence of wind from WSW and SW directions. The predominant wind speed was observed to be in the range of 11–15 km/h.

Synoptic scale wind was observed to be dominant over diurnal sea and land breezes thereby nullifying their effect.

Therefore, insignificant diurnal variation in wind pattern was observed during the study period. During the survey period predominant wind directions were observed to be WSW and SW (diurnal).

3.2 Modeling results

To delineate the zone of high nitrogen oxides concentration (impact zone) isopleths were plotted. *Fig. 3* presents the isopleths of predicted nitrogen oxides during different time periods.

During summer season, predominant wind blew from the S-W quadrant. During day time, the maximum predicted nitrogen oxides concentration of 37 $\mu g\ m^{-3}$ (10–18 hrs) occurs at a distance of 1 km in NE direction. The occurrence of higher concentration near to the sources may be due to the prevailing unstable atmospheric conditions and higher mixing heights during day

time. During night time (18–02 hrs), maximum predicted nitrogen oxides concentration of 37 $\mu g\ m^{-3}$ occurs at 9–10 km far in NE direction, whereas during 02–10 hrs, it was found to be 41 $\mu g\ m^{-3}$ at 10 km distance in NE direction. The predicted concentration at far off distance from sources may be attributed to the combination of high stacks and stable atmospheric conditions. It can be concluded from the figures that the impact zone is limited to the NE sector during summer season. However, the post-project air quality status i.e. the super-imposition of predicted air quality over baseline air quality is within the recommended ambient air quality status.

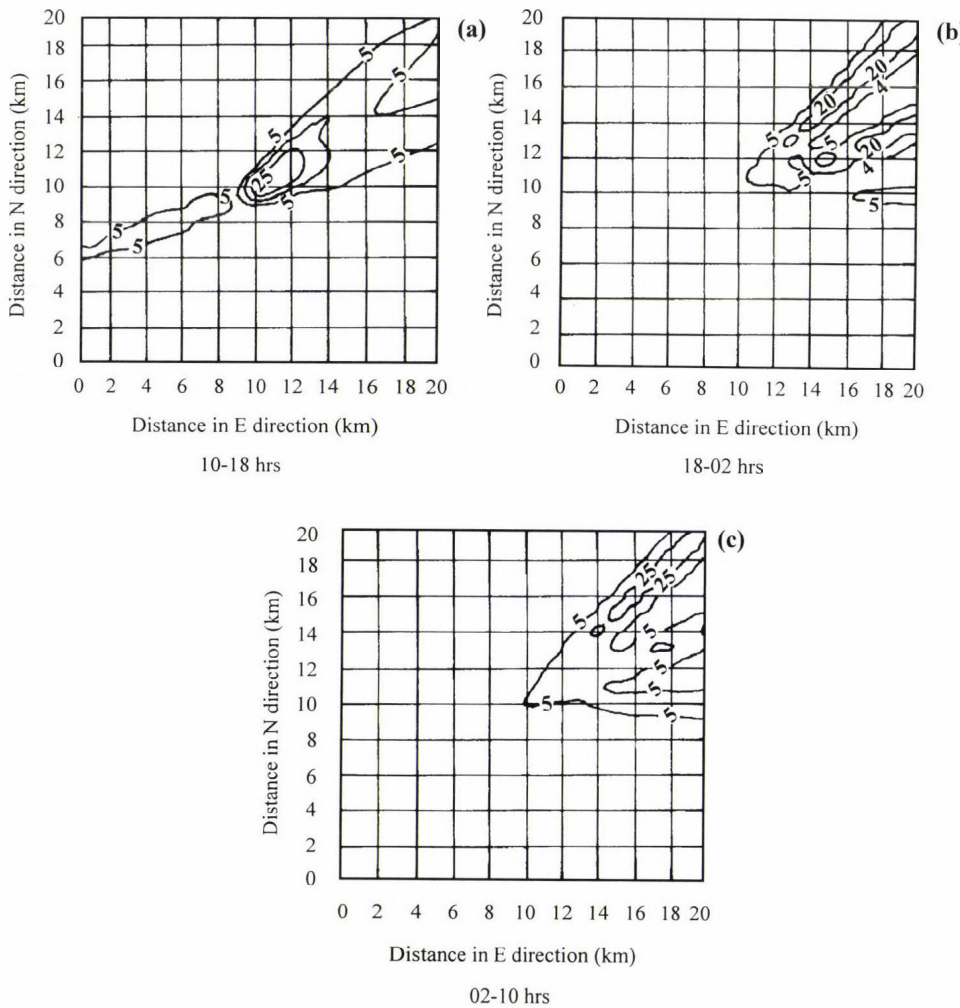

Fig. 3. Isopleths showing predicted NO_x concentration.

4. Recommendations

In order to avoid further degradation and maintain the ambient air quality status in Hazira region at least at the current levels in short run and improve the same the long run, following recommendations are made.

- The industrial area houses many industries as mentioned above (ESSAR, KRIBHCO, ONGC, GAIL); hence it is necessary to monitor the ambient air quality, stack emissions and meteorology on a regular basis through a well designed network.
- For reduction of nitrogen oxides, carbon monoxide, hydrocarbon emissions from various industries, the following measures are proposed:
  - proper burner maintenance,
  - good atomisation of liquid fuels,
  - optimum excess air levels,
  - staged combustion fuel gas recirculation.
- For reduction of hydrocarbons from storage tanks as fugitive emissions the following measures should be taken:
  - provision of floating roof or pressure storage for light hydrocarbons,
  - replacement of gland packing of pumps by mechanical seals,
  - proper maintenance of valves and other leakage prone areas.
- For reduction of particulates from the various industries, cyclones, scrubbers, or electrosatic precipitators or a combination of these can be used depending upon the type and size of the particulates.
- Greenbelt development should be undertaken to facilitate attenuation of pollutants from diverse industrial activities in the region. A minimum of 50–100 m greenbelt has been suggested around the proposed plant based on the attenuation of pollutants in the study area.

Acknowledgements—Authors wish to thank *Prof. P. Khanna*, Director of NEERI, for the kind approval to present the paper.

References

Indian Standards, 1969: *Methods for Measurements of Air Pollution — Sulfur dioxide*. 5182, Part II.

Indian Standards, 1974: *Suspended Particulate Matter*. 5182, Part IV.

Katz, M. (ed.), 1977: *Methods of Air Sampling and Analysis*. 2nd edition. American Public Health Association, Washington.

Pasquille, F., 1974: *Atmospheric Diffusion*. Wiley, New York.

Turner, D.B., 1970: *Workbook of Atmospheric Dispersion Estimates*. AP-26, Office of Air Programmes, USEPA, RTP, NC.

BOOK REVIEW

Richard J. Doviak, Dusan S. Zrnic: **Doppler Radar and Weather Observations.** Second edition. Academic Press Inc., 1993, San Diego, 11 chapters with problems to be solved, 5 appendices, 562 numbered pages, hundreds of figures, including many color plates, around 800 numbered formulae and equations, over 500 references.

This is a revised version of the book published under the same title in 1984. The many changes that have resulted in radar networking, development and implementation of new techniques in the USA explain this revision: changing the aged incoherent radars for Doppler-radars (NEXRAD with WSR-88D), implementation of Terminal Doppler Weather Radars (TDWR) at major airports, establishment of a demonstration network of wind profilers and radio acoustic sounding systems for vertical temperature distribution. This work is based on the authors' lectures on radar meteorology at the University of Oklahoma and their lecturing in different short courses, and on the comments received. The new material consists of an expanded Chapter 1, which now contains a short history of radar, sections on polarimetric measurements and data processing, an updated section on radio acoustic sounding systems and a section on wind profilers. Furthermore, Chapters 9-11 have been expanded and updated to include new figures of phenomena observed with the WSR-88D.

Chapter 1 provides historical background. Hungarian readers may find — with certain national pride — their country among those where efforts were made for radar developments already in the 1930s. *Chapter 2* introduces the essential properties of radio waves and describes the effects the atmosphere has on the path of the radar pulse and its echo. *Chapter 3* starts to develop weather radar theory, tracing the transmitted pulse to a single hydrometeor and considering the coherent or Doppler radar (equation can directly be applied to the commonly used incoherent weather radar). *Chapter 4* extends the radar principles to a conglomerate of hydrometeors that produces a continuous stream of echoes with random fluctuations of amplitude and phase, thus the weather radar equation is developed for the echo power in terms of radar and meteorological parameters. In *Chapter 5* the discrete Fourier transform is considered and applied to weather signals so as to make a connection between the Doppler spectrum and shear and turbulence of the flow. *Chapter 6* presents proven methods of weather signal processing with emphasis on obtaining the first three spectral moments and a section on methods to obtain simultaneously spectral moments and polarimetric measurements. *Chapter 7* examines limitations in pulsed Doppler radar observations of weather, presents various

techniques to mitigate them, and briefly considers how radar hardware affects measurement accuracy. *Chapter 8* deals with precipitation measurements by radar, describing the physics behind. Single- and multiple-parameter techniques and polarization diversity and its utility for quantitative precipitation measurements and discrimination between different types of hydrometeors are comprehensively discussed. Color plates ease evaluation of the various techniques. Following a brief introduction to storm structure the huge *Chapter 9* considers radar observations of winds, storms and related phenomena (tornadoes, density currents, convergence bands, downbursts and microbursts, lightning, etc.) in an illustrative manner. It discusses single- and multiple Doppler data analyses and interpretation of severe weather events with examples of wind fields, obtained from Doppler radar data analyses on storms and photographs of several significant phenomena associated with storms. The purpose of *Chapter 10* is to introduce the basic concepts of turbulence and to establish a firm connection between physical (statistical) properties of the atmosphere and Doppler-derived measurements. Relationships between turbulence and the mean Doppler velocity and the spectrum width are presented in this chapter. *Chapter 11* considers theories to explain radar echoes from clear-air refractive index irregularities. Relations between irregularity characteristics and Doppler-shifted signals are amply illustrated with specific examples and are used to explain actual observations. It also discusses vertical profiling of winds with specialized radars and measurements of temperature with radio acoustic sounding systems.

After reading through and studying the book one can confirm that the authors' intention, i.e. this book is meant to be a reference for users and developers of Doppler systems has been attained. Attaching a problem at the end of each chapter makes this edition more suitable for graduate courses on radar meteorology. To a meteorologist practicing at the borderland between meteorology and radar technique sometimes the language of the book (special words, terms, phrases) may sound slightly unusual, without causing confusion, however. Just very few and easily identifiable misprints occur in the enormous quantity of equations and formulae. This book shows great promise to be well received by the small but firm community of specialists that grew up in our country during the last decades.

Kapovits Albert

NEWS

VIIth Seminar on Surface and Meteorological Observations from Space

Budapest (Hungary), March 13–14, 1997

The seminar was organized by the Section of Earth Sciences and Department of Natural Sciences of the Hungarian Academy of Sciences and by the Hungarian Astronautical Society, with the sponsorship of the Hungarian Space Office and GRID-Budapest, the Budapest center of the Global Resource Information Database network.

The seminar began with the opening remarks by *Dr. I. Almár*, president of the Hungarian Astronautical Society, who reminded the participants that this series of seminars dates back to 1974, when the predecessor of the Hungarian Astronautical Society formed a working committee named *Earth Photography*. Since then Hungarian specialists in meteorology, cartography, geodesy, hydrology, geology, agriculture and Earth informatics (or *geomatics*) gather regularly to report on the recent national and international developments in their specific area. This occasion was not an exception; the presentations covered a number of topics of the above fields.

In addition to the six oral sessions, a poster session, including software presentations, was also held; this, considering the principal importance of the visualisation of satellite imagery in surface investigations, proved to be highly useful and efficient.

The presentations concentrated on various scientific, economic and educational aspects of the processing of satellite data with the final aim of obtaining geophysical information on the Earth's surface. Several talks discussed the retrieval of meteorological parameters needed for the accurate removal of atmospheric effects from the satellite signal, such as atmospheric profiling by GPS (Global Positioning System) and TOVS (TIROS-N Operational Vertical Sounder) systems, cloud detection and the retrieval of cloud properties. Other papers presented methods to derive surface physical parameters (land surface temperature, albedo etc.) or specific indexes characterizing the surface (vegetation "greenness" indexes etc.). A large number of presentations reported then on the application of the above information in vegetation cover identification, yield estimation, soil classification, geological investigations and water quality monitoring. As still there is no general consensus regarding some of these economically important topics, these sessions offered the possibility for a fruitful exchange of ideas.

The discussions also covered a wide range of satellite systems and instruments, from LANDSAT satellites that have been providing high spatial and spectral resolution imagery for a quarter of a century, through the operational meteorological satellites METEOSAT and NOAA, to the recently developed synthetic aperture radar (SAR) technology and many more. Almost all presentations placed their results in the context of international projects. An entire presentation was devoted to the participation of the Hungarian remote sensing community in the activities of various international organizations. Two speakers presented image processing software of leading commercial enterprises.

The organizers acknowledged the performance of the best young presenters. Among the awardees was *É. Borbás* (Hungarian Meteorological Service, Satellite Research Laboratory) for the presentation of her paper "GNSS applications in meteorology".

The seminar was concluded by a round-table discussion "The role of Earth Photograpy in the solution of the problems of the 90s". Here first *Dr. Gy. Tófalvi*, head of the Hungarian Space Office informed the community on the current financial situation of space research in Hungary. Then leaders of various research communities made their contributions, regarding financial, economic and scientific aspects. One of the main conclusions of the discussion was the need for further, more efficient collaboration between the institutions to ensure the continuation of the traditionally high quality application of satellite data for surface and atmospheric investigations in Hungary.

The presented papers have been published in the seminar proceedings.

I. Csiszár

ATMOSPHERIC ENVIRONMENT

an international journal

To promote the distribution of Atmospheric Environment *Időjárás* publishes regularly the *contents* of this important journal. For further information the interested reader is asked to contact *Prof. P. Brimblecombe,* School for Environmental Sciences, University of East Anglia, Norwich NR4 7TJ, U.K.; E-mail: atmos_env@uea.ac.uk

Volume 31 Number 8 1997

Volume 31 Number 9 1997

NOTES TO CONTRIBUTORS

The purpose of *Időjárás* is to publish papers in the field of theoretical and applied meteorology. These may be reports on new results of scientific investigations, critical review articles summarizing current problems in certain subject, or shorter contributions dealing with a specific question. Authors may be of any nationality but papers are published only in English.

Papers will be subjected to constructive criticism by unidentified referees.

* * *

The manuscript should meet the following formal requirements:

Title should contain the title of the paper, the names(s) of the author(s) with indication of the name and address of employment.

The title should be followed by an *abstract* containing the aim, method and conclusions of the scientific investigation. After the abstract, the *key-words* of the content of the paper must be given.

Three copies of the manuscript, typed with double space, should be sent to the Editor-in-Chief: *P.O. Box 39, H-1675 Budapest,* Hungary.

References: The text citation should contain the name(s) of the author(s) in Italic letter or underlined and the year of publication. In case of one author: *Miller* (1989), or if the name of the author cannot be fitted into the text: *(Miller,* 1989); in the case of two authors: *Gamov* and *Cleveland* (1973); if there are more than two authors: *Smith et al.* (1990). When referring to several papers published in the same year by the same author, the year of publication should be followed by letters a,b etc. At the end of the paper the list of references should be arranged alphabetically. For an article: the name(s) of author(s) in Italics or underlined, year, title of article, name of journal, volume number (the latter two in Italics or underlined) and pages. E.g. *Nathan, K. K.,* 1986: A note on the relationship between photosynthetically active radiation and cloud amount. *Időjárás 90,* 10-13. For a book: the name(s) of author(s), year, title of the book (all in Italics or underlined with except of the year), publisher and place of publication. E.g. *Junge, C. E.,* 1963: *Air Chemistry and Radioactivity.* Academic Press, New York and London.

Figures should be prepared entirely in black India ink upon transparent paper or copied by a good quality copier. A series of figures should be attached to each copy of the manuscript. The legends of figures should be given on a separate sheet. Photographs of good quality may be provided in black and white.

Tables should be marked by Arabic numbers and provided on separate sheets together with relevant captions. In one table the column number is maximum 13 if possible. One column should not contain more than five characters.

Mathematical formulas and *symbols:* non-Latin letters and hand-written marks should be explained by making marginal notes in pencil.

The final text should be submitted both in manuscript form and on *diskette.* Use standard 3.5" or 5.25" DOS formatted diskettes for this purpose. The following word processors are supported: WordPerfect 5.1, WordPerfect for Windows 5.1, Microsoft Word 5.5, Microsoft Word 6.0. In all other cases the preferred text format is ASCII.

* * *

Authors receive 30 *reprints* free of charge. Additional reprints may be ordered at the authors' expense when sending back the proofs to the Editorial Office.

Published by the Hungarian Meteorological Service

Budapest, Hungary

INDEX: 26 361

HU ISSN 0324-6329